

Kumulative Habilitationsschrift
zur Erlangung der Lehrbefugnis im Fach
Astrophysik

Physico-chemical Processes in Planet-forming Discs

vorgelegt von
Dr. rer. nat. Peter Voitke
aus Berlin

Institut für Theoretische Physik
Technische Universität Graz
Petersgasse 16
8010 Graz

Graz, im November 2023

Dr. Peter Voitke

Space Research Institute
(Institut für Weltraumforschung, IWF)
Austrian Academy of Science
Schmiedlstraße 6
8042 Graz, Austria

Tel: +43 316 4120320

peter.voitke@oeaw.ac.at

<https://www.oeaw.ac.at/en/iwf/institut/das-team/protoplanetare-scheiben-und-astrochemie/peter-voitke>

Nachstehende Publikationen werden als Habilitationsschrift eingereicht:

- P1** Voitke, P., Kamp, I., Thi, W.-F.: **Radiation thermo-chemical models of protoplanetary disks. I. Hydrostatic disk structure and inner rim,**
Astronomy & Astrophysics 501, 383–406, (2009)
- P2** Voitke, P., Pinte, C., Tilling, I., Ménard, F., Kamp, I., Thi, W.-F., Duchêne, G., Augereau, J.-C.: **Continuum and line modelling of discs around young stars – 300000 disc models for HERSCHEL/GASPS,**
Monthly Notices of the Royal Astronomical Society 405, L26–L30, (2010)
- P3** Voitke, P., Riaz, B., Duchêne, G., Pascucci, I., Lyo, A. -R., Dent, W. R. F., Phillips, N., Thi, W.-F., Ménard, F., Herczeg, G. J., Bergin, E., Brown, A., Mora, A., Kamp, I., Aresu, G., Brittain, S., de Gregorio-Monsalvo, I., Sandell, G.: **The unusual protoplanetary disk around the T Tauri star ET Chamaeleontis,**
Astronomy & Astrophysics 534, A44, (2011)
- P4** Voitke, P., Min, M., Pinte, C., Thi, W.-F., Kamp, I., Rab, C., Anthonioz, F., Antonellini, S., Baldovin-Saavedra, C., Carmona, A., Dominik, C., Dionatos, O., Greaves, J., Güdel, M., Ilee, J. D., Liebhart, A., Ménard, F., Rigon, L., Waters, L.B.F.M., Aresu, G., Meijerink, R., Spaans, M.: **Consistent dust and gas models for protoplanetary disks. I. Disk shape, dust settling, opacities, and PAHs,**
Astronomy & Astrophysics 586, A103, (2016)
- P5** Voitke, P., Min, M., Thi, W.-F., Roberts, C., Carmona, A., Kamp, I., Ménard, F., Pinte, C.: **Modelling mid-infrared molecular emission lines from T Tauri stars,**
Astronomy & Astrophysics 618, A57, (2018)
- P6** Voitke, P., Kamp, I., Antonellini, S., Anthonioz, F., Baldovin-Saavedra, C., Carmona, A., Dionatos, O., Dominik, C., Greaves, J., Güdel, M., Ilee, J. D., Liebhart, A., Ménard, F., Min, M., Pinte, C., Rab, C., Rigon, L., Thi, W. F., Thureau, N., Waters, L. B. F. M.: **Consistent Dust and Gas Models for Protoplanetary Disks. III. Models for Selected Objects from the FP7 DIANA Project**
Publications of the Astronomical Society of the Pacific 131, 064301, (2019)
- P7** Dionatos, O., Voitke, P., Güdel, M., Degroote, P., Liebhart, A., Anthonioz, F., Antonellini, S., Baldovin-Saavedra, C., Carmona, A., Dominik, C., Greaves, J., Ilee, J. D., Kamp, I., Ménard, F., Min, M., Pinte, C., Rab, C., Rigon, L., Thi, W. F., Waters, L. B. F. M.: **Consistent dust and gas models for protoplanetary disks. IV. A panchromatic view of protoplanetary disks,**
Astronomy & Astrophysics 625, A66, (2019)

Physico-chemical Processes in Planet-forming Discs

Peter Woitke

Space Research Institute (IWF), Austrian Academy of Science, Graz, Austria

Abstract

Planets form in clouds of gas and dust rotating around new-born stars, as a common byproduct of star formation. The physical and chemical conditions in these planet-forming discs decide upon when, where and how many planets will be formed, how massive they are, and which initial solid and gas composition they obtain. Recent exoplanet statistics have shown that the process of planet formation must be very robust indeed, as on average, every star is observed to have at least one planet.

This thesis summarises my scientific works in the research field of thermo-chemical modelling of planet-forming discs since 2009, in particular the development and applications of the Protoplanetary Disc Model (ProDiMo). By combining chemical rate networks with continuum & line radiative transfer, and the calculation of all relevant dust and gas heating & cooling rates in an axisymmetric disc structure, these models make detailed predictions about the molecular composition of the disc, the discs' internal gas and dust temperature structure, and the stability and composition of ice layers which form on top of the refractory dust grain surfaces. The development of ProDiMo was a process that took about 15 years, is still ongoing, and involved a team of international researchers, in particular Inga Kamp (Groningen University), Wing-Fai Thi and Christian Rab (both now in Garching), besides some of mine and some of their PhD-students. I have started the ProDiMo project, and am considered as the main developer, but without this team-work, ProDiMo would not have its capabilities and would not be at the level of international recognition that it has achieved to date.

Using formal solutions of the line & continuum radiative transfer equation along a bundle of parallel rays toward the observer, we can predict the spectral appearance of these discs from optical to millimetre wavelengths, for example the continuum and line fluxes, monochromatic images, radial intensity profiles, high-resolution line profiles that probe the disc dynamics, visibilities and channel maps. A large part of this thesis describes the publications that compared these predictions to disc observations that have been obtained by various space-borne and ground-based astronomical instruments, in particular Herschel/PACS, Spitzer/IRS, VLT/CRIRES, JWST/MIRI and ALMA, which observe at wavelengths between a few micron to a few millimetres. These observations probe the gas and the dust in different radial disc regions and in different layers above the midplane. Therefore, a recurring theme in my scientific work was to combine these multi-wavelength line and continuum observations, and to develop disc models that can predict all observations simultaneously, as good as possible, even at the expense of fitting certain observations less convincingly. Only if we succeed in combining the observational data from different instruments and different wavelength regions, a true holistic understanding of planet-forming discs can be achieved.

This thesis summarises the conclusions drawn from the ProDiMo thermo-chemical disc models about the chemical and physical state of protoplanetary discs as the birth places of exoplanets.

Acknowledgements

I would like to thank my wife Christiane Helling for her continuous support and scientific inspiration. Between 2007 and 2011, when most of ProDiMo was developed, she had to continue life together with our daughter Johanna, while I was commuting to Edinburgh and later working abroad in Vienna. When I became job-less in the wake of the 2008 financial crisis, I am not sure whether I would have managed to stay in science without her support. She gave me the motivation to carry on.

During my scientific career, I had the pleasure to discuss physics and chemistry and collaborate with a number of highly intelligent, knowledgeable, and inspiring scientists, from whom I learnt a lot. I want to mention a few names here: Erwin Sedlmayr, Carsten Dominik, Peter Cottrell, Vincent Icke, Sime-Jan Parrdekoper, Uffe Gråe Jørgensen, Wing-Fai Thi, Bill Dent, Inga Kamp, Christian Rab, Christophe Pinte, Francois Ménard, Geoffroy Lesur, Michiel Min, Manuel Güdel, Ken Rice, Peter Hauschildt, Guillaume Laibe, Will Rocha, Anders Johansen, Rens Waters, and Christiane Helling. I often found myself pondering about their views and insights, and their experience with numerical methods, which motivated me to try attacking the next level of physical consistency in my models.

I would also like to thank my former and current Master and PhD students, in particular Vasco Schirmacher, Gilles Niccolini, Ian Tilling, Oliver Herbort, Clayton Roberts, Aditya M. Arabhavi, Leoni Janssen, Marie-Luise Steinmeyer, Jayatee Kanwar, Thorsten Balduin and Till Käufer. They have found ways to develop and carry out new ideas which I could not, and some of their work has contributed to the development of ProDiMo.

I want to thank the IWF for welcoming me as a new group leader, in particular Werner Magnes, Aris Valavanoglou, Irmgard Jernej, Wolfgang Voller, Franz Ginner, Luca Fossati, Manfred Stellar, Ludmila Carone, Ruth Taubner, and Helmut Lammer. Their support made our start in Graz much easier.

Finally, I would like to thank the Graz University of Technology, in particular Prof. Von der Linden, for supporting my habilitation to obtain the *venia docendi* that will enable me to enrich the teaching programme at the TU Graz in the future.

Contents

List of submitted publications

Abstract

1	Introduction to Planet-forming Discs	9
1.1	Star, disc and planet formation	9
1.2	Observational appearance of discs	11
2	The ProDiMo Model	12
2.1	Disc geometry and density setup	13
2.2	Dust opacities and settling	14
2.3	Continuum radiative transfer	15
2.4	PAHs and other gas opacities	18
2.5	Chemistry	20
2.6	Gas heating/cooling balance	24
2.6.1	Line heating/cooling	25
2.6.2	Bound-free and free-free heating/cooling	26
2.6.3	Heating and cooling processes involving dust grains	27
2.6.4	High-energy heating processes	27
2.7	Numerical solution methods	30
2.8	Line transfer and predictions of observations	32
3	Results and Implications	34
3.1	Physical Processes and Code Development	34
3.2	Analysis of Herschel Observations	38
3.3	Analysis of ALMA Observations	40
3.4	Analysis of Other Observations	41
3.5	Application to Multi- λ observational data sets	43
4	Outlook	46
5	References	47
6	Submitted Publications	53
	Publication 1	53
	Publication 2	54
	Publication 3	55
	Publication 4	56
	Publication 5	57
	Publication 6	58
	Publication 7	59
7	International Research Activities	61
8	List of Teaching Courses	62
9	List of Publications	64

1 Introduction to Planet-forming Discs

1.1 Star, disc and planet formation

Star formation happens at the end of a line of complex developments in the cold galactic medium towards ever smaller spatial structures, driven by gravity, magnetic fields and turbulence, see reviews of the Protostars and Planets VII conference (Chevance et al., 2023; Zucker et al., 2023; Pineda et al., 2023). These structures span about five orders of magnitude, from spiral arms and giant molecular clouds (≈ 50 pc in diameter) to bubbles, filaments, cores and discs (≈ 100 au). When the cold cores of molecular clouds finally collapse under the pull of their own gravity, new stars are born in their centres. As the angular momentum of the in-falling matter is conserved and the collapse reduces the spatial scales by several orders of magnitude, the dust and gas begin to spin up, forming what is known as a protoplanetary disc (e.g. Yorke et al., 1993; Dominik, 2015).

These discs undergo several stages of evolution, as outlined in Fig. 1. The following classification of these evolutionary stages was developed originally by Lada & Wilking (1984), Kenyon & Hartmann (1995), and Williams & Cieza (2011): Class 0 objects are short-lived and are characterised by the first appearance of significant infall and angular motions, but yet without clear observational evidence for the nascent star at the centre. In Class I objects, the central star becomes visible and generates feedback by driving fast jets along the rotation axes. Nevertheless, the luminosity of the object is still generated mainly by frictional forces in the in-falling disc, i.e., the discs are self-luminous (active discs). In contrast, Class II objects are mainly powered by the star (passive discs), there is only little ongoing accretion, and the jets disappear. Class III is a designation for discs in

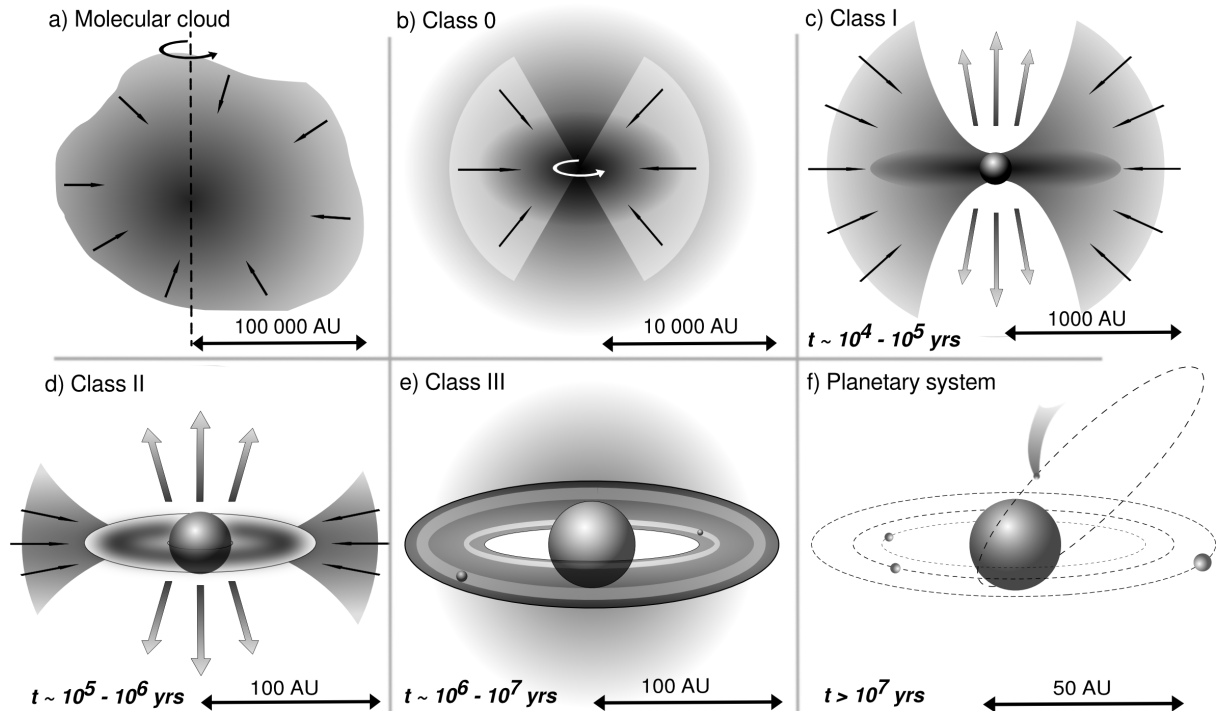


Figure 1: The phases of star and planet formation with timescales and spatial scales following the sketch developed by Drazkowska et al. (2022).

the clearing phase, where the matter in the disc is lost to space in the form of disc winds or is consumed by planet formation. Class III objects include the so-called debris discs, in which collisions of larger bodies re-create small dust particles and gas, causing the disc to become observable again in the infrared.

However, the exact definition and duration of the different phases is debated in the literature. The timescales stated in the sketch of Drazkowska et al. (2022, Fig. 1) are at the short end. For example, many of the so-called Herbig Ae/Be objects (Class II discs around massive stars of spectral type A or B) must be significantly older than 10^6 years, because these stars start as K-type stars and it takes at least 5 Myrs to evolve into A or B stars toward the main sequence (e.g. Siess et al., 2000), yet their discs belong to the most massive and most luminous Class II discs known. Hydro-models, which simulate the disc evolution, generally predict that the discs start small and then viscously spread in radius (e.g. Lynden-Bell & Pringle, 1974; Hartmann et al., 1998; Armitage, 2010; Vorobyov et al., 2020; Morbidelli et al., 2022), which would mean that the Class I discs are actually the smallest, however, they are still embedded into a much larger envelope that feeds them, so from an observational point of view, Class I discs are typically quite large.

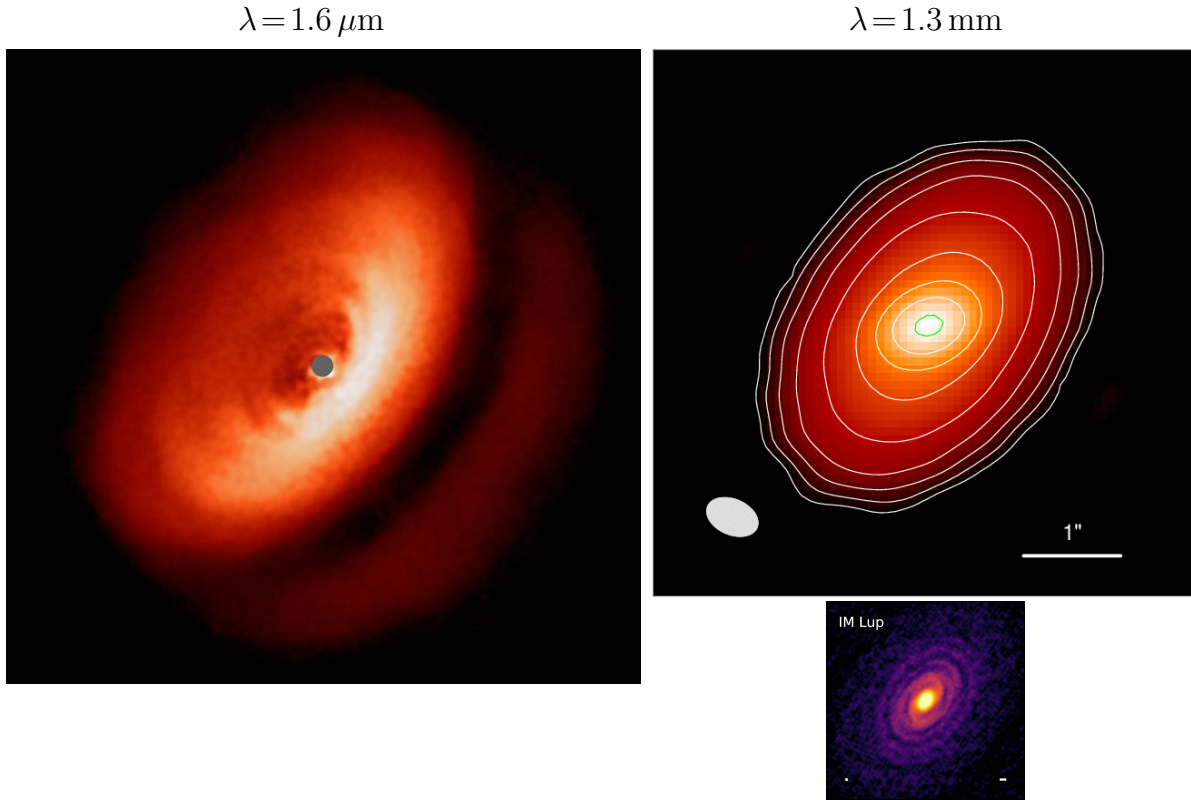


Figure 2: Three continuum images from the dusty disc around the young T Tauri star IM Lupi. The left is a polarimetric H-band ($1.6 \mu\text{m}$) image taken with the SPHERE instrument on ESO’s Very Large Telescope (Avenhaus et al., 2018). The right side shows two images at 1.3 mm taken with ALMA, using two different spatial resolutions, with PSFs and spatial scales as shown. The upper right shows the entire disc with a spatial resolution of about $0.4''$, with contours showing doubled intensities (Pinte et al., 2018). The lower right uses a different instrument setup (spatial resolution $0.045''$, the short bar shows a stretch of 10 au) to focus on the inner disc regions (Andrews et al., 2018). All three images are to scale, showing that the discs often appear significantly larger in gas than in dust. The left picture also shows that discs have a flared structure, whereas they appear to be flat at mm-wavelengths. With a radial disc extension of about 400 au in the left picture, IM Lupi is one of the largest T Tauri type discs known.

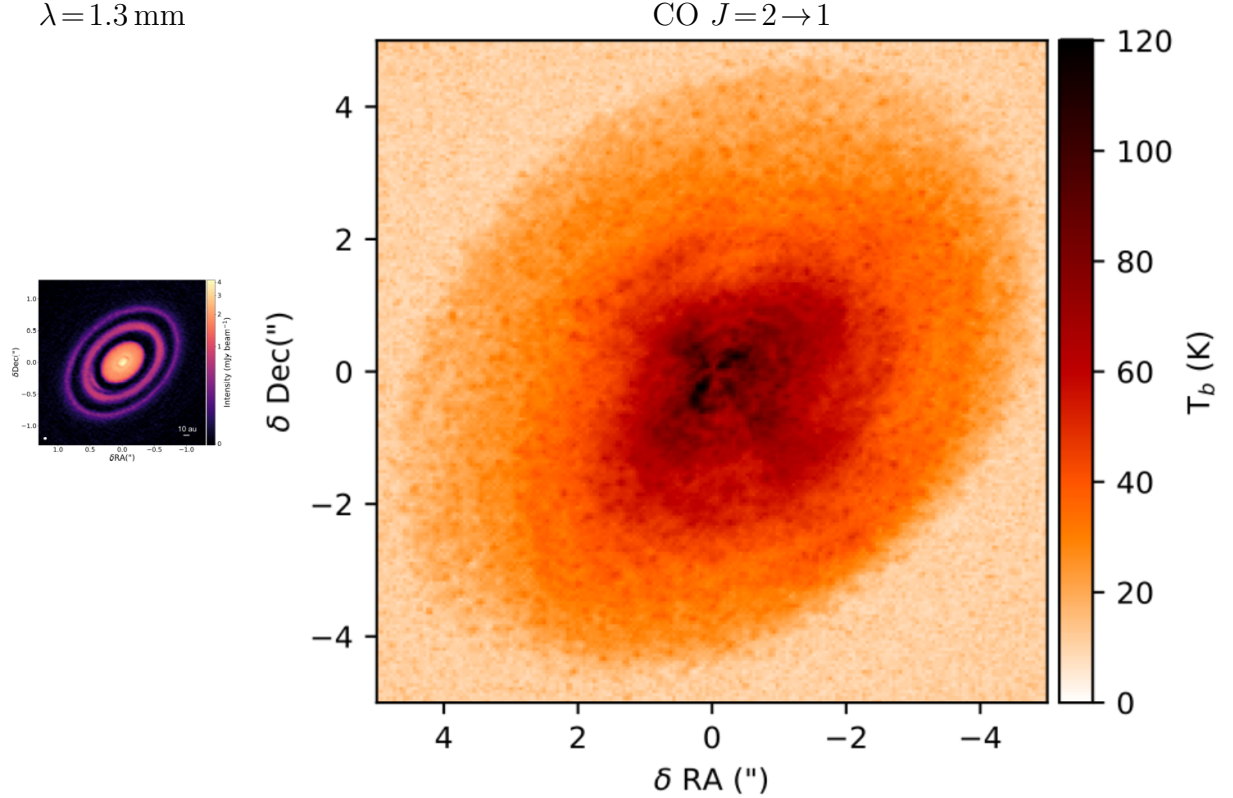


Figure 3: The Herbig Ae disc of HD 163296 as seen by ALMA (Isella et al., 2018). The picture on the left shows the band 6 continuum (about 1.3 mm) on a non-linear colour scale, with flat ring-like structures at radii of about 70 au and 100 au, similar to structures seen in other discs observed with high angular resolution by ALMA. In contrast, the CO $J=2 \rightarrow 1$ line map shows evidence for the CO gas being radially extended to at least 500 au, without clear rings. The images are to scale.

Growing evidence points towards the fact that planets are born at nearly the same time as their host stars in the same disc of material. First observational evidence of a ringed inner disc structure at millimetre wavelengths, which is interpreted as a signpost of ongoing planet formation, has been found in the object HL Tau (ALMA Partnership et al., 2015) which has an age of only about 5×10^5 years. But the same effects are still clearly seen in TW Hya, the age of which is estimated to be about 10 Myrs (Vacca & Sandell, 2011).

1.2 Observational appearance of discs

Protoplanetary discs have been first imaged at UV and optical wavelength, in particular the Hubble Space Telescope (HST) provided the first disc images (O’Dell & Wong, 1996). Since 2014, the Atacama Large Millimeter Array (ALMA) has started to provide disc images at mm-wavelengths with exquisite spatial resolution, and more recently the Spectro-Polarimetric High-contrast Exoplanet REsearch (SPHERE) instrument at the Very Large Telescope (VLT) has imaged discs in the H-band ($\sim 1.6 \mu\text{m}$), see a collection of continuum images of IM Lupi in Figs. 2 and 3.

2 The ProDiMo Model

The Protoplanetary Disc Model (ProDiMo) project was started in 2007, and the major software development was finished by myself in 2009 during my time as a post-doc at the UK Astronomy Technology Center (ATC) in Edinburgh in collaboration with Dr. Wing-Fai Thi (University of Edinburgh, now in Garching) and Prof. Inga Kamp (Groningen). The immediate scientific goal at the time was to predict the forbidden far infrared (far-IR) fine-structure emission lines of atoms and ions observed by the Herschel Space telescope (Herschel) using the PACS and SPIRE instruments, such as [OI] $2 \rightarrow 1$ ($63.18 \mu\text{m}$), [OI] $3 \rightarrow 2$ ($145.53 \mu\text{m}$), and [CII] $2 \rightarrow 1$ ($157.74 \mu\text{m}$), as well as a few far-IR high- J rotational emission lines of CO and H₂O between about $60 \mu\text{m}$ and $180 \mu\text{m}$, see Dent et al. (2013).

The first ProDiMo paper was published in *Astronomy & Astrophysics* in 2009 (Woitke et al., 2009b, see Publication 1 on page 53), immediately followed by an application to far-IR water emission lines in Herbig Ae discs (Woitke et al., 2009a). The physical and chemical roots of ProDiMo reach back to the COSTAR-program formerly developed by Inga Kamp (Kamp & Bertoldi, 2000; Kamp & van Zadelhoff, 2001), but ProDiMo was completely re-written in modern Fortran 90, with a modular parallel software architecture, and includes many more physical and chemical processes, which are consistently coupled to an in-built continuum and line radiative transfer. The basic setup and design of ProDiMo is nowadays known as a *thermo-chemical disc model*.

The basic modelling idea of ProDiMo is to assume a quasi-static 2D axisymmetric gas density structure $n_{\langle\text{H}\rangle}(r, z)$, where $n_{\langle\text{H}\rangle}$ is the hydrogen nuclei particle density, r is the distance from the rotation axis (often simply called “radius”), and z is the height over the midplane of the disc. The gas is assumed to be on stable circular Keplerian (or sub-Keplerian) orbits, which are pressure-supported to maintain their height z . Additional model parameters are the stellar irradiation properties, such as the stellar effective temperature and luminosity, the stellar non-photospheric UV and X-ray properties, and similar parameters describing the irradiation of the disc from the outside, i.e. the cosmic microwave background, interstellar UV irradiation, incident X-ray and cosmic ray fluxes. The interstellar irradiation properties are assumed to be isotropic. All parameters are assumed to be constant in time (neglecting, for example, stellar variability), and therefore, the resulting chemical and temperature structure in the disc will eventually also become time-independent. It is this disc structure that we primarily want to calculate with ProDiMo.

The slowest relaxation process in disc is usually the chemistry, in fact the transformation of some ice phases in the midplane into others can take longer than typical disc lifetimes, so when we refer to a “time-dependent ProDiMo model”, we mean a disc model where the densities and the radiation field in the disc is assumed to be constant, but we advance the chemistry at all points in the disc to a desired disc age (e.g. Helling et al., 2014). This concept can be relaxed to have different epochs with different irradiation parameters, for example to model the chemistry after an episodic accretion event (Rab et al., 2017a).

ProDiMo’s basic modelling method can shortly be described as a 2D XPDR-code, where PDR means photon dominated region (e.g. Röllig et al., 2007; Visser et al., 2009; Wolfire et al., 2022) and the X means additional X-ray physics and chemistry: In a given gas and dust density structure, radiative transfer is carried out to get the local radiation field and dust temperature. Based on these properties of the medium, a kinetic chemistry for gas and ice is solved (or advanced in time), and the gas temperature is calculated by solving the gas energy balance including all relevant heating and cooling processes.

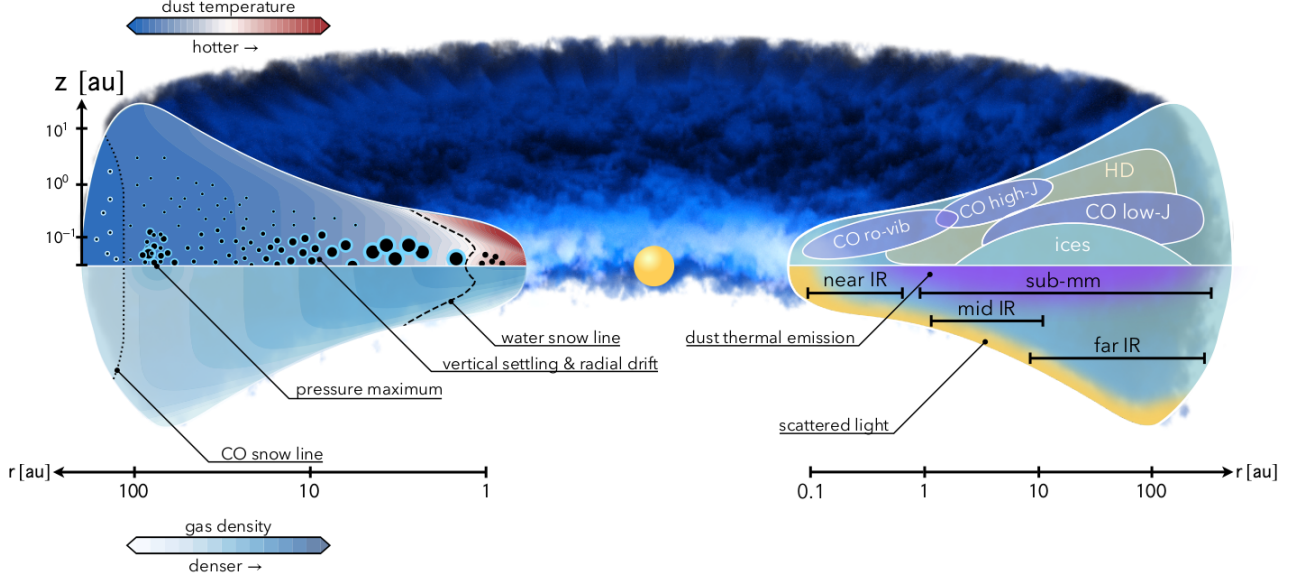


Figure 4: Sketch of the disc geometry and some of the important dust and gas phase physical and chemical processes. The right side shows which kind of continuum and line observations probe certain regions in the planet-forming discs (Miotello et al., 2022).

ProDiMo has been further developed ever since, adding more physics, chemistry and radiative transfer modules and enlarging its capabilities to predict various kinds of continuum and line observations based on the calculated chemical and temperature-structure in the disc. This habilitation thesis summarises the creation and subsequent development of ProDiMo, it's applications to various kinds of astronomical data, and the conclusions drawn from these simulations about the chemical and physical state of protoplanetary discs as the birth places of exoplanets.

2.1 Disc geometry and density setup

Figure 4, taken from Miotello et al. (2022), visualises the assumed disc geometry and some of the important dust and gas phase physical and chemical processes that are included in the ProDiMo disc simulations. The disc is assumed to have an axisymmetric density structure, which can be setup in various ways, either using the disc mass and various disc shape parameters, or by using the output of other, e.g. hydrodynamical programs like FEOSAD (Vorobyov et al., 2020), PLUTO (Mignone et al., 2007) or MOCCASIN (Ercolano et al., 2005, 2008). In the standard ProDiMo models, we assume pressure-supported Keplerian orbits of gas and dust with zero radial and vertical velocities, see Eqs.(1-6) in (Woitke et al., 2009b, Publication 1 on page 53). However, Rab et al. (2017a) used a density structure derived from disc evolution models for rotationally flattened in-falling envelopes, in this case these velocity components are non-zero in ProDiMo. The radial column density structure $\Sigma(r)$ can be setup by a radial powerlaw (Woitke et al., 2009b) or a combination of powerlaw and exponential tapering-off (Woitke et al., 2016, see Publication 4 on page 56). The vertical disc extension is either assumed to follow a Gaussian distribution with given scale height that only depends on radius (parametric radial powerlaw), or is calculated consistently with the resulting gas temperature structure and mean molecular weight (Woitke et al., 2009a; Thi et al., 2011b).

2.2 Dust opacities and settling

The assumptions about the dust opacities are described in (Woitke et al., 2016, see Publication 4 on page 56). We assume a powerlaw dust size distribution function $f(a)$ between a minimum and a maximum particle size, a_{\min} and a_{\max} , respectively, typically covering sub-micron to millimetre grains, about 4-5 orders of magnitude in size space. The grains are assumed to have the same uniform material composition. The wavelength-dependent scattering and absorption properties of the grains with a single size a are calculated by applying Mie-theory based on the effective optical constants given the assumed material mix, porosity, and shape. In Woitke et al. (2016), we established the “standard DIANA dust opacities” where we assume a mixture of two materials (silicate and amorphous carbon), 25% porosity, effective medium theory according to (Bruggeman, 1935), and a shape distribution of hollow spheres (Min et al., 2011). These assumptions were guided by the previous experience to fit disc continuum and line observations, and by a detailed study of optical properties of dust aggregates (Min et al., 2016), where the Discrete Dipole Approximation (DDA) is used to compute the interaction of light with complexly shaped, inhomogeneous aggregate particles. These computations are computationally too expensive to be included in complex disc models, but the simple method described above avoids several artefacts of Mie theory (spherical resonances), can account for the most important shape effects, and captures the co-called “antenna-effect”, where irregularly shaped inclusions of conducting materials result in a considerable increase of mm-cm absorption opacities, see Fig. 5.

These assumptions have partly been relaxed in Woitke et al. (2019, see Publication 6 on page 58), allowing for several disc zones with different dust/gas ratios, and different values for a_{\min} and a_{\max} . In Arabhavi et al. (2022), the “bare” grains made of refractory materials are assumed to be covered by a layer of ice of varying material and thickness. The position-dependent ice abundances are taken from the results of the chemistry, where ice formation is part of a kinetic chemical network. These models hence require iterations between the computation of the dust opacities, the radiative transfer, and the chemistry. However, in all other, more basic **ProDiMo** disc models, we assume temperature-independent dust opacities, which do not change with time, so we need to calculate the dust opacities only once during initialisation.

Another important model assumption is the treatment of vertical dust settling, where we assume a balance of upward directed turbulent mixing and downward directed gravitational settling, using the theoretical concepts of either Dubrulle et al. (1995) or Riols & Lesur (2018). In both cases, all grains in a given disc column are redistributed vertically such that the midplane becomes dust-enriched, in particular considering the larger dust particles, see Woitke et al. (2016) for details. In this way, the unsettled dust size distribution $f(a)$ mentioned above becomes a position-dependent quantity $f(a, r, z)$ in **ProDiMo**. The advantage of the new Riols & Lesur (2018)-setting is that the decrease of the midplane gas density with height is taken into account, whereas the in old Dubrulle et al. (1995)-settling treatment, that gas density is assumed to be constant in one column.

The assumptions about dust size distribution, opacities and settling determine how much UV radiation can penetrate into the disc, and how much grain surface per H-nucleus is present. Therefore, these assumption are crucial not only for the predicted continuum observations, but also for chemistry, heating, and line emission. In particular, other comparable thermo-chemical disc models (see summary in Table 1 of Woitke et al., 2016) often assume a single grain size, or a distribution of small grains around

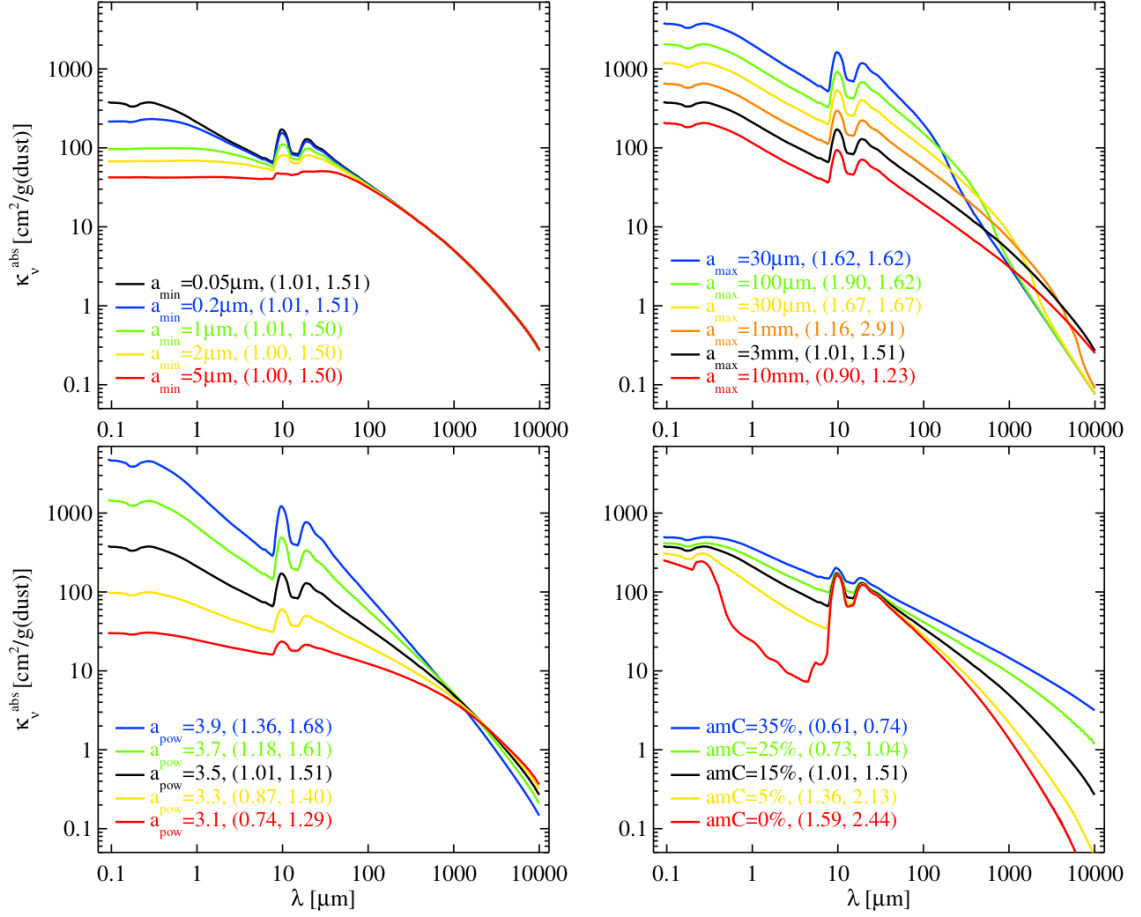


Figure 5: DIANA standard dust opacities, figure re-printed from Publication 4 (Woitke et al., 2016). All plots show the dust absorption coefficient per dust mass as function of dust size and material parameters. The upper two figures show the dependencies on minimum and maximum particle size, a_{min} and a_{max} . The lower two plots show the dependencies on dust size powerlaw index a_{pow} and on the maximum volume fraction of amorphous carbon amC . Fixed values for porosity (25%) and maximum hollow volume ratio $V_{\text{hollow}}^{\text{max}} = 0.8$ are assumed. The two numbers in brackets represent the log-log dust absorption opacity slopes between 0.85 mm and 1.3 mm, and between 5 mm and 1 cm. The black lines are all identical.

(sub-)micron sizes (Mathis et al., 1977), which produces far-UV dust extinction opacities that are larger by about a factor of 100 than our DIANA standard dust opacities, see discussion in (Woitke et al., 2016). Therefore, the various assumptions about the disc shape and the dust opacity parameters can result in a very different spectral appearance of the discs in line observations (Woitke et al., 2019, see Publication 6 on page 58).

2.3 Continuum radiative transfer

The first modelling step in ProDiMo is to solve the continuum radiative transfer problem of an irradiated disc, which results in the internal dust temperature structure $T_d(r, z)$ and the internal radiation field $J_\nu(r, z)$. The basic equations to be solved are the radiative transfer equation and the energy balance equation for the dust grains. The radiative transfer equation is given by

$$\frac{dI_\nu}{d\tau_\nu} = S_\nu - I_\nu \quad (1)$$

where $I_\nu = I_\nu(\vec{r}, \vec{n})$ is the spectral intensity at a certain 3D point \vec{r} in the disc into a certain direction \vec{n} . Assuming local thermodynamical equilibrium (LTE) and coherent isotropic scattering, the source function S_ν is given by

$$S_\nu = \frac{\kappa_\nu^{\text{abs}} B_\nu(T_d) + \kappa_\nu^{\text{sca}} J_\nu}{\kappa_\nu^{\text{ext}}} , \quad (2)$$

and the optical depth

$$\tau_\nu(s) = \int_0^s \kappa_\nu^{\text{ext}}(\vec{r}_0 - s' \vec{n}) ds' \quad (3)$$

is measured backwards along a ray, where \vec{r}_0 is the point of interest, s' is the distance backward along the ray \vec{n} , and $\vec{r}_0 - s' \vec{n}$ is the point where the ray enters the model volume. When this point is reached during the numerical integration of Eq. (1), the incident radiation $I_\nu^{\text{inc}} \exp(-\tau_\nu)$ is added, which can either be the stellar irradiation, or the (isotropic) interstellar irradiation, depending on whether the backward ray hits the star or not. $J_\nu = \frac{1}{4\pi} \int I_\nu d\Omega$ is the mean intensity, and B_ν the Planck function, and κ_ν^{abs} , κ_ν^{sca} and $\kappa_\nu^{\text{ext}} = \kappa_\nu^{\text{abs}} + \kappa_\nu^{\text{sca}}$ [cm^{-1}] are the dust absorption, scattering and extinction coefficients, respectively.

The energy balance of the dust grains is written as

$$\Gamma_{\text{dust}} + 4\pi \int \kappa_\nu^{\text{abs}} (J_\nu - B_\nu(T_d)) d\nu = 0 , \quad (4)$$

where Γ_{dust} [$\text{erg}/\text{cm}^3/\text{s}$] is a non-radiative net heating rate of the dust (for example via inelastic collisions with gas particles having a different temperature). In the standard **ProDiMo** models we assume $\Gamma_{\text{dust}} = 0$ and Eq. (4) simplifies to the condition of radiative equilibrium for the dust, appropriate for passive (Class II and III) discs.

Only very recently, we have included the process of viscous heating as a source for dust heating Γ_{dust} by means of a diffusion solver, see Appendix A in (Oberg et al., 2022), to be able to apply **ProDiMo** also to active protoplanetary and circumplanetary discs. Figure 6 shows a comparison between the dust temperatures calculated for a passive and non-settled T Tauri disc, and a viscously heated active disc with dust settling. Note the re-increase of the temperature towards the disc midplane in the inner, optically thick disc regions, due to viscous heating, and the sharp shadow that the inner disc casts onto the outer disc, resulting in very low temperatures, and another shadow forming in the outermost disc parts on the right, where the gas density is low and hence the dust strongly settled.

The actual solution of the radiative transfer problem in discs is numerically very challenging, because of the huge optical depths of order 10^6 involved, see e.g. the radiative transfer benchmark papers by Pascucci et al. (2004) and Pinte et al. (2009). **ProDiMo** follows a simple concept here, based on formal solutions of the radiative transfer equations on a given set of about 20×20 rays that all emanate from a single point in the disc to cover the 4π solid angle. Using a spatial grid of 100×100 radial and vertical grid points in cylinder coordinates (each cell is a torus in 3D), this concept requires to trace about $20 \times 20 \times 100 \times 100 = 4.000.000$ rays. The opacities and intensities are averaged over about 30 frequency bins that cover the electromagnetic spectrum from 91.2 nm (the far-UV threshold for neutral hydrogen ionisation) to about 1 cm.

Given an initial guess of $T_d(r, z)$ and $J_\nu(r, z)$, **ProDiMo** (i) calculates the source functions according to Eq. (2), (ii) numerically solves Eq. (1) backward along each ray that originates

in every grid point in all considered directions for all wavelengths, while also integrating the optical depths (Eq. 3), and (iii) re-calculates $J_\nu(r, z)$ and $T_d(r, z)$ from the definition of the mean intensity and from Eq. (4). This procedure is repeated until the results converge. While this simple concept (called Λ -iteration) actually works well for optically thin discs, it fails miserably for the usually optically thick discs, because the changes applied between iterations become tiny as the optical depths become large. In order to solve this problem, and a number of other numerical challenges, **ProDiMo**

- uses a log-interpolation of $S_\nu(r, z)$ between spatial grid points as the rays are integrated along s' ,
- varies the spatial step size Δs to make sure that the numerical deviations between one full step and two half steps are small,
- carefully auto-adjusts the ray directions during the radiative transfer (RT) iterations to focus on the incoming ray directions that causes the local dust heating,
- applies the geometrical extrapolation method from Auer (1984) after each 4th RT iteration, to accelerate the convergence, so **ProDiMo**'s RT method is an *accelerated* Λ -iteration.
- (since 2022) uses a 2D diffusion solver for the optically thick core on the midplane of the disc.

The numerical details are outlined in Woitke et al. (2009b, Sect. 4) and Oberg et al. (2022, Appendix A). In summary, **ProDiMo** uses a ray-based method to solve the continuum radiative transfer problem in discs with stellar and interstellar irradiation and internal

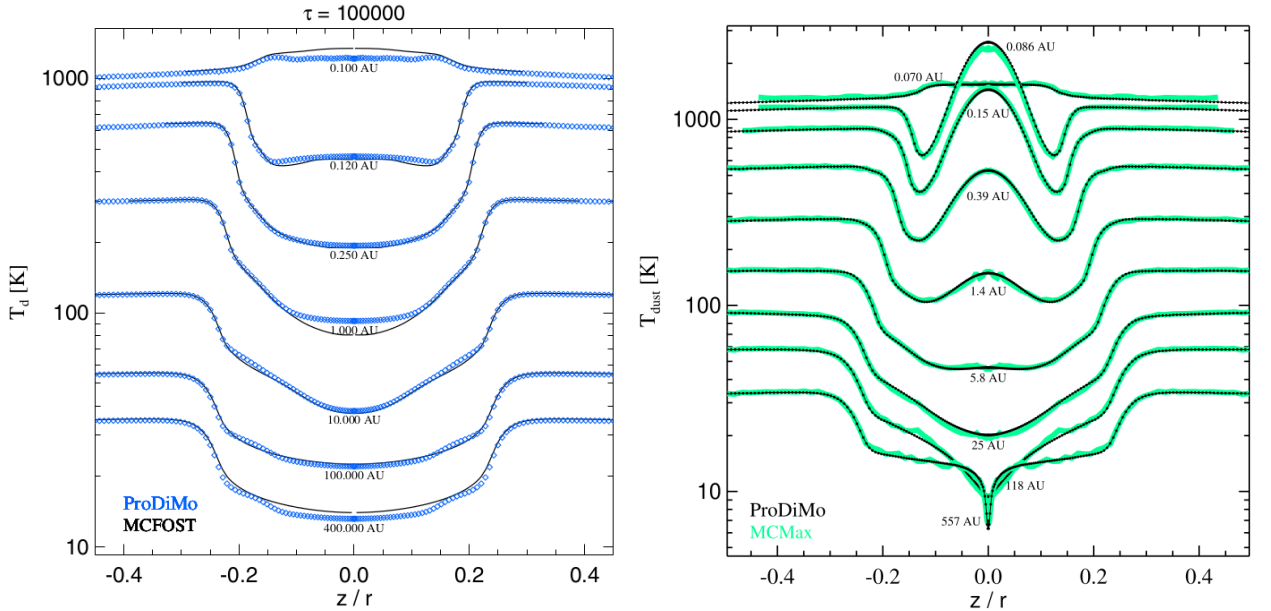


Figure 6: Resulting dust temperature structures $T_d(r, z)$ from **ProDiMo**'s continuum radiative transfer. The left plot shows a re-printed figure from Publication 1 (Woitke et al., 2009b) for a passive disc without dust settling. The right plot shows a re-printed figure from (Oberg et al., 2022) for an active disc with a mass accretion rate of $\dot{M}_{\text{acc}} = 10^{-8} M_\odot/\text{yr}$ and Dubrulle settling ($\alpha_{\text{settle}} = 0.01$). Both results are benchmarked against the leading Monte-Carlo radiative transfer programs MCFOST (Pinte et al., 2006) and MCMMax (Min et al., 2009). The comparison also reveals the progress on improving the details in the continuum radiative transfer module of **ProDiMo** over the years.

viscous heating. The results are well tested against the leading Monte Carlo radiative transfer codes MCFOST and MCMax. Compared to these MC codes, ProDiMo’s results are always noise-free and smooth, both spatially and in wavelength space, which is a huge advantage when discussing photo-chemistry, but it’s performance is slower and the solutions are limited by the assumption of isotropic scattering.

2.4 PAHs and other gas opacities

The inclusion of other opacities in ProDiMo’s radiative transfer is explained in Sect. 8 and Appendix B in Woitke et al. (2016, see Publication 4 on page 56). Polycyclic Aromatic Hydrocarbon molecules (PAHs) are observed via their strong mid-IR emission bands in many Herbig Ae/Be stars (e.g. Maaskant et al., 2014), whereas detection rates in T Tauri stars are much lower (Geers et al., 2006), likely because T Tauri stars generate much less blue and soft UV stellar radiation to heat the PAHs. PAHs in Herbig Ae/Be discs seem to have sizes of at least 100 carbon atoms (Visser et al., 2007), and to be somewhat less abundant than in the interstellar medium.

The PAH abundance in the disc is assumed to be given by the standard abundance in the interstellar medium (ISM, Tielens, 2008), modified by factor f_{PAH}

$$\frac{n_{\text{PAH}}}{n_{\text{(H)}}} = 3 \times 10^{-7} f_{\text{PAH}} \frac{50}{N_{\text{C}}} . \quad (5)$$

Here, $n_{\text{PAH}} [\text{cm}^{-3}]$ is the PAH particle density, $n_{\text{(H)}} [\text{cm}^{-3}]$ is the hydrogen nuclei density and N_{C} is the number of carbon atoms in the PAH. Values of $f_{\text{PAH}} \approx 0.1$ or lower seem typical in Herbig Ae discs.

The opacities of neutral and charged PAHs are calculated according to (Li & Draine, 2001) with updates in (Draine & Li, 2007), including the “graphitic” contribution in the near-IR and the additional “continuum” opacities of charged PAHs. We normally assume $N_{\text{C}} = 54$ carbon atoms and $N_{\text{H}} = 18$ hydrogen atoms (“circumcoronene”), resulting in a PAH mass of 666.7 amu and a PAH radius of 4.87 Å (Weingartner & Draine, 2001). However, N_{C} and f_{PAH} are free model parameters, as well as a decision whether to consider the neutral or charged PAH opacities, or a mixture of both.

To include PAHs in the radiative transfer, we neglect PAH scattering and extend the source function by two terms describing PAH emission and absorption

$$S_{\nu} = \frac{\kappa_{\nu}^{\text{dust,abs}} B_{\nu}(T_{\text{d}}) + \kappa_{\nu}^{\text{PAH,abs}} B_{\nu}(T_{\text{PAH}}) + \kappa_{\nu}^{\text{sca}} J_{\nu}}{\kappa_{\nu}^{\text{dust,abs}} + \kappa_{\nu}^{\text{PAH,abs}} + \kappa_{\nu}^{\text{sca}}} , \quad (6)$$

introducing the PAH temperature T_{PAH} . T_{d} and T_{PAH} are calculated as

$$0 = 4\pi \int \kappa_{\nu}^{\text{dust,abs}} (B_{\nu}(T_{\text{d}}) - J_{\nu}) d\nu , \quad (7)$$

$$0 = 4\pi \int \kappa_{\nu}^{\text{PAH,abs}} (B_{\nu}(T_{\text{PAH}}) - J_{\nu}) d\nu , \quad (8)$$

assuming independent radiative equilibria for the dust grains and the PAH molecules. The validity of these assumptions is discussed in Appendix B of (Woitke et al., 2016).

For PAH abundances or order $f_{\text{PAH}} = 0.01$ the PAH opacities can usually be neglected in the continuum radiative transfer, see Fig. 7. However, when dust settling is taken into

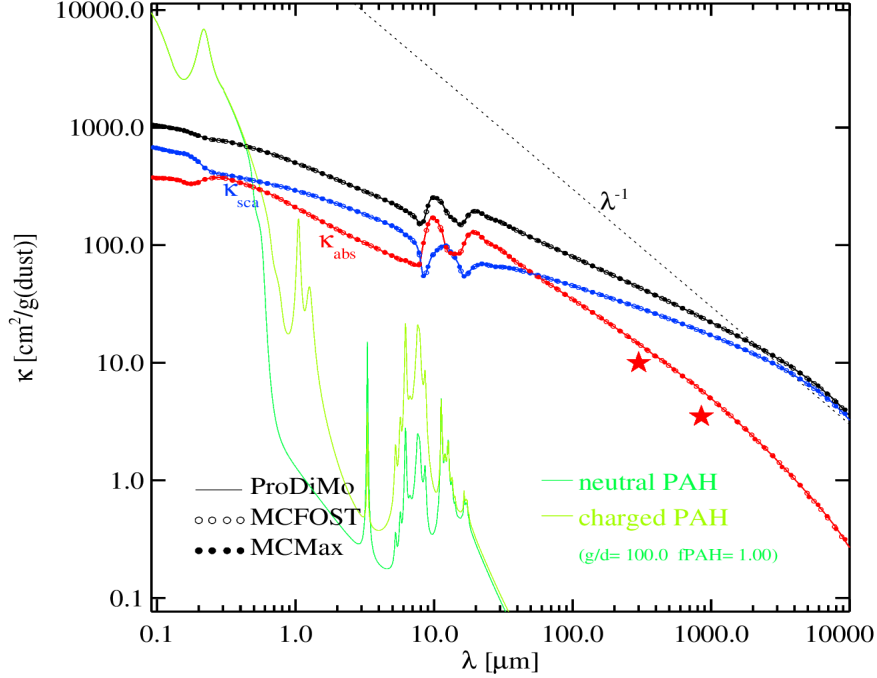


Figure 7: Comparison of unsettled DIANA standard dust opacities ($a_{\min} = 0.05 \mu\text{m}$, $a_{\max} = 3 \mu\text{m}$, $a_{\text{pow}} = 3.5$), as calculated by ProDiMo, MCFOST and MCMax, to the opacities of neutral and charged PAH molecules, assuming gas/dust = 100 and $f_{\text{PAH}} = 1$. The two red stars represent dust absorption opacities commonly used to derive disc masses from millimetre fluxes: $10 \text{ cm}^2/\text{g(dust)}$ at 1000 GHz (Beckwith et al., 1990) scaled to $3.5 \text{ cm}^2/\text{g(dust)}$ at $850 \mu\text{m}$.

account, the PAH UV opacities can dominate over the UV dust opacities in the uppermost disc layers, depending on the assumptions about the dust size distribution and settling. Because the PAHs are very small and therefore very inefficient scatterers, PAHs can effectively shield the disc from the stellar and interstellar UV by absorbing the UV and re-emitting this energy in form of the infrared PAH features at $3.3 \mu\text{m}$, $6.2 \mu\text{m}$, $7.6 \mu\text{m}$, $8.6 \mu\text{m}$, $11.3 \mu\text{m}$ and $13.5 \mu\text{m}$. This can have important consequences for the disc internal gas temperature and chemical structure, see Sect. 2.6.

Apart from the direct impact of PAHs on the internal radiation field via radiative transfer effects, PAHs can also be included in ProDiMo' chemistry via five charge states (Sect. 2.5) and the photoelectric heating rates of PAHs can be included in the gas energy balance (Sect. 2.6). There are various options in ProDiMo to include any combination of these effects. In the most consistent models, PAHs are included in chemistry and radiative transfer, and their opacities and photoelectric heating rates are calculated from the ambient radiation field and the calculated distribution of their charging states, which requires iterative models.

Molecular UV gas opacities can also be included in ProDiMo, but this is still an experimental, yet unpublished feature. The idea is to add the molecular opacities to $\kappa_{\nu}^{\text{PAH,abs}}$. In this case, T_{PAH} describes the thermal emission of a mixture of PAHs and molecules, but the molecules do not play a significant role here, because we only include molecular UV cross-sections, and the disc is certainly too cold for UV emission.

2.5 Chemistry

The chemical rate network is the core of all thermo-chemical disc models. In the most general case, we have a reaction-diffusion problem to solve

$$\frac{dn_i}{dt} = P_i - L_i - \nabla \cdot \Phi_i , \quad (9)$$

where n_i [cm⁻³] is the particle density of species i , t [s] is the time, P_i and L_i [cm⁻³s⁻¹] are the chemical production and destruction rates and Φ_i [cm⁻²s⁻¹] is a diffusive particle flux. Since we treat the disc as quasi-static, there is no advection term in Eq. (9).

The chemical production and destruction rates include 1st order processes, two-body and three-body reactions with rates

$$R_1 = k_1 \times n_A \quad (10)$$

$$R_2 = k_2 \times n_A n_B \quad (11)$$

$$R_3 = k_3 \times n_A n_B n_C , \quad (12)$$

where A, B, C are the reacting chemicals, and n_A , n_B , n_C their particle densities. The 1st order processes include photoprocesses, cosmic ray and X-ray induced processes, and spontaneous decay processes, each destroying A. For example, a photoionisation or photodissociation process



has a rate coefficient [s⁻¹]

$$k_{\text{ph}} = 4\pi \int \sigma_{\text{ph}}(\nu) \frac{J_\nu}{h\nu} d\nu , \quad (14)$$

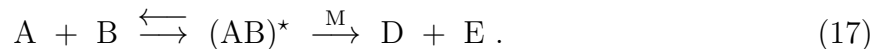
where ν is the photon frequency, $\sigma_{\text{ph}}(\nu)$ is the UV photo cross section and J_ν is the local direction-averaged UV intensity taken from the radiative transfer module (Sect. 2.3). The corresponding rate $R = k_{\text{ph}} n_A$ [cm⁻³s⁻¹] needs to be added three times, namely to the destruction rate of A, L_A , and to the two production rates of D and E, P_D and P_E . In a similar way, the gas-kinetic two-body reaction rates are computed, for example



using a modified Arrhenius law

$$k_2 = \alpha \left(\frac{T}{300 \text{ K}} \right)^\beta \exp \left(-\frac{\gamma}{T} \right) . \quad (16)$$

In this case, the rate coefficient k_2 has units [cm³s⁻¹], and the resulting rate $R = k_2 \times n_A n_B$ has again units [cm⁻³s⁻¹]. This rate is added to L_A , L_B , P_D and P_E . Concerning the three-body reactions $A + B + M \longrightarrow D + E + M$ there is, in most cases, an unspecified collision partner M involved, which stabilises an activated complex, following this scheme



Such reactions have low and high pressure limits, depending on the particle density of the collision partner n_M . However, the critical density of M of these reactions, where the low pressure limit changes gradually into the high pressure limit, is typically $10^{18} - 10^{21}$ cm⁻³.

Such high densities are typically not present in discs, so we can use the low pressure limit throughout, in which case the effective rate is given by $R = k_3 \times n_A n_B n_M [\text{cm}^{-3}\text{s}^{-1}]$, and $k_3 [\text{cm}^6\text{s}^{-1}]$ can again be expressed with a modified Arrhenius law.

The **ProDiMo** project started in 2009 with a small reaction network of 71 species and 911 reactions from the UMIST 2006 database (Woodall et al., 2007), which was originally designed by Kamp & Bertoldi (2000) to compute the concentrations of the small species relevant for the heating and cooling in discs, such as H_2 , OH, CO, and water. Since then, many publications using **ProDiMo** have expanded and refined the chemical network as we use it today. Here we list some of the most significant chemical processes added:

- A simple freeze-out chemistry with ice adsorption and thermal/photo-/Xray desorption was introduced by Woitke et al. (2009b), using the concept of an “active” surface layer (Aikawa et al., 1996), where only the top ~ 2 atomic layers of an ice mantel can be desorbed.
- An X-ray ionisation chemistry was added by Aresu et al. (2011), with primary X-ray ionisations and secondary ionisations via fast electrons, based on Meijerink & Spaans (2005) with doubly ionised atoms.
- The small and large DIANA standard chemical networks were introduced by Kamp et al. (2017), which have 100 and 235 chemical species, respectively, with reaction rates mostly taken from the UMIST 2012 database (McElroy et al., 2013). The paper also summarises the rates used for electronically excited molecular hydrogen H_2^* , which is a product of “failed” photoionisations of H_2 , and establishes our standard element abundances (see Table 5 in Kamp et al., 2017), which are close to solar except for the depleted metals Na, Mg, Si, S and Fe.
- The key process of H_2 -formation on grain surfaces is calculated according to Cazaux & Tielens (2002, 2004) with updates described in Cazaux & Spaans (2009); Cazaux & Tielens (2010).
- Thi et al. (2019) introduced a network for 5 charging states of PAH molecules of adjustable size, with the default choice being *circumcoronene* $\text{C}_{54}\text{H}_{18}$. The total abundance of the PAHs is treated as a free parameter.
- Instead of using the UMIST database for the base reactions, it is now also possible to use the KIDA standard network 2014 (Kinetic Database for Astrochemistry, Wakelam et al., 2012, 2013), or the OSU 2009 database (Ohio State University chemical network) from Eric Herbst.
- Surface chemistry was introduced by Thi et al. (2020b,a) and benchmarked against a standard setup for cold molecular clouds (Semenov et al., 2010). The application of surface chemistry in discs is subject of active research, many of the energy barriers are only poorly known, which becomes increasingly more relevant for higher temperatures. Thi et al. (2020a) have applied and tested the various surface chemical concepts to the formation of H_2 and HD on warm grain surfaces, and Thi et al. (2020b) have developed a model for the formation of phyllosilicates on warm grain surfaces.
- Thi et al. (2019) and Balduin et al. (2023) have developed an advanced chemical network for thousands of individual charging states of dust grains of different sizes.
- Kanwar et al. (2023, submitted to A&A) have developed an extended hydro-carbon network to simulate the formation of larger hydrocarbon molecules like benzene (C_6H_6) in the warm inner disc.

Some of the processes listed above do not follow the simple rate formulation (Eqs. 10-12), for example the active layer concept for ice desorption involves the relative composition of the surface layer (Woitke et al., 2009b), where all ice species appear in the denominator, and if one ice species is dominant, for example water ice, its desorption rate becomes independent of the ice concentration itself (0th-order rate) as long as the active surface layer is fully occupied. These special cases need to be treated carefully when it comes to the computation of the Jacobian matrix.

Ordered by increasing complexity, the following chemical models can be computed:

- | | |
|---|--|
| (1) thermo-chemical equilibrium: | minimisation of Gibb's free energy |
| (2) kinetic chemical equilibrium: | $0 = P_i - L_i$ |
| (3) time-dependent chemistry: | $\frac{dn_i}{dt} = P_i - L_i$ |
| (4) 1D time-independent reaction-diffusion: | $0 = P_i - L_i - \frac{\partial \Phi_i}{\partial z}$ |

The first variant is based on the principle of minimisation of the total local Gibb's free energy, given the local pressure and temperature, either just for the gas, or with condensation, using the chemical and phase equilibrium code **GGchem** by Woitke et al. (2018). This mode requires an equality between gas and dust temperature. It has rarely been used so far (e.g. Thi et al., 2020b), but is likely to be very useful to discuss the stability of refractory condensates in the inner disc.

The second option is the default, the work-horse of **ProDiMo**. Most publications using **ProDiMo** have assumed kinetic chemical equilibrium. Indeed, the chemical relaxation timescale (see Sect. 8.3 in Woitke et al., 2009b) is much shorter than typical disc evolutionary timescales in the observable, line-emitting, warm disc surface, which justifies this approximation when it comes to comparing disc models with observations. However, this simplification is not valid in the optically thick midplane, where the chemical transformation of one ice species into others can by far exceed the disc lifetime. Figure 8 shows a few selected results of our standard T Tauri disc model in kinetic chemical equilibrium, with physical disc parameters listed in Table 3 of Woitke et al. (2016). This model uses the large DIANA standard chemistry with 235 species and 3067 reactions.

For the third option, we fix the physical conditions at each point in the disc model in terms of temperatures, densities, and radiation field conditions, and solve the chemistry time-dependently, usually setting the initial chemical conditions by the results of a molecular cloud model. In this case, the disc chemistry evolves with disc age, as for example in Helling et al. (2014). Rab et al. (2017a) considered the time-dependent chemistry after an outburst of a young Class-I object going through episodic accretion events.

The forth option is the latest feature added to **ProDiMo**. Woitke et al. (2022) explored the effects of vertical turbulent mixing on the chemical structure of protoplanetary discs. As the more abundant species are mixed upwards and downwards, at the locations where these chemicals are finally destroyed, for example by photo-processes, the release of reaction products has important consequences for all other molecules. This generally creates a more active chemistry, with a richer mixture of ionised, atomic, molecular, and ice species, and new chemical pathways that are not relevant in the unmixed case.

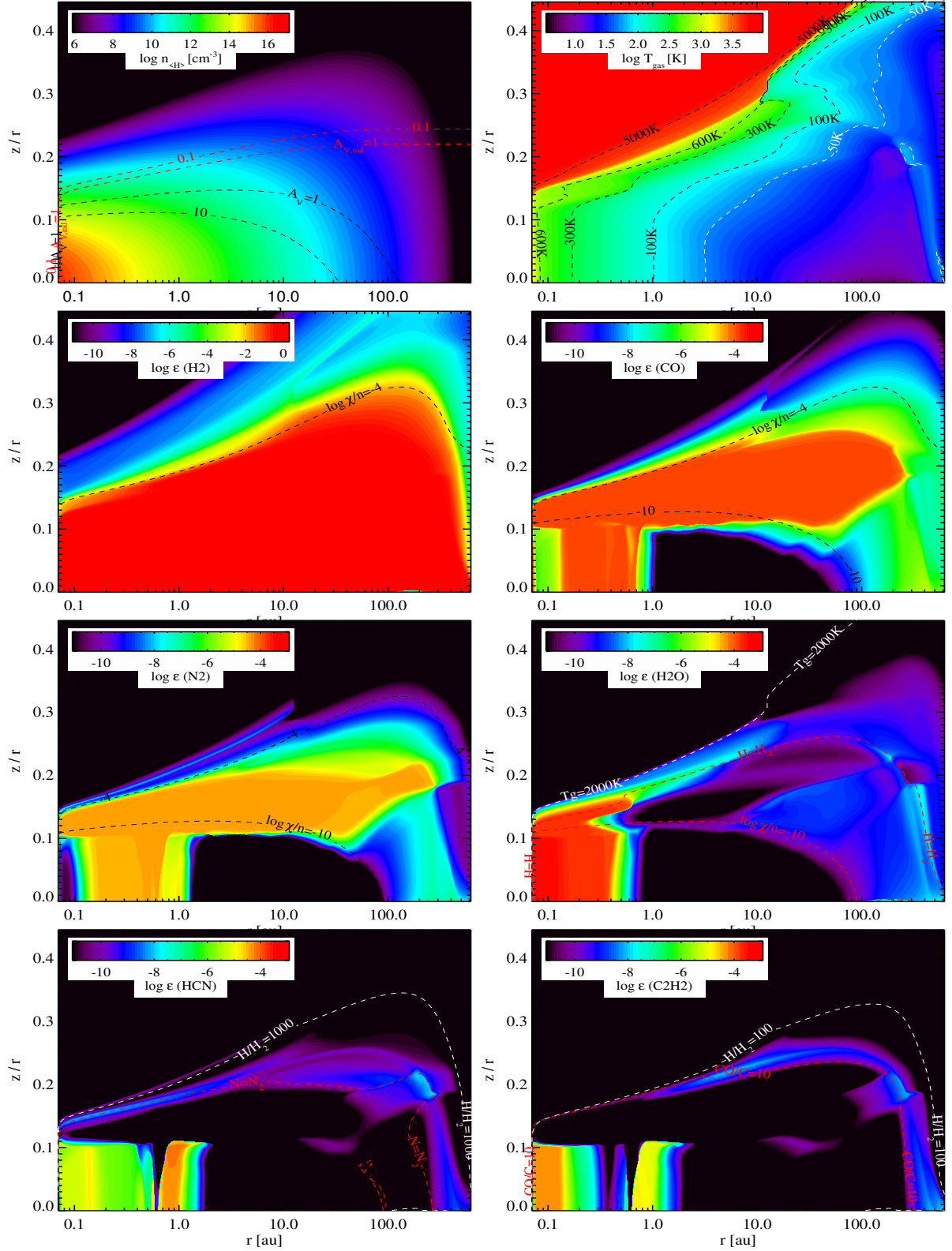


Figure 8: Selected results from the chemistry of a standard T Tauri model. The plots in the top row show the assumed gas density structure (left) and the calculated gas temperature structure (right) as function of radius r and relative height z/r over the midplane. The other plots show the calculated concentrations of the four major molecules H_2 , CO , N_2 , H_2O , and the two spectroscopically interesting molecules HCN and C_2H_2 , which only occur with lower concentrations in certain disc regions and layers. Additional contour lines include the vertical optical extinction A_V , the radial optical extinction $A_{V,\text{rad}}$, and the ionisation parameter χ/n (i.e. the UV field strength divided by gas particle density).

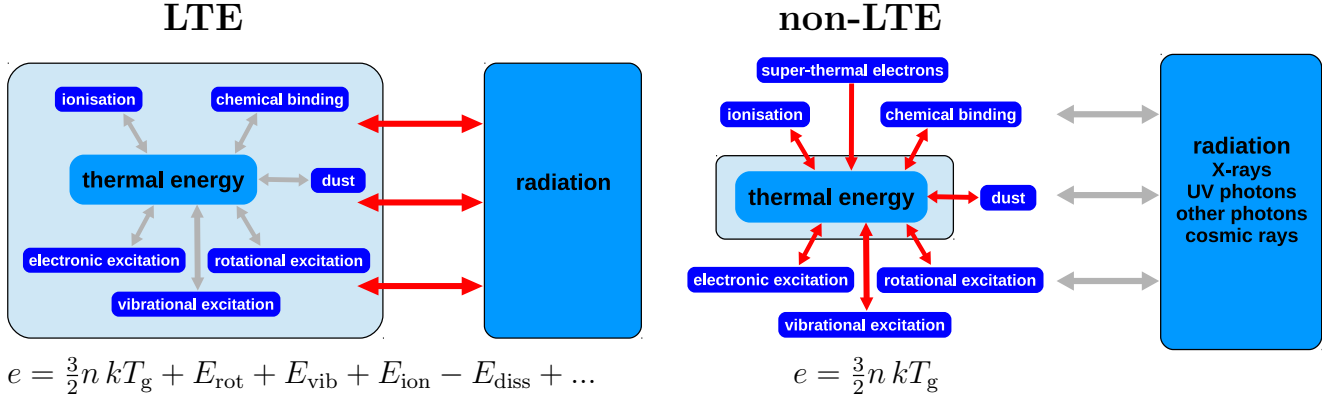


Figure 9: Two different approaches to apply the first law of thermodynamics. Following the LTE approach (left), the internal energy e contains all possible ways to store energy in a gas. According to the non-LTE approach (right) e is given by the thermal kinetic energy of the gas particles only. The red arrows visualise the energy fluxes considered to calculate the net heating/cooling rate Q . In contrast, the grey arrows visualise processes that are not directly included in the computation of Q . Figure reprinted from Woitke (2015).

2.6 Gas heating/cooling balance

The determination of the temperature of the gas in protoplanetary discs is an integral part of any disc modelling, and constitutes one of the four pillars of ProDiMo (radiative transfer, chemistry, heating & cooling, and hydrostatic structure), see Fig. 12. The resulting gas temperature is important for (i) the chemical processes, (ii) the production of emission lines connected to the observability of the gas phase, and (iii) the prediction of the hydrostatic vertical stratification and shape of the disc. The first law of thermodynamics is applied to the gas as shown on the right side of Fig. 9 as

$$\frac{d}{dt}\left(\frac{e}{\rho}\right) = -p\frac{dV}{dt} + \frac{1}{\rho}\left(\sum_i \Gamma_i - \sum_k \Lambda_k\right), \quad (18)$$

where e [erg/cm³] is the internal energy per volume, p [erg/cm³] the gas pressure, $V = 1/\rho$ [cm³/g] the specific volume, ρ [g/cm³] the mass density, and Γ_i (“gain”) and Λ_k (“loss”) are the various heating and cooling rates per volume [erg/cm³/s].

The $-pdV$ work is zero as long as the gas moves on stable, pressure-supported Keplerian orbits. In this case, ρ and V are constants, and Eq. (18) simplifies to

$$\frac{de}{dt} = Q(T_g) = \sum_i \Gamma_i - \sum_k \Lambda_k = 0, \quad (19)$$

which states the condition of thermal energy equilibrium. Since the net heating rate Q depends on the gas temperature, Eq. (19) states an implicit equation for the determination of the gas temperature in thermal equilibrium T_g^0 .

In order to assess the importance of the $-pdV$ work, we can compute the cooling relaxation timescale

$$\tau_{\text{cool}} = -\frac{\partial e}{\partial T_g} \bigg|_{T_g^0} \bigg/ \frac{\partial Q}{\partial T_g} \bigg|_{T_g^0}, \quad (20)$$

and compare it with the dynamical timescale τ_{dyn} given by the evolutionary timescale of the disc of the order of millions of years. However, in the case of winds, or hydrodynamical

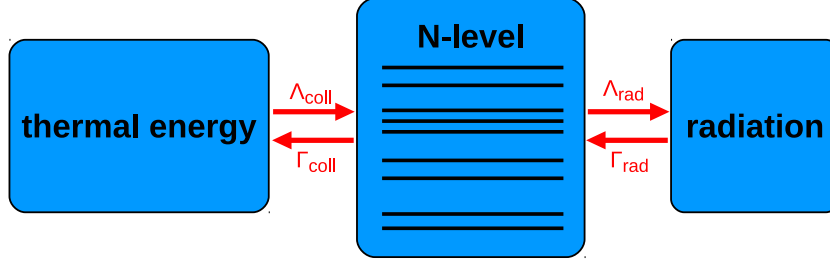


Figure 10: N -level heating and cooling rate. Energy fluxes from left to right are cooling, and from right to left heating. Subscript “coll” means collisional, and subscript “rad” means radiative.

instabilities such as spiral waves or vortices, τ_{dyn} will be much shorter, but not much shorter than the orbital timescale. The **ProDiMo** models show that, even in such strongly time-dependent cases, $\tau_{\text{cool}} \ll \tau_{\text{dyn}}$ often remains valid, such that Eq. (19) is justified. However, this may not be valid in highly optically thick regions in the midplane of massive discs where the excess energy can only escape diffusively, which is subject of ongoing research.

ProDiMo is known for its particularly detailed treatment of heating and cooling, taking into account various physical and chemical processes, and evaluating about 100 heating rates Γ_i and about 100 cooling Λ_k , which is summarised below.

2.6.1 Line heating/cooling

For the basic N -level bound-bound (line) heating and cooling rates, we use a non-LTE formulation with escape probability theory, see Voitke et al. (2009b) and Voitke (2015). It is important to realise that spectral lines do not only cause cooling by collisional excitation followed by line emission, but can also do the reverse, namely heating by line absorption followed by collisional de-excitation, see Fig. 10. In statistical equilibrium, the net energy exchange rate between the gas thermal energy and the radiation field [erg/cm³/s] can be measured on either side of the energy buffer labelled with N -level

$$Q_{N\text{-level}} = \Gamma_{\text{rad}} - \Lambda_{\text{rad}} = \Gamma_{\text{coll}} - \Lambda_{\text{coll}} , \quad (21)$$

$$\Gamma_{\text{col}} = \sum_{l=1}^{N-1} \sum_{u=l+1}^N n_u C_{ul} \Delta E_{ul} \quad (22)$$

$$\Lambda_{\text{col}} = \sum_{l=1}^{N-1} \sum_{u=l+1}^N n_l C_{lu} \Delta E_{ul} \quad (23)$$

$$\Gamma_{\text{rad}} = \sum_{\text{lines}} n_l \Delta E_{ul} P_{ul}^{\text{pump}} B_{lu} J_{\nu_{ul}}^{\text{cont}} \quad (24)$$

$$\Lambda_{\text{rad}} = \sum_{\text{lines}} n_u \Delta E_{ul} (P_{ul}^{\text{esc}} A_{ul} + P_{ul}^{\text{pump}} B_{ul} J_{\nu_{ul}}^{\text{cont}}) . \quad (25)$$

$\Delta E_{ul} = E_u - E_l$ is the energy difference between an upper state u and a lower state l , $C_{ul} = \sum_p n_p \gamma_{ul}^p(T_g)$ [s⁻¹] are the collisional de-excitation rates, C_{lu} the collisional excitation rates, n_p is the density of a collision partner p and $\gamma_{ul}^p(T_g) = \langle v_p \sigma_{ul} \rangle$ its collisional rate coefficient [cm³ s⁻¹] for de-excitation $u \rightarrow l$. A_{ul} , B_{lu} and B_{ul} are the Einstein coefficients for spontaneous emission, absorption and stimulated emission.

P_{ul}^{esc} and P_{ul}^{pump} are the escape and pumping probabilities, expressing the probability that a locally emitted line photon is not re-absorbed again in the neighbourhood in the

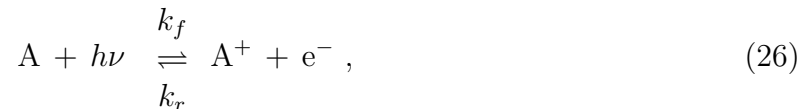
same line, and the probability that a continuum photon makes it to the considered location given the existence of line opacity in the disc, respectively. Both probabilities become very small when the line is optically thick. Various authors have presented different ideas and formula for P_{ul}^{esc} and P_{ul}^{pump} , for example Gorti & Hollenbach (2009), Voitke et al. (2009b), Woods & Willacy (2009), Du & Bergin (2014) and Bruderer et al. (2014) use different assumptions about disc geometry, and approximations about velocity gradients, and line broadening. Recently, Voitke et al. (2023, A&A submitted) have developed a new escape probability theory for 2D disc geometries, where local continuum radiative transfer effects in the line resonance regions are taken into account, leading to expressions for P_{ul}^{esc} and P_{ul}^{pump} that depend on radial and vertical line and continuum optical depths.

In order to evaluate the non-LTE equations (22) to (25), the respective atomic and molecular data are required. The data includes the level energies E_i and statistical weights g_i , the radiative data (transition wavelengths λ_{ul} and Einstein coefficients A_{ul}), and, in particular, the collisional data for all important collision partners, including e^- , H, He, and H_2 , as function of temperature, which are often incomplete or entirely missing. Over the years, we have collected such data from various sources and databases, combining experimental data, or quantum-mechanical predictions, or a combination of both. A selection of atomic data sources is listed in Table A.1 of Voitke et al. (2009b), updated with larger model atoms in Table 4 of Voitke et al. (2011), using the CHIANTI database (Atomic Database for Spectroscopic Diagnostics of Astrophysical Plasmas) and the NIST database (National Institute of Standards and Technology).

Concerning the molecules, we mostly use the LAMDA database (Leiden Atomic and Molecular Database), but there have been additional efforts to collect more extensive data in form of ro-vibronic data (i.e. electronically, vibrationally and rotationally excited states) of the two key molecules H_2 and CO, see Thi et al. (2013a). The data situation is particularly challenging for the ro-vibrational transitions of larger molecules, and for some molecules like CO_2 , C_2H_2 and HCN, we are simply forced to assume LTE, in which case a line list is sufficient. For this purpose, we mostly use the HITRAN 2020 database (High-resolution Transmission Molecular Absorption Database).

2.6.2 Bound-free and free-free heating/cooling

In addition to the interaction of the gas with line photons via excited states, there are a couple of bound-free and free-free processes to be taken into account, for example photo-ionisation of neutral C, Fe, Si, and H^-



where k_f is the photo-ionisation rate (see Eq. 14) and k_r the direct recombination rate. Here, it is the excess kinetic energy of the created free electron that is thermalising with the gas. From the threshold frequency ν_{thr} and the energy conservation $h\nu = h\nu_{\text{thr}} + E_{\text{th}}$ we find the photo-ionisation heating rate to be

$$\Gamma = n_A 4\pi \int_{\nu_{\text{thr}}}^{\infty} J_\nu \frac{\nu - \nu_{\text{thr}}}{\nu} \sigma^{\text{bf}}(\nu) d\nu , \quad (27)$$

where $\sigma^{\text{bf}}(\nu)$ is the bound-free cross section. The reverse process, the recombination cooling rate, is slightly more difficult to understand. A direct recombination destroys one thermal electron, so the recombination cooling rate should be of order

$$\Lambda = n_{\text{A}+} n_{\text{e}^-} k_r(T_{\text{g}}) \langle E_{\text{th}} \rangle , \quad (28)$$

where $\langle E_{\text{th}} \rangle$ is the mean thermal energy of the captured electron. By considering an equilibrium between photo-ionisation and direct recombination in thermal equilibrium, where $J_{\nu} = B_{\nu}(T_{\text{g}})$, called Milne relations, it is possible to derive the recombination cooling rate just from the bound-free cross sections as

$$\Lambda = \frac{n_{\text{A}+} n_{\text{e}^-} k_r(T_{\text{g}})}{k_f|_{J_{\nu}=B_{\nu}(T_{\text{g}})}} 4\pi \int_{\nu_{\text{thr}}}^{\infty} B_{\nu}(T_{\text{g}}) \frac{\nu - \nu_{\text{thr}}}{\nu} \sigma^{\text{f}}(\nu) d\nu . \quad (29)$$

Depending on the spectral shape of $\sigma^{\text{bf}}(\nu)$, Eq. (29) typically results in $\langle E_{\text{th}} \rangle \approx (1.5 - 2.5) kT_{\text{g}}$. In applications to discs, we find that the photo-ionisation of neutral carbon is an important heating process in the outer disc, and the photo-attachment of H^- , i.e. $\text{H} + \text{e}^- \rightarrow \text{H}^- + h\nu$, can be an important cooling process in the inner disc.

2.6.3 Heating and cooling processes involving dust grains

The presence of dust particles in the disc, which are “outside” of the thermodynamical system considered for the gas internal energy and the first law of thermodynamics (Fig. 11), leads to a number of additional heating and cooling processes. Such processes include inelastic collisions of gas particles with dust grains, and the injection of super-thermal electrons or gas particles just formed by certain physical and chemical processes taking place on the surface of the dust grains, such as UV photon absorption or surface chemical processes. Table 1 summarises the heating/cooling processes included in ProDiMo.

2.6.4 High-energy heating processes

The young star in the centre of the disc is usually active and accreting, therefore it is a strong source of UV radiation, X-rays, and stellar energetic particles (SEPs). When this high-energy radiation interacts with the upper disc surface, a number of additional high-energy processes are triggered, which usually dominate the heating of these regions, see Table 1. In addition, the disc is also irradiated from the outside in form of interstellar UV photons and cosmic rays. The hard X-rays and in particular the cosmic rays can penetrate quite deep into the disc, where they provoke some chemical activity even in the UV-shielded regions that can still be relevant for the heating of the gas.

Figure 11 shows which of these heating and cooling processes are found to be the relevant ones in a standard ProDiMo model for a T Tauri disc without viscous heating and PAHs. The hot upper disc regions are controlled by X-ray Coulomb heating versus Lyman- α and forbidden [O III] and [O I] line cooling. The warm surface layers above the $A_{\text{V,rad}} = 1$ -line are heated by UV-induced processes, in particular the heating by collisional de-excitation of H_2^* , chemical heating by exothermal reactions, photo-dissociation, and photo-ionisation of neutral carbon. This heating is balance by line cooling in particular of OH, water and CO. Below the $A_{\text{V,rad}} = 1$ line, the efficient line cooling creates a situation where the gas temperatures are slightly lower than the local dust temperatures, and the gas is heated by

Table 1: High-energy heating and miscellaneous heating/cooling processes in ProDiMo

process	physical description	formula (reference)
dust thermal accommodation	Inelastic collisions of gas particles with dust grains cause an equilibration of T_g and T_d – can be heating or cooling.	Burke & Hollenbach (1983)
heating by formation of H_2 on dust	The H_2 molecules forming on grain surfaces are ejected with super-thermal velocities in vibrationally highly excited states. The kinetic part is assumed to get thermalised by collisions.	Black & Dalgarno (1976)
background/formation heating by H_2	In addition to the radiative and collisional excitation of its ro-vibrational states, the vibrational states of H_2 are pumped by the formation of H_2 on grain surfaces. The excess energy on ejection is partly thermalised by de-exciting collisions. This effect is part of the non-LTE modelling of H_2 in ProDiMo.	Duley & Williams (1986)
heating by collisional de-excitation of H_2^*	The fluorescent excitation of H_2 by UV photons pumps the vibrational levels of H_2 , which can be converted into thermal energy by collisions.	Tielens & Hollenbach (1985)
dust photo-electric heating	UV photons impinging on dust grains can eject electrons with super-thermal velocities (photoeffect) which then thermalise through collisions with the gas. The efficiency of this process decreases strongly with grain charge.	Kamp & Bertoldi (2000)
PAH heating	Photoeffect on PAH molecules, similar to dust photo-electric heating, depends on PAH charging.	Thi et al. (2019)
X-ray Coulomb heating	The absorption of X-rays in the K -shells of the various elements dissociates and ionises the gas, which produces fast electrons. If the degree of ionisation in the gas is high, these super-thermal electrons predominantly undergo elastic Coulomb collisions with ambient electrons, which can very efficiently heat the gas.	Dalgarno et al. (1999)
X-ray H_2 dissociation heating	If the gas is mostly molecular, the fast electrons produced X-ray interactions mostly interact with H_2 , creating H_2^+ , which will recombine or produce H_3^+ . These reactions are exotherm, heating the gas.	Meijerink & Spaans (2005)

Table 1: continued

process	physical description	formula (reference)
cosmic ray heating	Energetic particles (cosmic rays or SEPs) loose their energy in small steps, characterised by the energy to create an ion pair. We use a simple formula for the energy thermalised by the subsequent physical and chemical processes per ionised H-atom and H ₂ -molecule.	Jonkheid et al. (2004)
viscous heating	The transport of angular momentum in the disc is physically connected to the creation of heat by frictional forces. It also leads to mass accretion. We use a formula that expresses the heat production due to viscous heating as function of the mass accretion rate.	D'Alessio et al. (1998)
photo-dissociation heating	Similar to bound-free ionisation heating, but more complicated, as only a small fraction of the excess energy over binding energy is liberated in form of kinetic energy. However, the reaction products can be in excited ro-vibronic states, the energy of which might get thermalised by collisions.	Glassgold & Najita (2015)
chemical heating	Chemical reactions generally liberate or consume chemical binding energy. We multiply the reaction rates of all exotherm and endotherm gas phase reactions with their reaction enthalpies and sum them up, excluding the UV, cosmic ray and X-ray reactions. The stable molecules destroyed by these reactions typically undergo a series of exotherm reactions before they eventually re-form.	Woitke et al. (2011)
Lyman- α cooling	Once an H-atom is collisionally excited to its $n=2$ level, it will emit a Lyman- α photon. These photons are absorbed and re-emitted many times, until they eventually leave the disc (resonance scattering).	Tielens & Hollenbach (1985)

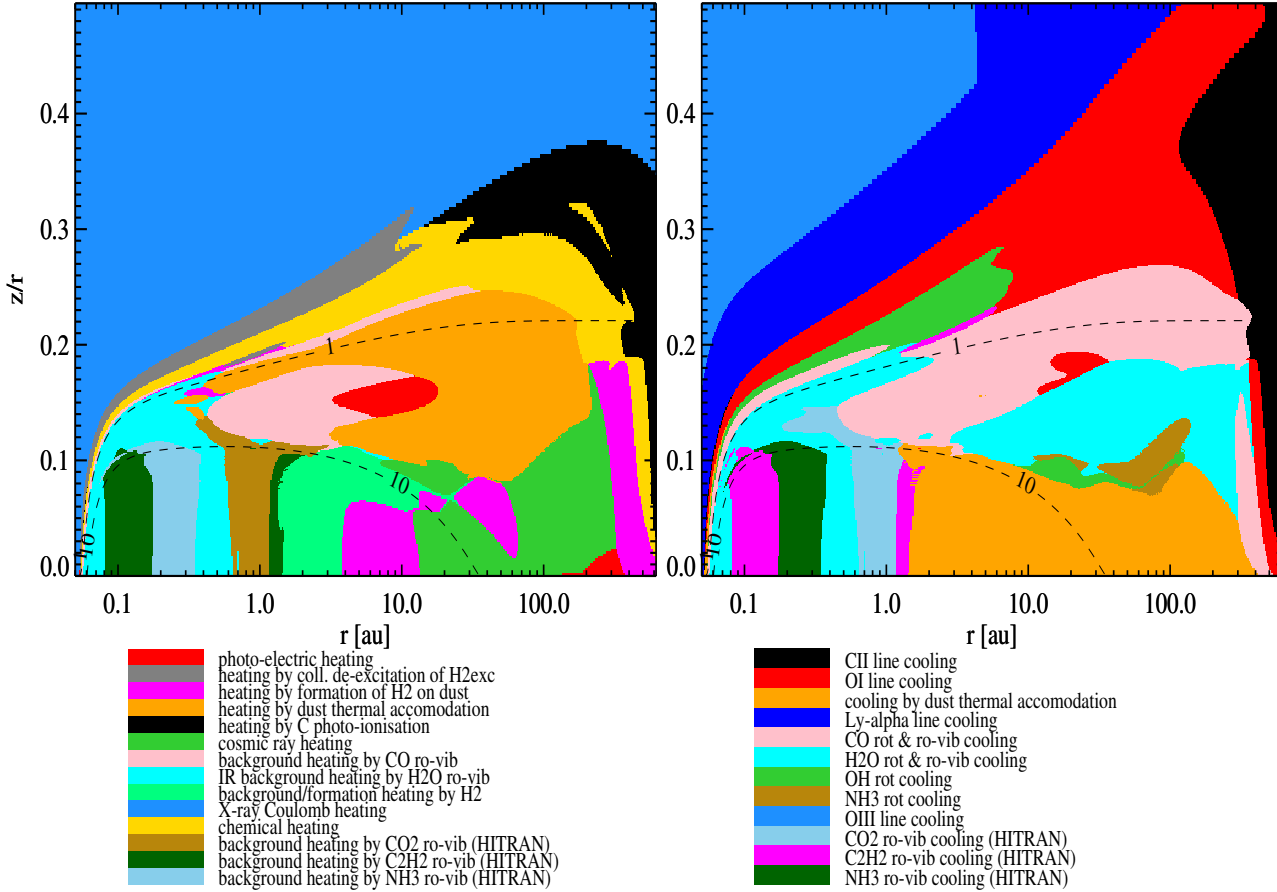


Figure 11: The leading heating process (left) and the leading cooling process (right) in a ProDiMo standard T Tauri disc model. Processes are only plotted when they fill in at least 1% of the depicted area in these plots. The dashed lines mark the visual disc surface ($A_{V,\text{rad}} = 1$) and a vertical optical extinction of $A_V = 10$. The model includes 103 heating and 95 cooling processes, with altogether 64910 spectral lines.

thermal accommodation in addition to the heating via absorption of continuum photons by the CO, water and CO₂ lines. In the optically thick part of the disc ($A_V \gtrsim 10$), where $J_\nu \approx B_\nu(T_d)$ and $T_g \approx T_d$, dust and gas exchange energy mostly via photons, i.e. the gas absorbs continuum photons in the lines, and the dust absorbs the line photons emitted by the gas.

2.7 Numerical solution methods

The previous sections have laid out how the radiative, physical and chemical processes are interlinked in protoplanetary discs. The chemistry can only be calculated when the radiation field and the local dust and gas temperatures are known, and the calculation of the heating/cooling rates requires to know the radiation field, the gas and dust temperatures, and the local concentrations of all relevant atoms, ions, electrons and molecules. Finally, the hydrostatic structure of the disc can only be calculated when the gas temperatures and the mean molecular weights are known, and that structure changes the disc shape and hence the results of the continuum radiative transfer.

In order to solve these dependencies, ProDiMo uses a sequence of internal and global

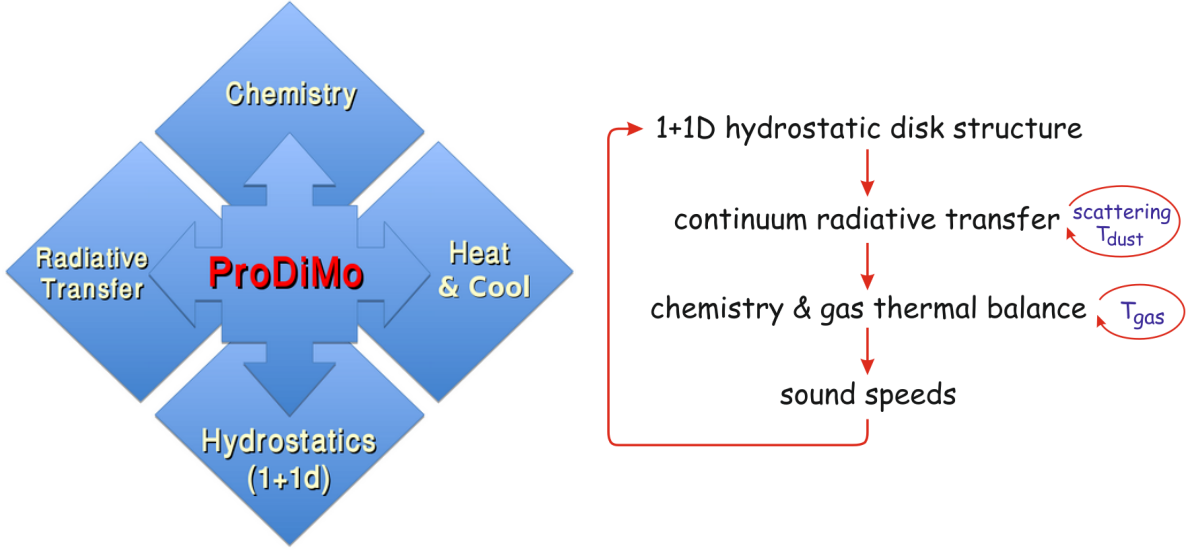


Figure 12: Schematic description of the thermo-chemical disc modelling code ProDiMo and the course of actions and global iterations. The right figure is adopted from Woitke et al. (2009b).

iterations, see Fig. 12. We start by setting the stellar and interstellar irradiation properties and (a guess of) the disc density structure $\rho(r, z)$. After determining the dust settling (Sect. 2.2), we calculate the dust absorption and scattering opacities (Sect. 2.2) and solve the continuum radiative transfer problem (Sect. 2.3), which involves an iteration to find the correct dust temperature structure and source functions including scattering.

Next, we solve the chemistry on a given point for a given gas temperature, and determine the net gas heating function $Q(T_g)$. We then vary the gas temperature, re-calculate the chemistry and net gas heating, and repeat this process until the gas temperature T_g^0 in thermal balance is found, where $Q(T_g^0) = 0$, which on average requires about 5-10 calls of the chemistry module per point. Due to dependencies of the photo-dissociation rates on radial and vertical molecular column densities (shielding factors) in the chemistry, and the dependencies of the line escape probabilities on radial and vertical line optical depths for the gas heating/cooling balance, the chemistry on the various spatial grid points must be solved in a particular order. A new point can only be calculated once all points above that point, and all points inside of that point are already completed. But different processors can still work on several disc columns in parallel, which leads to a filling of the computed points in a “diagonal” way, where the computations start with the closest highest grid point, and end with the most distant midplane point.

Once the chemistry and the gas energy balance have been determined on all grid points, we can compute the local sound speeds and then solve the following equation for the vertical hydrostatic equilibrium by numerical integration to obtain the vertical disc structure

$$p = \sum n_i k T_g = c_s^2(r, z) \rho \quad (30)$$

$$\frac{1}{\rho} \frac{dp}{dz} = c_s^2(r, z) \frac{d \ln p}{dz} = - \frac{z GM_\star}{(r^2 + z^2)^{3/2}}. \quad (31)$$

Such models require an additional outer iteration, in which the resulting disc density structure $\rho(r, z)$ is passed back to the continuum radiative transfer, see Fig. 12. Such hydrostatic disc models are very slow and tend to have convergence problems, so they are rarely used in practise, see however Sect. 2.1 for published examples.

But even if the disc density structure $\rho(r, z)$ is fixed in a parametric way, some disc models still require global iterations, in cases where the opacities used in the continuum radiative transfer depend on the results of the chemistry, for example

- inclusion of X-ray gas opacities in the radiative transfer (Rab et al., 2018).
- PAH opacities in the radiative transfer with consistent charging (Thi et al., 2019),
- inclusion of position-dependent ice opacities (Arabhazi et al., 2022).

2.8 Line transfer and predictions of observations

Once a disc model has been completed, we solve the line and continuum radiative transfer equation in 3D, along a bundle of parallel rays, to produce observable quantities. The basics of this ray-tracing technique are explained in Appendix A.7 of Publication 3 (Woitke et al., 2011), and the setup of the parallel rays forming the image plane, to observe the disc under an inclination angle i , is described in Section 2.3 of Thi et al. (2011b). This ray-tracing technique has been used to connect the disc models to various kinds of observations, and is the key to our endeavour to compare and verify our modelling results with observations.

The observations predicted this way are the spectral energy distribution (Thi et al., 2011b), continuum images and radial continuum intensity profiles (Woitke et al., 2019), infrared molecular line spectra (Woitke et al., 2018), line and continuum visibilities (Woitke et al., 2016, 2019), line velocity profiles (e.g. Woitke et al., 2011; Tilling et al., 2012; Thi et al., 2013b) and channel maps (e.g. Rab et al., 2020). Applying additional instrument-specific input data, such as filter transmission curves and baseline configurations, we can simulate the observations available on different platforms, with different instruments and observational techniques this way, for example photometric fluxes from UV to millimetre wavelengths for the SED, the Submillimeter Array (SMA) for continuum images at

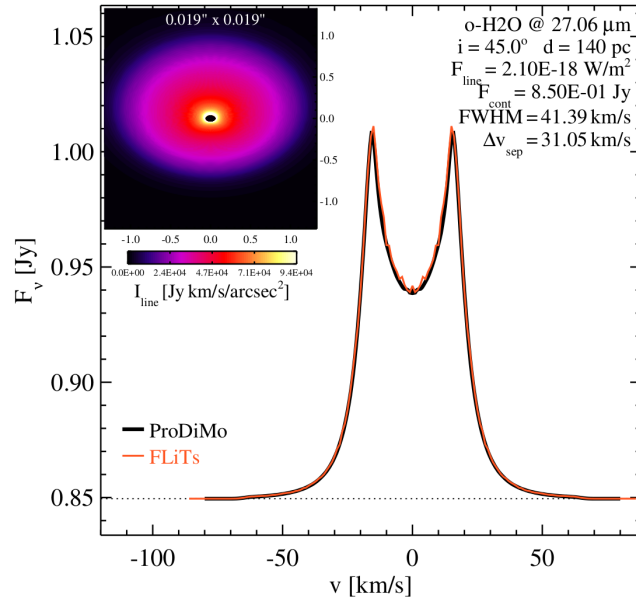


Figure 13: The o-H₂O rotational line $8_{5,4} \rightarrow 8_{2,7}$ in the mid-IR at $27.06 \mu\text{m}$ emitted from a T Tauri disc as simulated with ProDiMo and FLiTs. The line is emitted from the disc surface within about 1 au. The Keplerian velocity field creates a symmetric double-peaked profile. The line sits on a continuum of about 0.85 Jy, figure re-printed from Publication 5 (Woitke et al., 2018).

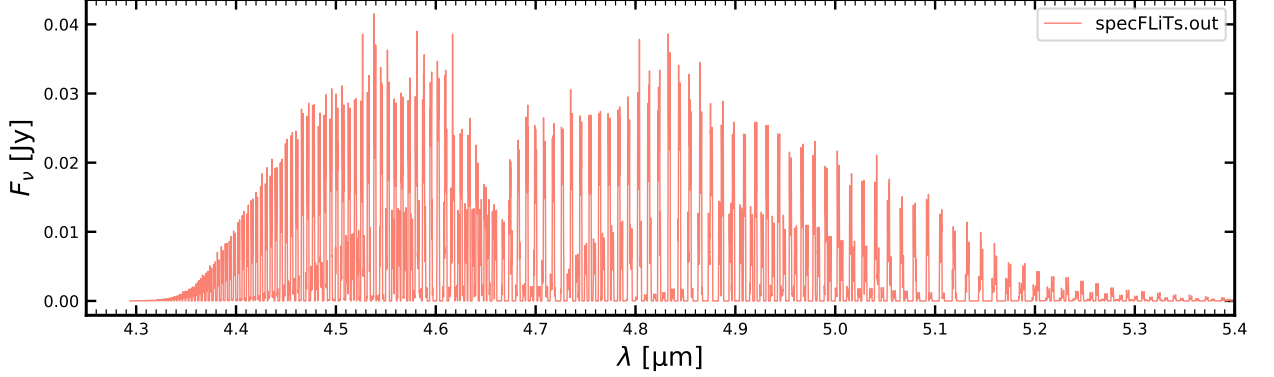


Figure 14: The CO fundamental ro-vibrational spectrum around $4.7\ \mu\text{m}$ emitted from a T Tauri disc simulated with ProDiMo and FLiTs. We see the P and R branches of the vibrational $v=1\rightarrow 0$, $v=2\rightarrow 1$ and $v=3\rightarrow 2$ bands in emission after continuum subtraction. One ro-vibrational line creates a narrow, symmetric double-peaked profile as in Fig. 13, but the superposition of all lines from the three different vibrational bands can make the individual lines appear asymmetric.

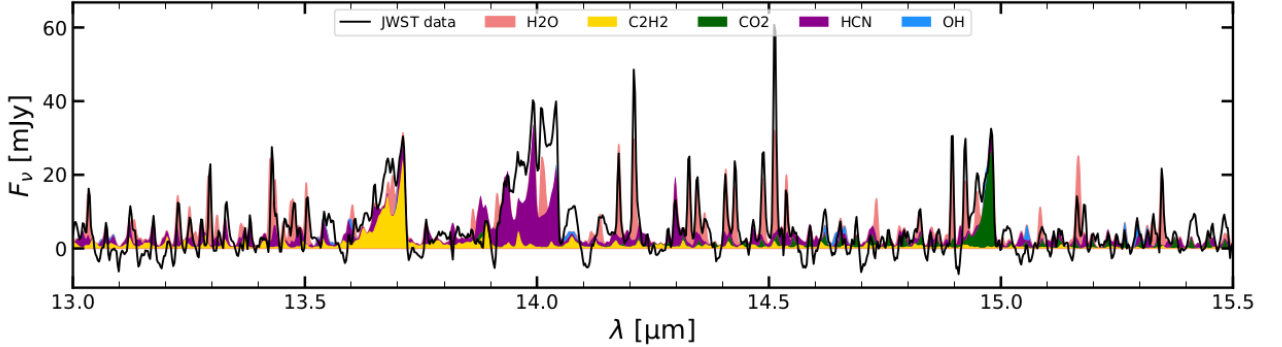


Figure 15: The continuum-subtracted spectrum of the T Tauri star EX Lupi observed with JWST (Kóspál et al., 2023, black line) compared to fitted ProDiMo–FLiTs 2D disc model, convolved to a spectral resolution of $R=2500$, showing the contributions of the various molecules (Woitke et al., 2023).

sub-millimetre images, VLT/CRIRES for velocity-resolved CO fundamental line spectra, VLT/MIDI and VLT/PIONIER for visibilities, the Spitzer Space Telescope and JWST for IR spectra, and the Atacama Large Millimeter Array (ALMA) for channel maps.

The physical assumptions going into the continuum and line transfer at this stage are (i) pressure-supported Keplerian velocity field, (ii) Gaussian line profile function with thermal + turbulent broadening, (iii) non-LTE population of the molecular states computed with escape probability, and (iv) isotropic and coherent continuum scattering. The assumption of Keplerian orbits can be relaxed (yet without consistent feedback on the escape probabilities), for example to discuss the asymmetric line profiles caused by disc winds (Rab et al., 2022). The non-LTE populations are computed as laid out in Sect. 2.6.1, when the gas line heating/cooling rates are determined, and the continuum source functions are calculated as laid out in Sect. 2.3 for the continuum radiative transfer.

A major improvement of this techniques was the development of the Fast Line Tracer (FLiTs) by Michiel Min (see Woitke et al., 2018), which allows us to compute thousands of spectral lines at a time, to efficiently produce the complicated infrared molecular line spectra that we can now observe with the James Webb Telescope (JWST). Figures 13, 14 and 15 show three examples. FLiTs uses the level populations, dust opacities and

continuum source functions from ProDiMo, on the same (r, z) -grid, and applies a fast numerical technique to trace all lines simultaneously, including line overlaps and a clever randomisation of the ray positions to avoid Nyquist-like artefacts.

3 Results and Implications

The following section provides a brief historical overview of the development of the ProDiMo radiation thermo-chemical disc model, its application to various physical processes in discs, and the results obtained with ProDiMo to analyse and interpret various observational data obtained with different instruments in different wavelengths domains.

3.1 Physical Processes and Code Development

Code Basics: The first published results of ProDiMo appeared in Pinte et al. (2009), who performed a dust radiative transfer benchmark for optically thick discs. It was an important milestone for the development of ProDiMo to pass these tests, showing that the ray-based continuum radiative transfer provides reliable results. The full modelling concept of ProDiMo was then presented by Woitke et al. (2009b, see Publication 1 on page 53). The paper introduces the considered axi-symmetric disc geometry, the foundations of the dust radiative transfer, the formulation of the chemical rate network including UV photo-rates and a simple freeze-out ice chemistry, and the treatment of the gas energy balance via the calculation of various heating and cooling rates. This paper has meanwhile reached over 300 citations.

First line predictions: In Woitke et al. (2009a), far-IR water emission lines from Herbig Ae discs were calculated in consideration up the upcoming ESA Herschel Space Observatory mission (Herschel). To predict these lines, we utilised the non-LTE Monte Carlo radiative transfer program RATRAN by Hogerheijde & van der Tak (2000), and discussed the differences between LTE population, non-LTE population calculated by ProDiMo’s escape probability theory, and the full non-LTE computations performed internally by RATRAN. These investigations showed that the escape probability model (in the 2009 formulation) slightly underpredicts the water emission lines by about 5-20%, whereas assuming LTE leads to critical line overpredictions by a factor of about 2-3. These same technique was used by Kamp et al. (2010) to make detailed predictions for the [OI] $2 \rightarrow 1$ ($63.18 \mu\text{m}$), [OI] $3 \rightarrow 2$ ($145.53 \mu\text{m}$), and [CII] $2 \rightarrow 1$ ($157.74 \mu\text{m}$) forbidden atomic lines targeted by the Herschel open time key program GASPS “*GAS evolution in Protoplanetary Systems*”.

Deuteration of water: Thi et al. (2010b) expanded ProDiMo’s chemical network by a small set of deuterated species $\{\text{D}^+, \text{D}, \text{HD}, \text{HD}^+, \text{OD}, \text{OD}^+, \text{HDO}, \text{HDO}^+, \text{H}_2\text{DO}^+\}$ to discuss the chemical pathways to form deuterated water and the resulting HDO/H₂O fractionation ratio in discs. The results show that it is possible to obtain a surprisingly high water fractionation ratio of order 10% when the gas is warm ($T_g \gtrsim 200 \text{ K}$), with interesting consequences for the delivery of water to Earth.

SEDs and inner rims: In Thi et al. (2011b), we presented the first post-processing tool included in ProDiMo to predict observational quantities from the results of the disc models. The continuum radiative transfer is numerically solved along a bundle of parallel rays, allowing us to calculate the integrated spectral flux under inclination angle i and

predicting monochromatic images. In this particular paper, we consider hydrostatic disc models which have tall inner rims in the case of Herbig Ae discs. These “puffed-up” inner rims cast a shadow onto the outer disc, which is important for near-IR excess and the shape of the spectral energy distribution (SED) at longer wavelengths.

Detailed line-transfer as post-processing: In Appendix A.7 of Woitke et al. (2011), we introduced a method to calculate the line and continuum radiative transfer equation along a bundle of parallel rays intersecting the disc midplane under inclination angle i . This tool is similar to the SED tool presented by Thi et al. (2011b), but on a fine, velocity-resolving frequency grid, where the Doppler-shift of the line-emitting gas according to a Keplerian velocity field is taken into account. The line-transfer post-processing tool is very robust and fast, but only applicable to spectroscopically isolated lines. The results typically show a double-peaked line profile as e.g. observed by SMA and ALMA in the (sub-)mm spectral region. The tool replaced the previously used calls of RATRAN or MCFOST in all publications after 2011. Besides properly predicting the line fluxes, it allows us to calculate spatially resolved line intensity maps and channel maps. Both the SED and the line tools are actually equipped with Fourier transform algorithms to calculate visibilities for user-selected baselines, which so far was only used once in Woitke et al. (2016).

X-ray chemistry: Aresu et al. (2011) introduced an X-ray chemistry to ProDiMo with primary ionisations and secondary ionisations by fast electrons, based on Meijerink & Spaans (2005), with doubly ionised atoms. These high-energy processes are particularly relevant for T Tauri stars that have high X-ray to UV luminosity ratios. The penetration of the stellar X-rays is treated by a radial extinction law using X-ray gas opacities from the literature. The X-rays generally reach only slightly deeper layers in the disc when compared to far-UV radiation, but cannot change the midplane ionisation. However, X-rays can specifically unblock the CO, which can lead to the formation of molecules like HCN and C₂H₂ in an oxygen-rich environment, which has now become an active research topic in view of the first results from the James Webb Space Telescope (JWST), see Woitke et al. (2023). Meijerink et al. (2012) and Aresu et al. (2012) presented a grid of X-ray disc models for T Tauri stars and studied the impact of the X-rays on the forbidden far-IR lines of [OI] and [CII], as well as on the [NeII] line at 12.8 μ m, which has been frequently observed with the Spitzer Space Telescope (Spitzer). Neon cannot be ionised by far-UV radiation, so this line is a prime indicator for X-ray driven chemistry in discs. The same code was later used by Meijerink et al. (2013) to discuss the time-chemistry in Active Galactic Nuclei (AGN) discs, making line ratio predictions, such as HCN/HCN⁺ for the Atacama Large Millimeter Array (ALMA).

CO ro-vibronic model molecule: Thi et al. (2013a) collected molecular data for the CO energy levels, radiative transitions, and rates for collisional excitation by H₂, H, He, and e⁻, for the ground $X^1\Sigma^+$ and electronic $A^1\Pi$ state, up to 9 vibrational states each, and up to 50 rotational sub-states, creating a large ro-vibronic CO model molecule. This implementation allows us to discuss the fluorescent pumping by UV light of the $X^1\Sigma^+$ vibrational states, which is an important observational diagnostic of the physical state of the gas around the inner rim and in the upper surface layers of Herbig Ae discs close to the star, which often show rotationally “cool” but vibrationally “hot” line spectra.

Ice evolution: In Helling et al. (2014), we studied the evolution of ices in the midplane of protoplanetary discs. By setting up time-dependent disc models with chemical abundances

from molecular clouds as initial condition, we simulated how ices form in the disc, such as $\text{H}_2\text{O}\#$, $\text{CO}\#$, $\text{CO}_2\#$, $\text{CH}_3\text{OH}\#$, $\text{CH}_4\#$, $\text{N}_2\#$ and $\text{NH}_3\#$. Since the midplane is rather cold, the molecules with stable ice phases can freeze out very quickly (within a few 100 yrs), but then it takes millions of years to convert the remaining gas phase molecules without stable ice phases into those which can freeze out, and this conversion is triggered by cosmic rays to break the bonds of already existing molecules such as O_2 . The gas composition reflects these fast and slow changes, finally leading to a gas that is devoid of oxygen and nitrogen (i.e. carbon-rich) between the water iceline and the CO iceline, and devoid of all elements with stable ice phases (i.e. pure hydrogen and noble gases) beyond the CO iceline. These are the chemical pre-conditions for planet formation.

DIANA basics: Between 2012 and 2016, I have been leading the FP7-SPACE collaboration project “DiscAnalysis” (DIANA), bringing together disc experts from five different European countries. In *Woitke et al. (2016, see Publication 4 on page 56)* we summarised our agreements about the modelling foundations of protoplanetary discs, such as a power-law surface density profile with exponential tapering-off, dust settling, standard dust opacities and treatment of PAHs. With over 230 citations to date, this is my second best cited publication. *Kamp et al. (2017)* is a follow-up publication where we published standard element abundances and the setups of our enlarged chemical networks for the disc modelling, with excited molecular hydrogen, with PAHs in five different charging states and X-ray processes. All neutral gas species (except for H, H_2 and noble gases) can freeze out, and all molecules can be protonated. These rate networks became later known as the “small and large DIANA standard” chemical networks with 100 and 235 chemical species, respectively.

High-Energy Physics: The FP7-DIANA project triggered three important inclusions of high-energy physics into *ProDiMo*. *Rab et al. (2017b)* included Stellar Energetic Particles (SEPs) and compared their impact on T Tauri disc models to the impact of Cosmic Rays (CRs) and radioactive decays. *Rab et al. (2017a)* studied the time-dependent chemistry after episodic accretion events, where the stellar luminosity suddenly increases by a factor of 100, showing that the ices in the inner disc regions all sublime quickly, but it takes tens of thousands of years for the chemistry in the outer disc regions to return to quiescent state, with implications on ALMA line observations. The paper also introduces a way to include an in-falling extended envelope to the disc modelling. Furthermore, *Rab et al. (2018)* included X-ray radiative transfer including Compton scattering to *ProDiMo*, showing that the scattering enhances the X-ray impact on disc ionisation in deeper disc layers. *Brunn et al. (2023)* have used *ProDiMo* to predict the midplane ionisation of inner T Tauri discs affected by magnetic re-connection events, where the magnetic field of the star interacts with the magnetic field of the disc, which produces SEPs that ionise the disc.

IR Molecular Emission Lines: In *Woitke et al. (2018, see Publication 5 on page 57)* we introduced the Fast Line Tracer (FLiTs) developed by Michiel Min, which allows us to calculate thousands of velocity-resolved IR molecular emission lines at a time as post-processing. This tool, which uses the disc structure, dust opacities and molecular abundances calculated by *ProDiMo*, is nowadays key to interpret JWST spectra. In this paper, we showed that the IR molecular emission lines are expected to be emitted from different layers close to the star, from OH (highest) – CO – H_2O – CO_2 – HCN – C_2H_2 (deepest), and discuss the differences between molecular emissions coming from the disc surface and from distant walls behind disc gaps. *Greenwood et al. (2019b)* studied the IR line-emitting

regions of H_2O , OH , CO_2 , HCN and C_2H_2 in T Tauri discs by means of *ProDiMo* models, and reported on the changes of the predicted line spectra with the stellar UV and X-ray luminosities, the disc flaring angle, and dust settling.

Dust Evolution: Greenwood et al. (2019a) coupled *ProDiMo* to the dust evolution model called “two-pop-py” by Birnstiel et al. (2012, 2015). This 1D-model includes dust growth, fragmentation and radial drift by means of a simplified version of Birnstiel et al. (2010), only using two dust size bins. The small grains remain coupled to the gas, whereas the large grains are affected by radial drift and can eventually disappear. As the dust population evolves and diminishes, the continuum optical depths in the disc surface are reduced, which can increase the IR line fluxes of H_2O , OH , CO_2 , HCN and C_2H_2 by up to a factor of 100.

Brown Dwarf Discs: Greenwood et al. (2017) extended *ProDiMo*’s range of applicability to brown dwarf discs, using the Drift-Phoenix brown dwarf synthetic spectra by Witte et al. (2009, 2011), and discussed observable ALMA line ratios such as ^{13}CO 3-2/ HCO^+ 4-3, and their difference to T Tauri stars.

Dust charging, MRI, and Lightning in Discs: Thi et al. (2019) introduced a moment method to include dust grains with arbitrarily large positive or negative charges into *ProDiMo*’s chemical rate network. In the midplane, the dust grains collect most of the free electrons created by cosmic rays, leading to highly negatively charged grains, which has a significant impact on the midplane ionisation. The paper discusses further how the gas ionisation is connected to the dynamical coupling between gas and magnetic field, and how it therefore changes the effective viscosity parameter α of the magneto-rotational instability (MRI), which drives mass accretion and disc evolution. Balduin et al. (2023) have recently expanded this model to include size-dependent charging of dust particles, showing that the grains eventually reach a charge proportional to their size, where $\langle Q \rangle/a$ ranges from a few hundreds of negative charges per micron in the midplane to several thousands of positive charges per micron in the upper irradiated disc layers. The paper also includes a simple model for the electrification of the disc due to turbulent motions of the charged dust grains, concluding however, that this mechanism is too inefficient to create electric fields of the order of the critical electric field for a run-away collisional ionisation (lightning).

Surface Chemistry and Phyllosilicates: Thi et al. (2020a) implemented a state of the art surface chemical rate network in *ProDiMo*, benchmarked against Semenov et al. (2010). This paper, however, concentrates first and foremost on the H_2 and HD formation on warm grain surfaces. Thi et al. (2020b) then expanded the network to discuss the formation and stability of chemisorbed water, and simulated how chemisorbed water might diffuse into the silicate lattice on timescales of millions of years to form phyllosilicates (hydrated silicates), which are stable up to about 700 K. In a related work by D’Angelo et al. (2019), *ProDiMo* models have been used to estimate the content of chemisorbed water present in form of hydrated silicates. They conclude that, only taking into account the first mono-layer on $0.1 \mu\text{m}$ grains, 0.5-10 Earth oceans of chemisorbed water can be present in protoplanetary discs, showing how water might have been delivered to planet Earth.

Miscellaneous Chemical and Physical Processes Meisner et al. (2019) quantified Arrhenius parameters for gas phase reactions that are enhanced by atomic tunnelling at low temperatures. They used *ProDiMo* models to test the impact of their improved rates on disc chemistry and mid-IR water lines. Oberg et al. (2020) have used *ProDiMo* to model the dust radiative transfer in circumplanetary discs, for the conditions expected for the

young Jupiter, using a hierarchical approach, where a model for the circumstellar disc provides the boundary conditions for the circumplanetary disc model. Using the resulting FUV radiation field, photoevaporative mass loss rates from the Jovian circumplanetary disc are computed, causing a truncation outside of the orbit of Callisto. In Oberg et al. (2022) the ice formation and viscous evolution of circumplanetary discs is simulated, and further conclusions are drawn about the formation of Jupiter’s icy moons. The paper also introduced a diffusion solver for the continuum radiative transfer that has become standard for all **ProDiMo** disc models after 2022. Rocha et al. (2023) simulated the UV-irradiation of CH_3OH ice (UV photolysis) under laboratory conditions and compared the theoretical **ProDiMo** results with lab data, considering the time-dependent destruction of the methanol ice, the growth curves of the photolysis products, including branching ratios, and the re-formation of methanol ice, which turns out to be critical for the interpretation of the lab data. Guadarrama et al. (2022) studied the effect of metallicity on molecules in the disc observable with ALMA, in particular CO, HCN, CN, HCO^+ and N_2H^+ with **ProDiMo**.

Arabhavi et al. (2022) included position-dependent ice opacities in **ProDiMo**. Depending on the results of **ProDiMo**’s ice chemistry, the thickness and composition of the ice layers of the grains are calculated, the opacities are interpolated in pre-computed multi-dimensional opacity tables, and these opacities are fed back to the radiative transfer (RT) calculations. This procedure requires iterations between RT and chemistry, but is found to converge after just a few global iterations. The paper discusses the observability of near and mid-IR ice features with JWST. Without mixing (see below), the **ProDiMo** models only show abundant ices deep in the disc (vertical optical extinction $A_{V,\text{ver}} \gtrsim 10$, because of UV-desorption). According to these models, the ices hardly produce any observable spectral features. Woitke et al. (2022): explored the effects of vertical turbulent mixing on the chemical structure of protoplanetary discs. The mixing leads to an additional vertical transport of molecules and icy grains into lower and higher disc layers where these species do not form in-situ. At the locations where they are finally destroyed, for example by photo-processes, the release of reaction products creates a more active chemistry, with a richer mixture of ionised, atomic, molecular, and ice species, and new chemical pathways that are not relevant in the unmixed case. In particular, the paper shows that icy grains can be transported upwards faster than photo-desorption can sublimate the icy mantles, and in this case, already for slow mixing $\alpha = 10^{-4}$, the ices start to produce spectral emission features observable with JWST. Another principle effect is that molecules and atoms, which form in higher, warmer and more illuminated layers, can be transported downward into the midplane, which can be relevant for ALMA observations.

3.2 Analysis of Herschel Observations

Since **ProDiMo** was originally developed to interpret the far-IR gas emission line observations of the Herschel open-time key program GASPS (see review by Dent et al. (2013)), the first applications of **ProDiMo** to actual observational data in the early years (2010-2014) were almost exclusively centred around these data.

Preparations for the Herschel mission: Even before the first Herschel observations were carried out, (Woitke et al., 2010, see Publication 2 on page 54) prepared a large grid (called the DENT grid) of 300000 disc models where 11 stellar, disc and dust parameters were varied systematically, including the total disc mass, several disc shape parameters and the dust-to-gas ratio. In this grid, the Monte Carlo radiative transfer program MCFOST

(Pinte et al., 2009) was used to perform the dust continuum RT, the resulting radiation field and dust temperatures were then passed on to ProDiMo to calculate the gas chemistry and determine the gas temperature structure, and those results were passed back to MCFOST to do the line transfer calculations. For each model, dust continuum and line radiative transfer calculations were carried out to predict 29 far-IR and (sub-)mm lines of [OI], [CII], CO and H₂O under five disc inclination angles.

Early Herschel/GASPS results: The first Herschel/GASPS results about the [OI] 63.18 μm , [OI] 145.53 μm and [CII] 157.74 μm emission lines reported by Mathews et al. (2010) were within the expectations from the DENT grid for the T Tauri stars and HD 169142, see (Pinte et al., 2010), but the non-detections of these lines for the bright Herbig Ae star HD 181327 were puzzling. Later, Lebreton et al. (2012) concluded that HD 181327 is likely an object which has passed the stage of gaseous planet formation already and the observations led to a classification of the disc around HD 181327 to be an icy Kuiper belt. Meeus et al. (2010) presented the first serious attempt to derive the gas and dust masses of the disc around the young Herbig Ae star HD 169142 from the Herschel/GASPS data together with a collection of auxiliary photometric and CO millimetre line data. A ProDiMo model was convincingly fitted to these observations which could explain the SED, fitted all Herschel/GASPS line flux detections and non-detections, and the CO 2-1 and ¹³CO 2-1 lines. The model featured an inner disc, a gap, and a continuous disc between 20 and 200 au with a gas-to-dust ratio of about 20–50. In a similar way, Thi et al. (2010a) presented a ProDiMo disc model for the ~ 10 Myrs old T Tauri star TW Hya using the Herschel/GASPS data together with auxiliary photometric and CO millimetre line data. The paper concluded that the gas-to-dust ratio has decreased to only about 3–25 which is significantly lower than standard interstellar value of 100, suggesting that a significant fraction of the primordial gas has already disappeared. Thi et al. (2011a) reported on the detection of a series of rotational lines of CH⁺ at from $J=5 \rightarrow 4$ at 72.16 μm down to $J=2 \rightarrow 1$ at 179.59 μm by Herschel in HD 100546. They provided a ProDiMo disc model for HD 100546, to fit these and other Herschel and sub-mm CO line fluxes, deriving a gas mass of about $10^{-3} M_{\odot}$, which corresponds to a gas-to-dust ratio of about 8.

Subsequent analysis of observations and models: Based on the DENT grid created for the Herschel/GASPS open-time key program, Kamp et al. (2011) presented a thorough analysis of the correlations found between the predicted line fluxes in the models, and the trends and dependencies of these line fluxes on continuum fluxes and disc parameters. The paper aimed at providing simple diagnostic tools to derive integrated disc properties based on the measured Herschel and sub-mm line fluxes, but a simple formula to derive e.g. the disc mass from these line observations was shown to be difficult. Riviere-Marichalar et al. (2012) presented the results of the Herschel/GASPS program concerning the T Tauri stars in the Taurus-Auriga star formation region. From the 68 objects, 33 were detected in the forbidden [OI] 63.18 μm fine structure line, and 8 T Tauri stars were detected in the o-H₂O emission line close by at 63.32 μm as a by-product. These detection rates are clearly limited by the S/N ratio of the Herschel/PACS observations. ProDiMo models were used to interpret these data in terms of the line excitation temperatures and line emission regions. Additional Herschel observations and fitted disc models have been published for the debris disc 49 Cet (Roberge et al., 2013), the active T Tauri star DG Tau (Podio et al., 2013), the young luminous B9.5 star 51 Ophiuchi (Thi et al., 2013b), the low-mass disc of HD 141569A Thi et al. (2014), and the exceptionally bright source T Tau N with extended

envelope (Podio et al., 2014). Despite the very different nature of these objects, **ProDiMo** models have been shown to be a powerful tool to analyse and interpret the Herschel line observations.

Analysis of larger data samples: In later stages of the Herschel data analysis, more in-depth studies were presented, and larger data samples were considered. For example, Kamp et al. (2013) challenged the **ProDiMo** models to see how the chemical network, the assumed metallicity and the carbon-to-oxygen ratio might need to be modified to improve our understanding of the water line formation in TW Hya, combining the data from several Herschel observational programs. van der Wiel et al. (2014) examined the Herschel SPIRE spectroscopic observations between 240 and 660 μm towards 18 protoplanetary discs, publishing series of high- J emission line fluxes of CO and ^{13}CO from 11–10 down to 4–3, beside additional line fluxes of water, HCN, CH^+ , and [CI]. **ProDiMo** models were used to fit the CO spectral line energy distributions (SLEDs) and to understand which disc regions are possibly populated with warm gas that is required to excite these lines.

Aresu et al. (2014) analysed [OI] 63.2 μm line data obtained with Herschel GASPS and studied the impact of the UV and X-ray luminosities of the central stars on these line fluxes, both observationally and using **ProDiMo** models. According to the models, the gas temperatures above the $\text{H}\rightarrow\text{H}_2$ transition, which is crucial for the [OI] 63.2 μm line emission, should critically depend on the UV and X-ray irradiation by the star, however, the sample of observations does not seem to support this hypothesis. Keane et al. (2014) collected Herschel line and continuum data for 21 transitional discs in Taurus, Chameleon, Lupus and Ophiuchus. They used statistical tests to search for correlations with known stellar properties, such as effective temperature, stellar mass, accretion rate and UV luminosity, and disc properties like the radius of the inner cavity. The DENT grid of **ProDiMo** models was used to extract the expected trends from the disc models. The study remained largely inconclusive.

Antonellini et al. (2015) used **ProDiMo** models to compare the predicted behaviour of the far-IR water lines of T Tauri discs observable with Herschel to those in the mid-IR observable with Spitzer. The paper discussed which stellar, disc and dust parameters are important for the line formation for the two families of water lines. Antonellini et al. (2016) studied a puzzling result obtained with Herschel and Spitzer, namely that water line detection rates for T Tauri stars are remarkably lower than those for the more luminous Herbig Ae/Be stars. The explanation given in the paper is that the brighter stars also produce a brighter IR continuum flux, and the line data reduction techniques actually depend critically on the relative continuum flux noise, so lines with the same flux on a brighter continuum could not be detected. However, this explanation might not entirely explain this clear observational trend.

3.3 Analysis of ALMA Observations

Pinte et al. (2018) published a spectacular paper in which the accurate ALMA channel maps of three CO 2-1 isotopologue lines of the T Tauri star IM Lupi allowed for a direct determination of the geometrical height over the midplane from where the CO is emitting, as well as its emission temperature as function of radius. There are two emitting CO surfaces (see Fig. 16), corresponding to the close disc side and the far disc side that we see through the midplane. These two layers are separated by the icy midplane in which the CO is frozen out, and the upper boundary of the CO emitting layer corresponds to CO

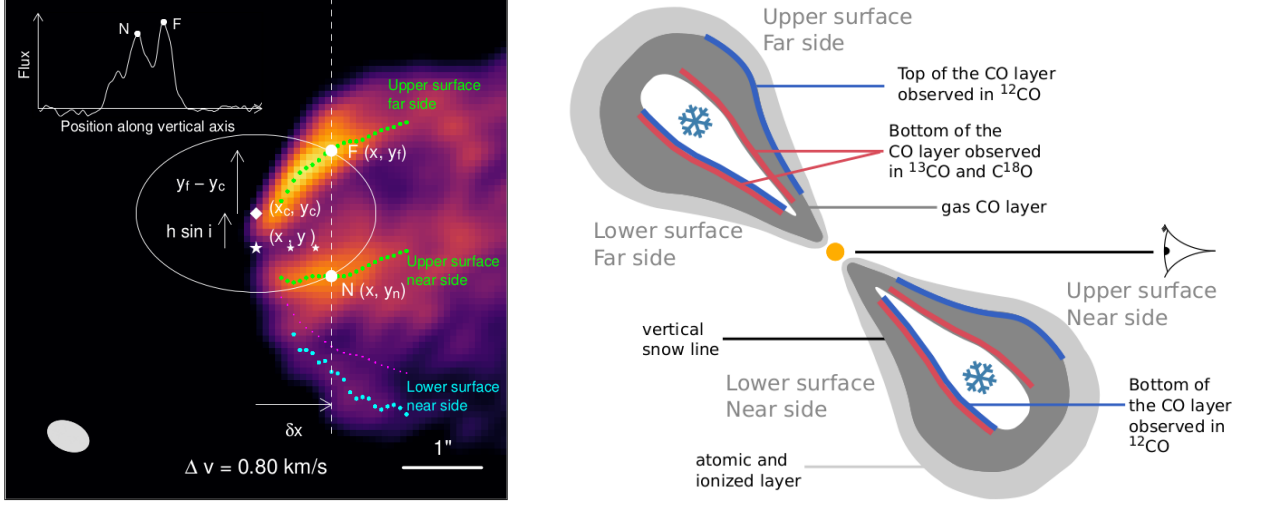


Figure 16: Left: observed channel map of ^{12}CO 2–1 of the T Tauri star IM Lupi. Right: schematic view of the CO emitting surfaces of IM Lupi, re-printed from Pinte et al. (2018).

photo-dissociation. Since the CO-rich layer is optically thick, we only see the surface, which is warm where the CO photo-dissociates, and cold where it freezes out, and the ALMA observations allow us to measure these two temperatures directly from the observations, as function of radius. Many of these observed CO properties are very close to the expectations from ProDiMo models, for example the authors derive $21 \pm 2 \text{ K}$ for the CO freeze-out temperature. In the ProDiMo models we see values between about 20 and 25 K.

Rab et al. (2019) modelled circumstellar discs around the T Tauri stars known to host planet-mass companions (PMCs), which are likely still embedded in the disc and have circumplanetary discs (CPDs) around them. By using hypothetical circumplanetary disc properties, for example a planet mass of 20 Jupiter masses and a PMC luminosity of 0.01 to $0.001 L_{\odot}$, they discussed whether these CPDs might be detectable with VLT/SPHERE and with ALMA in continuum and in CO lines. Rab et al. (2020) presented a detailed study of the rings observed with ALMA in the disc around the Herbig Ae star HD 163296. By analysing the CO line photons coming from the far side of the disc through the dust gaps (which are dark and optically thin in the continuum), the authors were able to derive the gas column densities in the gaps, which are much less deficient than the dust column densities.

3.4 Analysis of Other Observations

Optical and Near-IR spectroscopy: Rab et al. (2022) have used the density structure of 2D XUV photoevaporative disc wind models calculated with the PLUTO hydrodynamics code (Mignone et al., 2007) in ProDiMo. In addition, the complex 3D wind velocity structure was used during the line post-processing to predict o-H_2 $2.12 \mu\text{m}$ and $[\text{OI}]$ 6300\AA line fluxes and asymmetric line profiles. The results are compared to high-resolution observations of the Telescopio Nazionale Galileo (**TNG**) in the GIARPS observing mode for the near-IR, and the high-resolution spectrograph **HARPS-N** for the optical. The results are found to be generally consistent with the observed wind signatures for both the $[\text{OI}]$ 6300\AA and the o-H_2 $2.12 \mu\text{m}$ spectral lines.

L-band and M-band spectroscopy: Fedele et al. (2011) obtained high-resolution ($R \approx 10^5$) L-band spectroscopic data with **VLT/CRIRES** of 11 Herbig AeBe stars, detecting a number of hot water and OH lines. The authors discussed the principal chemical formation and destruction paths of OH and H₂O, and studied the line forming regions on the basis of the predictions from by means **ProDiMo** models. Their conclusion was that there must be some kind of particular depletion of water in Herbig AeBe discs. Hein Bertelsen et al. (2014) obtained VLT/CRIRES observations of CO fundamental ro-vibrational lines from HD 100546. They used **ProDiMo** models with the large ro-vibronic CO model molecule of Thi et al. (2013a) to determine the CO line excitation mechanism, and compare these models to the observations. The authors concluded about the spatial extent of the CO emissions, with the final goal of using the CO ro-vibrational lines as a diagnostic tool to determine the inner disc structure in the context of planet formation. Hein Bertelsen et al. (2016a) observed CO fundamental ro-vibrational emission lines from six Herbig Ae stars with VLT/CRIRES and found different types of line profiles including narrow single-peaked, broad single-peaked and double-peaked. **ProDiMo** models were used to relate these different line profiles to flared and self-shadowed disc geometries, and the presence of large gas holes or gaps. Hein Bertelsen et al. (2016b) observed CO fundamental ro-vibrational emission lines from HD 163296 for different epochs 10 years apart. They found the central line profiles to change from double-peaked to single peaked, whereas the line wings remained similar. Antonellini et al. (2020) used archival VLT/CRIRES observations of fundamental ro-vibrational CO emission lines from 37 T Tauri stars, and compared the behaviour of these lines, in form of line flux ratios and line widths, to the predictions from **ProDiMo** models. They concluded that the complex shapes of the inner disc, in particular disc gaps and inner cavities, need to be considered to understand these observations. Oberg et al. (2023) have studied the possibilities to observe CO fundamental ro-vibrational emission lines with the mid-infrared ELT imager and spectrograph (**METIS**), which provides an exquisite combination of high spectral with high angular resolution. Circumplanetary discs have been identified as very promising targets, as their gas rotation in the circumplanetary disc leaves detectable signals in the background of the gas performing circumstellar motions. These simulations are performed with two **ProDiMo** disc models, one for the circumstellar disc and one for the circumplanetary disc.

Mid-IR spectroscopy: Antonellini et al. (2017) used **ProDiMo** models to analyse the behaviour of three water emission line blends observed by **Spitzer/IRS** around 15.2 μm , 17.2 μm and 29.9 μm . The authors discussed the predicted line emission regions and expected trends with dust and stellar parameters such as spectral type and stellar luminosity. They found a correlation with the amplitude of the 10 μm silicate dust emission feature. Petit dit de la Roche et al. (2021) used the **VLT/VISIR** instrument, and its upgrade VLT/VISIER-NEAR, to observe high-resolution mid-IR images between 8.5 and 11.3 μm . They measured the apparent sizes of the discs at these wavelengths covering several PAH features. The authors used the DIANA standard model of HD 100546 (Woitke et al., 2019) and compared their observations with these model predictions. After slight modifications of the inner radius of the outer disc and the PAH abundance, they obtained a good fit. Ercolano et al. (2022) have studied the potential of the exoplanet missions **TWINKLE** and **ARIEL** to detect PAHs in the atmospheres of discs and exoplanets. Using the PAH opacities from **ProDiMo**, the 3.3 μm feature was identified as the most promising PAH indicator in transmission spectroscopy, possibly related to haze cloud layers. Similar detections might

be possible with **JWST/NEARspec** or, at longer wavelengths, with **JWST/MIRI**. Woitke et al. (2023) have published the first fit of a JWST/MIRI spectrum by a full 2D thermochemical disc model. The JWST observations of the T Tauri star EX Lupi showed emission lines by CO, H₂O, OH, CO₂, HCN, C₂H₂ and H₂. The fitted **ProDiMo** model can roughly reproduce all these lines, and provides the disc structure, all molecular concentrations as function of (r, z) , the gas and dust temperature structures and, in case of CO, H₂O and OH, the non-LTE level populations in a consistent way. According to the fitted model, the inner disc has a slowly ascending surface density profile combined with strong dust settling. The HCN and C₂H₂ molecules form in the close midplane via X-ray chemistry in the oxygen-rich gas. All emission lines observable with JWST originate from a layered molecular structure in the inner disc < 0.7 au.

Sub-mm line Observations: Drabek-Maunder et al. (2016) observed the HCO⁺ 4–3 line at $840.38 \mu\text{m}$ of Lk Ca 15 with the James Clerk Maxwell Telescope (**JCMT**) and showed that the extended wings of this emission line probe the gas inside of the well-known dust rim at the inner cavity at about 50 au. They used **ProDiMo** models to provide a detailed 2-zone fit of the SED and the HCO⁺ line flux and profile, concluding that the gas-to-dust mass ratio in the inner cavity must be as large as 10^6 to 10^7 . White et al. (2019) obtained **APEX** observations of the CO gas in the envelope of the young FUor-type star V883 Ori. They used **ProDiMo** models to test several envelope configurations. They found that an envelope with a mass of $0.2\text{--}0.4 M_{\odot}$ and a mass-infall rate of $\dot{M} = (1 - 2) \times 10^{-6} M_{\odot}/\text{yr}$ fits the observations best, however the outflow structure around V883 Ori is likely caused by multiple outburst events, consistent with episodic accretion.

3.5 Application to Multi- λ observational data sets

Woitke et al. (2011, see Publication 3 on page 55) published a detailed **ProDiMo** disc model for the low-mass T Tauri star ET Cha, fitting a large set of continuum and line observations. The observational data included new optical/near-IR ANDICAM photometric measurements, Herschel/PACS line flux results for 10 far-IR lines (only [OI] $63.2 \mu\text{m}$ was detected), APEX/LABOCA observations for the $870 \mu\text{m}$ continuum and the CO 3–2 line, archival data for the o-H₂ $2.12 \mu\text{m}$ line, and a high-resolution optical spectrum taken with the Anglo-Australian Telescope AAT and University College London coudé Echelle Spectrograph (UCLES) showing blue-shifted emission lines [OI] 6300 \AA , [SII] 6731 \AA , [SII] 6716 \AA and [NII] 6583 \AA . Three archival HST/COS and HST/STIS spectra were used to determine the incident far-UV spectrum of the star. The non-detection of CO 3–2, which is very surprising for this type of objects, was explained in the paper by assuming an extremely small disc with an outer radius of only (6–9) au. This conclusion was later beautifully confirmed by ALMA CO 3–2 observations (Woitke et al., 2013) showing a weak but very broad line from which we were able to confirm a disc outer radius of about 5 au.

Tilling et al. (2012) developed a detailed **ProDiMo** disc model for the bright and very well-known Herbig Ae star HD 163296. They fitted a compilation of photometric fluxes for the SED, a number of UV spectra to determine the UV input spectrum, a near-IR SpeX/IRTF spectrum, a mid-IR Spitzer/IRS spectrum, the measured Herschel fluxes of 13 [OI], [CII], o/p-H₂O and CO lines between 63 and $181 \mu\text{m}$ (all non-detections but [OI] $63.2 \mu\text{m}$), and three (sub-)mm CO and ¹³CO lines. The fit showed the necessity to assume a large disc with exponentially tapering-off surface density profile. Ian Tilling was a former PhD student in Edinburgh (UK) under my supervision.

Carmona et al. (2014) collected continuum and line observations for the transitional Herbig Ae disc of HD 135344B from 14 different instruments, among them HST/COS, VLT/UVES, VLT/CRIRES, VLTI/PIONIER, Subaru/HICIAO, Herschel/PACS, SMA and ALMA. The observational data included the SED, near-IR polarised dust scattered light images, IR visibilities and closure phases, [OI] 6300 Å, CO fundamental ro-vibrational observations including spectro-astrometry signals, 11.2 μm PAH emission, [OI] 63.2 μm , [OI] 145.5 μm , [CII] 157.7 μm , CO 6–5, CO 3–2 and CO 2–1. Using both MCFOST and ProDiMo disc models, the authors fitted the disc geometry including a disc gap, the dust-to-gas ratio and a carbon-enriched inner disc. One of their conclusions was that the CO

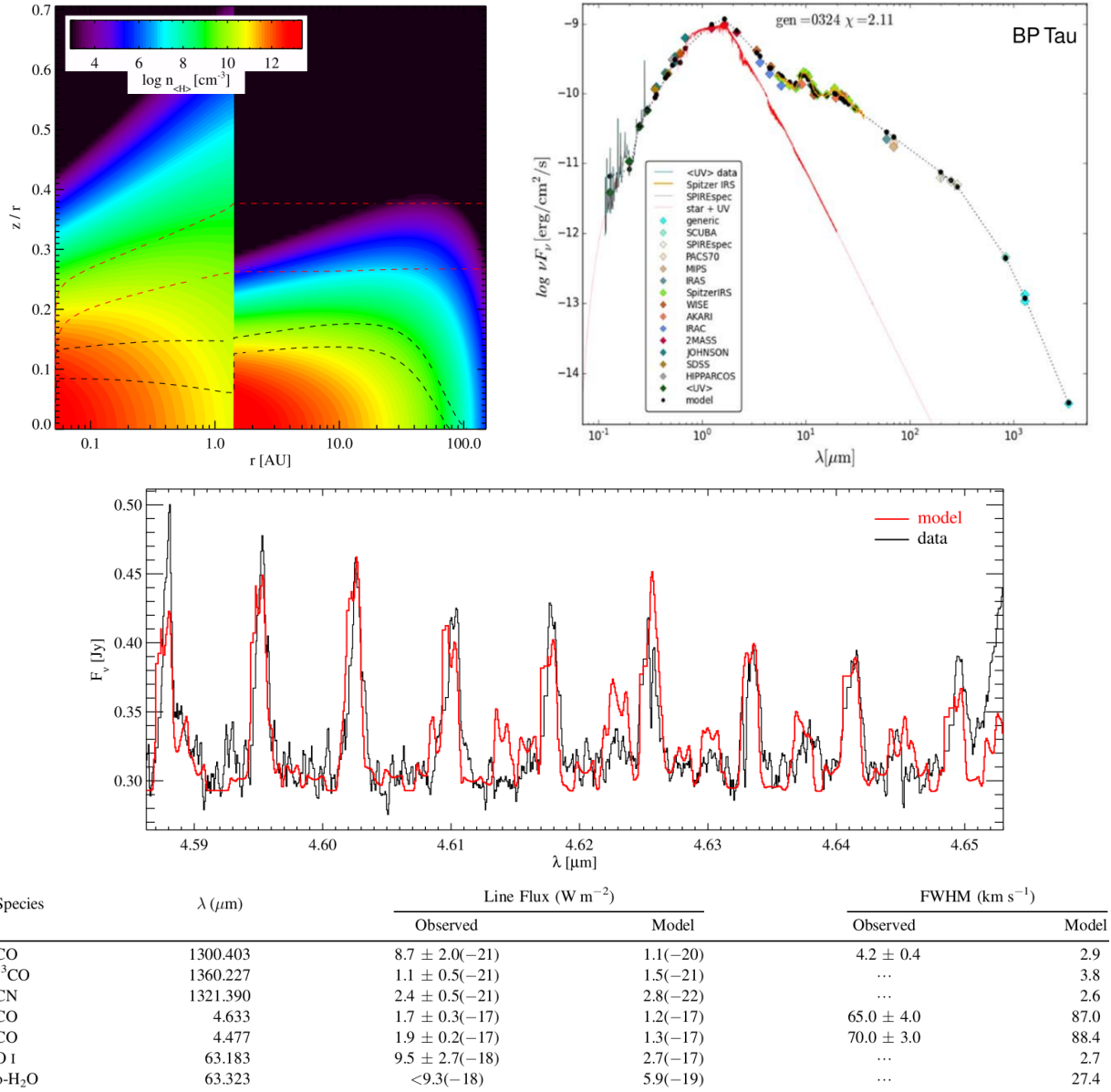


Figure 17: Multi-wavelength fit of various observations of the disc of T Tauri star BP Tau. The upper row of figures shows the assumed disc density structure $n_{\text{H}}(r, z)$ and the computed spectral energy distribution in comparison to multi- λ observations. The central figure shows a small part of the M-band IR spectrum of fundamental ro-vibrational lines of CO with FLiTs-fit, and the lower table shows the fit of other lines and line widths.

fundamental ro-vibrational lines must be partly emitted from the gas in the gap between an inner and an outer dusty disc.

Garufi et al. (2014) used **ProDiMo** models to fit a large multi- λ observational data set for the young low-mass T Tauri star FT Tau that included an optical spectrum from TNG (La Palma Observatory), a J-band spectrum taken with the long-slit Intermediate Resolution Infrared Spectrograph at the WHT (La Palma Observatory), a K-band spectrum taken with NOTCAM (Nordic Optical Telescope CAMera), a high-resolution M-band Keck/NIRSPEC observations with CO fundamental ro-vibrational emission lines, and diverse photometric, Herschel/PACS and Spitzer/IRS observations. The modelling of FT Tau with **ProDiMo** revealed a massive disc ($0.02 M_{\odot}$) with a close inner rim (0.05 au) that is obscured by interstellar dust clouds (optical extinction $A_V = 1.8$).

Woitke et al. (2019, see Publication 6 on page 58) summarised the main modelling results of the FP7 DIANA project. Similar to the papers described above, we collected large multi- λ observational data sets for 27 well-known protoplanetary discs. The data collection included X-ray stellar properties and modelled X-ray input spectra as seen by the disc, low resolution UV-spectra, spectra from various instruments to cover the optical and near-IR wavelengths, high-resolution M-band spectra for the ro-vibrational CO lines, continuum images, interferometric data, emission line fluxes, line velocity profiles and line maps. These observations probe the dust, polycyclic aromatic hydrocarbons (PAHs) and the gas in these objects. A standardised modelling procedure was presented to fit these by our disc modelling codes (**ProDiMo**, **MCFOST**, **MCMAX**), solving the continuum and line radiative transfer, disc chemistry, and the heating and cooling balance for both the gas and the dust. Dionatos et al. (2019, see Publication 7 on page 59) published all collected observations in an open-access database. The aim was to fit all available observations of one object by one single disc model each.

A daunting question initially hanging over the DIANA project was “*does this work?*” The answer was a surprisingly clear yes. In reality, discs are very complicated objects, individual, time-dependent and not strictly axi-symmetric. Yet, by allowing just for two disc zones, an inner and an outer disc, we could find parameter combinations for our models, which predict observations that resemble most of the continuum and line data we could find, simultaneously. One of the resulting fits is shown in Fig. 17. As a result of these efforts, we were able to discuss the average disc geometry of the fitting disc structures, the scale heights, the disc masses, the dust opacities, the dust-to-gas ratios and the PAH properties. For example, the mean viscosity parameter for the dust settling was found to be $\log_{10} \alpha = -2.9 \pm 0.9$, the PAH abundance with respect to interstellar standards $f_{\text{PAH}} = 0.005 - 0.8$, and the mean dust opacity $\kappa_{850 \mu\text{m}}^{\text{abs}} = 6.3^{+3.5}_{-2.3} \text{ cm}^2/\text{g}(\text{dust})$. We found that some discs can be so cold in the distant settled midplane, which contains most of the dust mass, that the dust barely emits at $850 \mu\text{m}$ and 1.3 mm , which causes the standard method to derive disc masses from millimetre fluxes to fail. We found indeed considerably larger gas masses as compared to the values derived from this standard method.

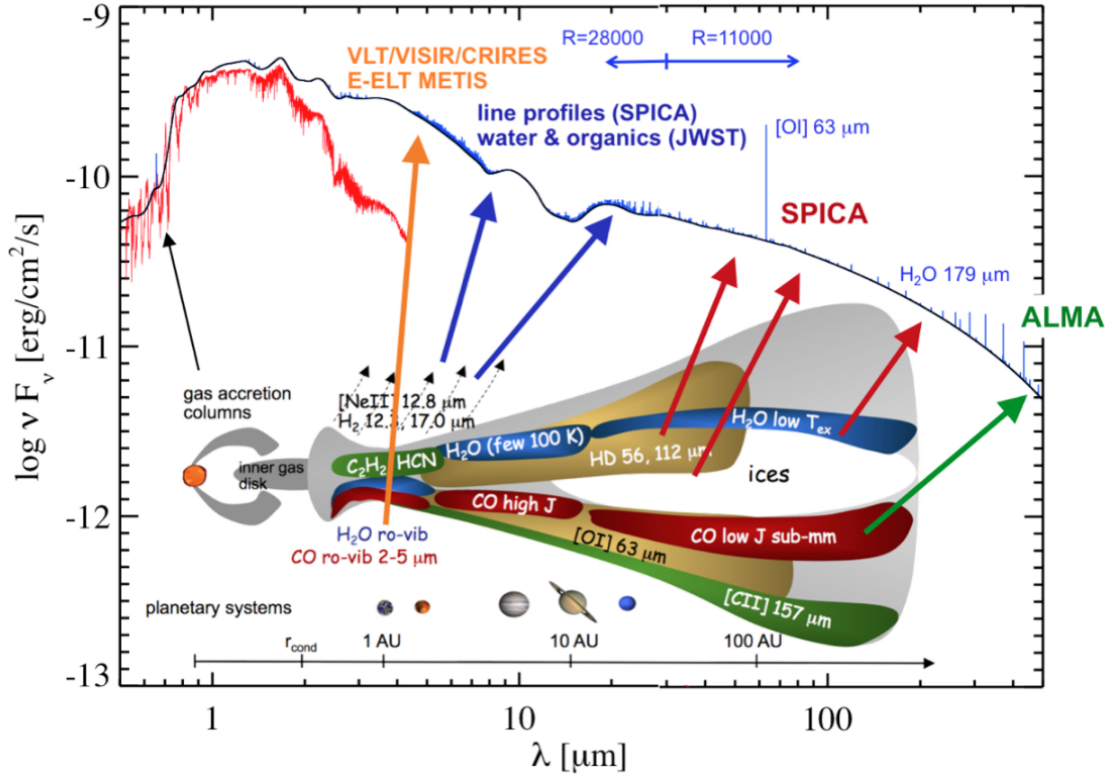


Figure 18: Multi-wavelength observations of protoplanetary discs – which spectral tracers probe which disc locations, disc physics and chemistry? Figure re-printed from Kamp (2020).

4 Outlook

The ProDiMo disc models have been proven to be a very useful tool to analyse and explain various disc observations, from optical emission lines probing disc winds and outflows to continuum observations at different wavelengths, and from mid-IR molecular emission lines probing the inner disc to millimetre line observations and channel maps probing the outer disc. A summary of line emission mechanisms, line emitting disc regions, and corresponding wavelength domains is shown in Fig. 18. The figure includes current observational platforms and instruments, such as ALMA and JWST, as well as future instruments like E-ELT/METIS and SPICA. Unfortunately for disc research, the European Space Agency ESA decided in 2020 to no longer consider the SPace Infrared telescope for Cosmology and Astrophysics (SPICA) as candidate M5 mission. However, hope is not entirely lost, as space missions with similar mid-IR and far-IR instrument capabilities have been proposed, for example LIFE, GREX-PLUS, and SALTUS.

In the near future, the focus of the research of my group will be on ALMA and JWST. **ALMA** observations are the prime choice to probe the outer disc, the chemistry and ice formation, its time-dependence, dust evolution, dust dynamics and the gas energy balance. With the high-spatial and high frequency resolution of ALMA, we can directly (model-free) locate the line emitting regions and emission temperatures of certain molecules from the observations and can compare these data against the predictions from ProDiMo models.

With **JWST**, the ro-vibrational lines of the molecules in the mid-infrared spectral region can be studied, emitted from the upper layers of the inner disc, where these molecules have temperatures between a few hundred to a few thousand Kelvin. These studies have just

begun, but first results (e.g. Woitke et al., 2023) look very promising, because we can interpret and understand the main characteristics of these molecular line emissions (e.g. column densities and emission temperatures) in terms of physically consistent 2D models, in similar ways as astronomers have learnt to interpret stellar spectra to conclude about the element composition of stars in the last century. Among the current hot JWST topics with regard to protoplanetary discs are the shape of the inner disc, transport processes and oxygen depletion, and the dynamic structure of the underlying dust particles. Models are also required here to connect these measurements to the chemical composition of the midplane in the planet-forming disc regions, as these regions cannot be observed directly.

In this current spirit of optimism in the community, however, one should not forget about the idea of a pan-chromatic (i.e. multi-wavelength) modelling approach. Certain observations can only tell us about certain layers of the disc in certain radial domains. Only if we succeed in combining the observational data from different instruments and wavelength regions, a holistic understanding of planet-forming discs can be achieved. Are here, ground-based facilities such as **VLT/CRILES** and **ELT/METIS** can provide additional constraints which probe the dynamics of the gas emitting in the infrared, thereby searching for signatures of planets in the making.

Further future topics of research include our understanding of disc and dust evolution over millions of years, where we need hydrodynamical disc models that can predict the dynamical behaviour of dust and gas, and the instabilities that can occur, which eventually trigger the process of dust growth and planet formation. Here, **ProDiMo** models can be used to predict the spectral appearance of the dust and gas in snapshots of these “patterns of planet formation”, to help interpreting the complex molecular structures that we are bound to see quite soon.

Finally, the formation of refractory materials, phyllosilicates and ices during the early disc evolution is key to understand the current material composition of primitive bodies in the solar system, which can be probed directly by solar system exploration missions. **ProDiMo** disc models can potentially make an impact here as well, in combination with the **GGchem** phase equilibrium models (Woitke et al., 2018). For example, (Steinmeyer et al., 2023) presented a study about the sublimation of refractory minerals during pebble accretion. Once our disc chemistry is equipped with more isotopologues, we will be able to predict the material composition and isotopic ratios of pebbles, comets, and planetesimals at different radii – the building blocks for planet formation, including planet Earth.

References

- Aikawa, Y., Miyama, S. M., Nakano, T., & Umemoto, T. 1996, *ApJ*, 467, 684
 ALMA Partnership, Brogan, C. L., Pérez, L. M., et al. 2015, *ApJL*, 808, L3
 Andrews, S. M., Huang, J., Pérez, L. M., et al. 2018, *ApJL*, 869, L41
 Antonellini, S., Banzatti, A., Kamp, I., Thi, W. F., & Woitke, P. 2020, *A&A*, 637, A29
 Antonellini, S., Bremer, J., Kamp, I., et al. 2017, *A&A*, 597, A72
 Antonellini, S., Kamp, I., Lahuis, F., et al. 2016, *A&A*, 585, A61
 Antonellini, S., Kamp, I., Riviere-Marichalar, P., et al. 2015, *A&A*, 582, A105
 Arabhavi, A. M., Woitke, P., Cazaux, S. M., et al. 2022, *A&A*, 666, A139
 Aresu, G., Kamp, I., Meijerink, R., et al. 2014, *A&A*, 566, A14
 Aresu, G., Kamp, I., Meijerink, R., et al. 2011, *A&A*, 526, A163
 Aresu, G., Meijerink, R., Kamp, I., et al. 2012, *A&A*, 547, A69

- Armitage, P. J. 2010, *Astrophysics of Planet Formation* (Cambridge University Press)
- Auer, L. 1984, in *Numerical Radiative Transfer*, ed. W. Kalkhofen (Cambridge Univ. Press, Cambridge), 101
- Avenhaus, H., Quanz, S. P., Garufi, A., et al. 2018, *ApJ*, 863, 44
- Balduin, T., Woitke, P., Thi, W.-F., Gråe Jørgensen, U., & Narita, Y. 2023, arXiv e-prints, arXiv:2308.04335
- Beckwith, S. V. W., Sargent, A. I., Chini, R. S., & Guesten, R. 1990, *AJ*, 99, 924
- Birnstiel, T., Andrews, S. M., Pinilla, P., & Kama, M. 2015, *ApJL*, 813, L14
- Birnstiel, T., Dullemond, C. P., & Brauer, F. 2010, *A&A*, 513, A79
- Birnstiel, T., Klahr, H., & Ercolano, B. 2012, *A&A*, 539, A148
- Black, J. H. & Dalgarno, A. 1976, *ApJ*, 203, 132
- Bruderer, S., van der Marel, N., van Dishoeck, E. F., & van Kempen, T. A. 2014, *A&A*, 562, A26
- Bruggeman, D. A. G. 1935, *Annalen der Physik*, 416, 636
- Brunn, V., Marcowith, A., Sauty, C., et al. 2023, *MNRAS*, 519, 5673
- Burke, J. R. & Hollenbach, D. J. 1983, *ApJ*, 265, 223
- Carmona, A., Pinte, C., Thi, W. F., et al. 2014, *A&A*, 567, A51
- Cazaux, S. & Spaans, M. 2009, *A&A*, 496, 365
- Cazaux, S. & Tielens, A. G. G. M. 2002, *ApJL*, 575, L29
- Cazaux, S. & Tielens, A. G. G. M. 2004, *ApJ*, 604, 222
- Cazaux, S. & Tielens, A. G. G. M. 2010, *ApJ*, 715, 698
- Chevance, M., Krumholz, M. R., McLeod, A. F., et al. 2023, in *Astronomical Society of the Pacific Conference Series*, Vol. 534, *Protostars and Planets VII*, ed. S. Inutsuka, Y. Aikawa, T. Muto, K. Tomida, & M. Tamura, 1
- D’Alessio, P., Canto, J., Calvet, N., & Lizano, S. 1998, *ApJ*, 500, 411
- Dalgarno, A., Yan, M., & Liu, W. 1999, *ApJS*, 125, 237
- D’Angelo, M., Cazaux, S., Kamp, I., Thi, W. F., & Woitke, P. 2019, *A&A*, 622, A208
- Dent, W. R. F., Thi, W. F., Kamp, I., et al. 2013, *PASP*, 125, 477
- Dionatos, O., Woitke, P., Güdel, M., et al. 2019, *A&A*, 625, A66
- Dominik, C. 2015, in *European Physical Journal Web of Conferences*, Vol. 102, *European Physical Journal Web of Conferences*, 00004
- Drabek-Maunder, E., Mohanty, S., Greaves, J., et al. 2016, *ApJ*, 833, 260
- Draine, B. T. & Li, A. 2007, *ApJ*, 657, 810
- Drazkowska, J., Lichtenberg, T., Schönbächler, M., Golabek, G., & Hands, T. 2022, in *European Astronomical Society Annual Meeting*, Valencia Conference Centre, June 27 – July 1, 2022
- Du, F. & Bergin, E. A. 2014, *ApJ*, 792, 2
- Dubrulle, B., Morfill, G., & Sterzik, M. 1995, *ICARUS*, 114, 237
- Duley, W. W. & Williams, D. A. 1986, *MNRAS*, 223, 177
- Ercolano, B., Barlow, M. J., & Storey, P. J. 2005, *MNRAS*, 362, 1038
- Ercolano, B., Drake, J. J., Raymond, J. C., & Clarke, C. C. 2008, *ApJ*, 688, 398
- Ercolano, B., Rab, C., Molaverdikhani, K., et al. 2022, *MNRAS*, 512, 430
- Fedele, D., Pascucci, I., Brittain, S., et al. 2011, *ApJ*, 732, 106
- Gangi, M., Nisini, B., Antonucci, S., et al. 2020, *A&A*, 643, A32
- Garufi, A., Podio, L., Kamp, I., et al. 2014, *A&A*, 567, A141
- Geers, V. C., Augereau, J.-C., Pontoppidan, K. M., et al. 2006, *A&A*, 459, 545
- Glassgold, A. E. & Najita, J. R. 2015, *The Astrophysical Journal*, 810, 125
- Gorti, U. & Hollenbach, D. 2009, *ApJ*, 690, 1539
- Greenwood, A. J., Kamp, I., Waters, L. B. F. M., Woitke, P., & Thi, W. F. 2019a, *A&A*, 626, A6
- Greenwood, A. J., Kamp, I., Waters, L. B. F. M., Woitke, P., & Thi, W. F. 2019b, *A&A*, 631, A81
- Greenwood, A. J., Kamp, I., Waters, L. B. F. M., et al. 2017, *A&A*, 601, A44

- Guadarrama, R., Vorobyov, E. I., Rab, C., & Güdel, M. 2022, *A&A*, 667, A28
- Hartmann, L., Calvet, N., Gullbring, E., & D'Alessio, P. 1998, *ApJ*, 495, 385
- Hein Bertelsen, R. P., Kamp, I., Goto, M., et al. 2014, *A&A*, 561, A102
- Hein Bertelsen, R. P., Kamp, I., van der Plas, G., et al. 2016a, *A&A*, 590, A98
- Hein Bertelsen, R. P., Kamp, I., van der Plas, G., et al. 2016b, *MNRAS*, 458, 1466
- Helling, C., Woitke, P., Rimmer, P. B., et al. 2014, *Life*, 4, 142
- Hogerheijde, M. R. & van der Tak, F. F. S. 2000, *A&A*, 362, 697
- Isella, A., Huang, J., Andrews, S. M., et al. 2018, *ApJL*, 869, L49
- Jonkheid, B., Faas, F. G. A., van Zadelhoff, G.-J., & van Dishoeck, E. F. 2004, *A&A*, 428, 511
- Kamp, I. 2020, in *Origins: From the Protosun to the First Steps of Life*, ed. B. G. Elmegreen, L. V. Tóth, & M. Güdel, Vol. 345, 115–123
- Kamp, I. & Bertoldi, F. 2000, *A&A*, 353, 276
- Kamp, I., Thi, W. F., Meeus, G., et al. 2013, *A&A*, 559, A24
- Kamp, I., Thi, W. F., Woitke, P., et al. 2017, *A&A*, 607, A41
- Kamp, I., Tilling, I., Woitke, P., Thi, W. F., & Hogerheijde, M. 2010, *A&A*, 510, A18
- Kamp, I. & van Zadelhoff, G.-J. 2001, *A&A*, 373, 641
- Kamp, I., Woitke, P., Pinte, C., et al. 2011, *A&A*, 532, A85
- Keane, J. T., Pascucci, I., Espaillat, C., et al. 2014, *ApJ*, 787, 153
- Kenyon, S. J. & Hartmann, L. 1995, *ApJS*, 101, 117
- Kóspál, Á., Ábrahám, P., Diehl, L., et al. 2023, *ApJL*, 945, L7
- Lada, C. J. & Wilking, B. A. 1984, *ApJ*, 287, 610
- Lebreton, J., Augereau, J. C., Thi, W. F., et al. 2012, *A&A*, 539, A17
- Li, A. & Draine, B. T. 2001, *ApJ*, 554, 778
- Lynden-Bell, D. & Pringle, J. E. 1974, *MNRAS*, 168, 603
- Maaskant, K. M., Min, M., Waters, L. B. F. M., & Tielens, A. G. G. M. 2014, *A&A*, 563, A78
- Mathews, G. S., Dent, W. R. F., Williams, J. P., et al. 2010, *A&A*, 518, L127
- Mathis, J. S., Rumpl, W., & Nordsieck, K. H. 1977, *ApJ*, 217, 425
- McElroy, D., Walsh, C., Markwick, A. J., et al. 2013, *A&A*, 550, A36
- Meeus, G., Pinte, C., Woitke, P., et al. 2010, *A&A*, 518, L124
- Meijerink, R., Aresu, G., Kamp, I., et al. 2012, *A&A*, 547, A68
- Meijerink, R. & Spaans, M. 2005, *A&A*, 436, 397
- Meijerink, R., Spaans, M., Kamp, I., et al. 2013, *Journal of Physical Chemistry A*, 117, 9593
- Meisner, J., Kamp, I., Thi, W. F., & Kästner, J. 2019, *A&A*, 627, A45
- Mignone, A., Bodo, G., Massaglia, S., et al. 2007, *ApJS*, 170, 228
- Min, M., Dullemond, C. P., Dominik, C., de Koter, A., & Hovenier, J. W. 2009, *A&A*, 497, 155
- Min, M., Dullemond, C. P., Kama, M., & Dominik, C. 2011, *ICARUS*, 212, 416
- Min, M., Rab, C., Woitke, P., Dominik, C., & Ménard, F. 2016, *A&A*, 585, A13
- Miotello, A., Kamp, I., Birnstiel, T., Cleeves, L. I., & Kataoka, A. 2022, *PPVII*, Chapter 14, arXiv e-prints, arXiv:2203.09818
- Morbidelli, A., Baillié, K., Batygin, K., et al. 2022, *Nature Astronomy*, 6, 72
- Oberg, N., Kamp, I., Cazaux, S., & Rab, C. 2020, *A&A*, 638, A135
- Oberg, N., Kamp, I., Cazaux, S., Rab, C., & Czoske, O. 2023, *A&A*, 670, A74
- Oberg, N., Kamp, I., Cazaux, S., Woitke, P., & Thi, W. F. 2022, *A&A*, 667, A95
- O'Dell, C. R. & Wong, K. 1996, *AJ*, 111, 846
- Pascucci, I., Wolf, S., Steinacker, J., et al. 2004, *A&A*, 417, 793
- Petit dit de la Roche, D. J. M., Oberg, N., van den Ancker, M. E., et al. 2021, *A&A*, 648, A92
- Pineda, J. E., Arzoumanian, D., Andre, P., et al. 2023, in *Astronomical Society of the Pacific Conference Series*, Vol. 534, *Protostars and Planets VII*, ed. S. Inutsuka, Y. Aikawa, T. Muto, K. Tomida, & M. Tamura, 233
- Pinte, C., Harries, T. J., Min, M., et al. 2009, *A&A*, 498, 967

- Pinte, C., Ménard, F., Duchêne, G., & Bastien, P. 2006, *A&A*, 459, 797
- Pinte, C., Ménard, F., Duchêne, G., et al. 2018, *A&A*, 609, A47
- Pinte, C., Woitke, P., Ménard, F., et al. 2010, *A&A*, 518, L126
- Podio, L., Kamp, I., Codella, C., et al. 2013, *ApJL*, 766, L5
- Podio, L., Kamp, I., Codella, C., et al. 2014, *ApJL*, 783, L26
- Rab, C., Elbakyan, V., Vorobyov, E., et al. 2017a, *A&A*, 604, A15
- Rab, C., Güdel, M., Padovani, M., et al. 2017b, *A&A*, 603, A96
- Rab, C., Güdel, M., Woitke, P., et al. 2018, *A&A*, 609, A91
- Rab, C., Kamp, I., Dominik, C., et al. 2020, *A&A*, 642, A165
- Rab, C., Kamp, I., Ginski, C., et al. 2019, *A&A*, 624, A16
- Rab, C., Weber, M., Grassi, T., et al. 2022, arXiv e-prints, arXiv:2210.15486
- Riols, A. & Lesur, G. 2018, *A&A*, 617, A117
- Riviere-Marichalar, P., Ménard, F., Thi, W. F., et al. 2012, *A&A*, 538, L3
- Roberge, A., Kamp, I., Montesinos, B., et al. 2013, *ApJ*, 771, 69
- Rocha, W. R. M., Woitke, P., Pilling, S., et al. 2023, *A&A*, 673, A70
- Röllig, M., Abel, N. P., Bell, T., et al. 2007, *A&A*, 467, 187
- Semenov, D., Hersant, F., Wakelam, V., et al. 2010, *A&A*, 522, A42
- Siess, L., Dufour, E., & Forestini, M. 2000, *A&A*, 358, 593
- Steinmeyer, M.-L., Woitke, P., & Johansen, A. 2023, arXiv e-prints, arXiv:2308.05647
- Thi, W. F., Hocuk, S., Kamp, I., et al. 2020a, *A&A*, 634, A42
- Thi, W. F., Hocuk, S., Kamp, I., et al. 2020b, *A&A*, 635, A16
- Thi, W. F., Kamp, I., Woitke, P., et al. 2013a, *A&A*, 551, A49
- Thi, W. F., Lesur, G., Woitke, P., et al. 2019, *A&A*, 632, A44
- Thi, W. F., Mathews, G., Ménard, F., et al. 2010a, *A&A*, 518, L125
- Thi, W. F., Ménard, F., Meeus, G., et al. 2013b, *A&A*, 557, A111
- Thi, W. F., Ménard, F., Meeus, G., et al. 2011a, *A&A*, 530, L2
- Thi, W. F., Pinte, C., Pantin, E., et al. 2014, *A&A*, 561, A50
- Thi, W. F., Woitke, P., & Kamp, I. 2010b, *MNRAS*, 407, 232
- Thi, W. F., Woitke, P., & Kamp, I. 2011b, *MNRAS*, 412, 711
- Tielens, A. G. G. M. 2008, *ARA&A*, 46, 289
- Tielens, A. G. G. M. & Hollenbach, D. 1985, *ApJ*, 291, 747
- Tilling, I., Woitke, P., Meeus, G., et al. 2012, *A&A*, 538, A20
- Vacca, W. D. & Sandell, G. 2011, *ApJ*, 732, 8
- van der Wiel, M. H. D., Naylor, D. A., Kamp, I., et al. 2014, *MNRAS*, 444, 3911
- Visser, R., Geers, V. C., Dullemond, C. P., et al. 2007, *A&A*, 466, 229
- Visser, R., van Dishoeck, E. F., & Black, J. H. 2009, *A&A*, 503, 323
- Vorobyov, E. I., Khaibrakhmanov, S., Basu, S., & Audard, M. 2020, *A&A*, 644, A74
- Wakelam, V., Herbst, E., Loison, J.-C., et al. 2012, *ApJS*, 199, 21
- Wakelam, V., Smith, I. W. M., Loison, J. C., et al. 2013, arXiv e-prints, arXiv:1310.4350
- Weingartner, J. C. & Draine, B. T. 2001, *ApJS*, 134, 263
- White, J. A., Kóspál, Á., Rab, C., et al. 2019, *ApJ*, 877, 21
- Williams, J. P. & Cieza, L. A. 2011, *ARA&A*, 49, 67
- Witte, S., Helling, C., Barman, T., Heidrich, N., & Hauschildt, P. H. 2011, *A&A*, 529, A44
- Witte, S., Helling, C., & Hauschildt, P. H. 2009, *A&A*, 506, 1367
- Woitke, P. 2015, in *European Physical Journal Web of Conferences*, Vol. 102, European Physical Journal Web of Conferences, 00011
- Woitke, P., Arabhavi, A. M., Kamp, I., & Thi, W. F. 2022, *A&A*, 668, A164
- Woitke, P., Dent, W. R. F., Thi, W.-F., et al. 2013, in *Protostars and Planets VI Posters*, 13
- Woitke, P., Kamp, I., Antonellini, S., et al. 2019, *PASP*, 131, 064301
- Woitke, P., Kamp, I., & Thi, W. F. 2009a, *A&A*, 501, 383

- Woitke, P., Min, M., Pinte, C., et al. 2016, *A&A*, 586, A103
- Woitke, P., Min, M., Thi, W. F., et al. 2018, *A&A*, 618, A57
- Woitke, P., Pinte, C., Tilling, I., et al. 2010, *MNRAS*, 405, L26
- Woitke, P., Riaz, B., Duchêne, G., et al. 2011, *A&A*, 534, A44
- Woitke, P., Thi, W.-F., Arabhavi, A. M., et al. 2023, submitted to *A&A*, –
- Woitke, P., Thi, W. F., Kamp, I., & Hogerheijde, M. R. 2009b, *A&A*, 501, L5
- Wolfire, M. G., Vallini, L., & Chevance, M. 2022, *ARA&A*, 60, 247
- Woodall, J., Agúndez, M., Markwick-Kemper, A. J., & Millar, T. J. 2007, *A&A*, 466, 1197
- Woods, P. M. & Willacy, K. 2009, *ApJ*, 693, 1360
- Yorke, H. W., Bodenheimer, P., & Laughlin, G. 1993, *ApJ*, 411, 274
- Zucker, C., Alves, J., Goodman, A., Meingast, S., & Galli, P. 2023, in *Astronomical Society of the Pacific Conference Series*, Vol. 534, *Protostars and Planets VII*, ed. S. Inutsuka, Y. Aikawa, T. Muto, K. Tomida, & M. Tamura, 43

Publication 1:

Radiation thermo-chemical models of protoplanetary disks – I. Hydrostatic disk structure and inner rim

Woitke, P.; Kamp, I.; Thi, W.-F.

Astronomy & Astrophysics, 2009, Volume 501, Issue 1, 2009, pp. 383–406

Abstract: Emission lines from protoplanetary disks originate mainly in the irradiated surface layers, where the gas is generally warmer than the dust. Therefore, interpreting emission lines requires detailed thermo-chemical models, which are essential to converting line observations into understanding disk physics. We aim at hydrostatic disk models that are valid from 0.1 AU to 1000 AU to interpret gas emission lines from UV to sub-mm. In particular, our interest lies in interpreting far IR gas emission lines, such as will be observed by the Herschel observatory, related to the GASPS open time key program. This paper introduces a new disk code called ProDiMo. We combine frequency-dependent 2D dust continuum radiative transfer, kinetic gas-phase and UV photo-chemistry, ice formation, and detailed non-LTE heating & cooling with the consistent calculation of the hydrostatic disk structure. We include FeII and CO ro-vibrational line heating/cooling relevant to the high-density gas close to the star, and apply a modified escape-probability treatment. The models are characterised by a high degree of consistency between the various physical, chemical, and radiative processes, where the mutual feedbacks are solved iteratively. In application to a T Tauri disk extending from 0.5 AU to 500 AU, the models show that the dense, shielded and cold midplane ($z/r \lesssim 0.1$, $T_g \approx T_d$) is surrounded by a layer of hot ($T_g \approx 5000$ K) and thin ($n_{\text{H}} \approx 10^7$ to 10^8 cm^{-3}) atomic gas that extends radially to about 10 AU and vertically up to $z/r \approx 0.5$. This layer is predominantly heated by the stellar UV (e.g. PAH-heating) and cools via FeII semi-forbidden and O I 630 nm optical line emission. The dust grains in this “halo” scatter the starlight back onto the disk, which affects the photochemistry. The more distant regions are characterised by a cooler flaring structure. Beyond $r \gtrsim 100$ AU, T_g decouples from T_d even in the midplane and reaches values of about $T_g \approx 2 T_d$. Our models show that the gas energy balance is the key to understanding the vertical disk structure. Models calculated with the assumption $T_g = T_d$ show a much flatter disk structure. The conditions in the close regions (< 10 AU) with densities $n_{\text{H}} \approx 10^8$ to 10^{15} cm^{-3} resemble those of cool stellar atmospheres and, thus, the heating and cooling is more like in stellar atmospheres. The application of heating and cooling rates known from PDR and interstellar cloud research alone can be misleading here, so more work needs to be invested to identify the leading heating and cooling processes.

Own contribution: This paper established ProDiMo as a new modelling code for protoplanetary discs and is my best cited paper until the present day (317 citations on November 2023). It required more than 2 years of programming work from scratch done by myself as a post-doc at the ATC in Edinburgh, UK. The overall disc modelling approach was based on Inga Kamp’s COSTAR-program, but was considerably enhanced and generalised by us in the code re-writing process. Some important non-LTE atomic and molecular, and other physical and chemical data was contributed by Wing-Fai Thi, including some related code parts. All paper text was written by me, and all figures were created by myself.

Link: <https://ui.adsabs.harvard.edu/abs/2009A%26A...501..383W>

Publication 2:

Continuum and line modelling of discs around young stars – 300000 disc models for HERSCHEL/GASPS

Woitke, P.; Pinte, C.; Tilling, I.; Ménard, F.; Kamp, I.; Thi, W.-F.; Duchêne, G.; Augereau, J.-C.

Monthly Notices of the Royal Astronomical Society, 2010, Letters, Vol. 405, Issue 1, pp. L26–L30

Abstract: We have combined the thermo-chemical disc code ProDiMo with the Monte Carlo radiative transfer code MCFOST to calculate a grid of ~ 300000 circumstellar disc models, systematically varying 11 stellar, disc and dust parameters including the total disc mass, several disc shape parameters and the dust-to-gas ratio. For each model, dust continuum and line radiative transfer calculations are carried out for 29 far-infrared, sub-mm and mm lines of [OI], [CII], ^{12}CO and o/p- H_2O under five inclinations. The grid allows us to study the influence of the input parameters on the observables, to make statistical predictions for different types of circumstellar discs and to find systematic trends and correlations between the parameters, the continuum fluxes and the line fluxes. The model grid, comprising the calculated disc temperature and chemical structures, the computed spectral energy distributions, line fluxes and profiles, will be used in particular for the data interpretation of the HERSCHEL open time-key program GASPS. The calculated line fluxes show a strong dependence on the assumed ultraviolet excess of the central star and on the disc flaring. The fraction of models predicting [OI] and [CII] fine-structure lines fluxes above HERSCHEL/PACS and SPICA/SAFARI detection limits is calculated as a function of disc mass. The possibility of deriving the disc gas mass from line observations is discussed.

Own contribution: This paper marked the starting point of a long-lasting, fruitful collaboration with disc researchers from the Laboratoire d'Astrophysique de Grenoble (later called IPAG), in particular Christophe Pinte and Francois Ménard. For the production of 300000 disc models, it was necessary to use the fast MCFOST Monte Carlo radiative transfer code, developed by C. Pinte, to calculate the dust temperature structure and UV radiation field and to pass these results to our thermo-chemical disc code. C. Pinte modified MCFOST accordingly, and I modified PRODIMO to skip the radiative transfer parts and use the MCFOST results instead. A lot of code testing and double-checking was done by myself. My former PhD student I. Tilling helped to create an idl-tool to visualise the grid results, but most of that work I actually did myself, too. The other co-authors mostly had advisory functions. All paper text was written by myself and all figures and tables were created by myself. The modelling grid was later used in subsequent papers, in particular by Kamp et al. (2011). This grid of thermo-chemical models is still available to the community via the IWF webpage.

Link: <https://ui.adsabs.harvard.edu/abs/2010MNRAS.405L..26W>

Publication 3:

The unusual protoplanetary disk around the T Tauri star ET Chamaeleontis

Woitke, P.; Riaz, B.; Duchêne, G.; Pascucci, I.; Lyo, A.-R.; Dent, W.R.F.; Phillips, N.; Thi, W.-F.; Ménard, F.; Herczeg, G.J.; Bergin, E.; Brown, A.; Mora, A.; Kamp, I.; Aresu, G.; Brittain, S.; de Gregorio-Monsalvo, I.; Sandell

Astronomy & Astrophysics, 2011, Volume 534, id. A44, 27, pp. 1-27

Abstract: We present new continuum and line observations, along with modelling, of the faint (6-8) Myr old T Tauri star ET Cha belonging to the η Chamaeleontis cluster. We have acquired Herschel/PACS photometric fluxes at 70 μm and 160 μm , as well as a detection of the [OI] 63 μm fine-structure line in emission, and derived upper limits for some other far-IR OI, CII, CO and o-H₂O lines. These observations were carried out in the frame of the open time key programme GASPS, where ET Cha was selected as one of the science demonstration phase targets. The Herschel data is complemented by new simultaneous ANDICAM B-K photometry, new HST/COS and HST/STIS UV-observations, a non-detection of CO $J=3 \rightarrow 2$ with APEX, re-analysis of a UCLES high-resolution optical spectrum showing forbidden emission lines like [OI] 6300 Å, [SII] 6731 Å and 6716 Å, and [NII] 6583 Å, and a compilation of existing broad-band photometric data. We used the thermo-chemical disk code ProDiMo and the Monte-Carlo radiative transfer code MCFOST to model the protoplanetary disk around ET Cha. The paper also introduces a number of physical improvements to the ProDiMo disk modelling code concerning the treatment of PAH ionisation balance and heating, the heating by exothermic chemical reactions, and several non-thermal pumping mechanisms for selected gas emission lines. By applying an evolutionary strategy to minimise the deviations between model predictions and observations, we find a variety of united gas and dust models that simultaneously fit all observed line and continuum fluxes about equally well. Based on these models we can determine the disk dust mass with confidence, $M_{\text{dust}} \approx (2 - 5) \times 10^{-8} M_{\odot}$ whereas the total disk gas mass is found to be only little constrained, $M_{\text{gas}} \approx (5 \times 10^{-5} - 3 \times 10^{-3}) M_{\odot}$. Both mass estimates are substantially lower than previously reported. In the models, the disk extends from 0.022 AU (just outside of the co-rotation radius) to only about 10 AU, remarkably small for single stars, whereas larger disks are found to be inconsistent with the CO $J=3 \rightarrow 2$ non-detection. The low velocity component of the [OI] 6300 Å emission line is centred on the stellar systematic velocity, and is consistent with being emitted from the inner disk. The model is also consistent with the line flux of H₂ $v=1 \rightarrow 0$ S(1) at 2.122 μm and with the [OI] 63 μm line as seen with Herschel/PACS. An additional high-velocity component of the [OI] 6300 Å emission line, however, points to the existence of an additional jet/outflow of low velocity 40-65 km/s with mass loss rate $\approx 10^{-9} M_{\odot}/\text{yr}$. In relation to our low estimations of the disk mass, such a mass loss rate suggests a disk lifetime of only $\sim 0.05 - 3$ Myr, substantially shorter than the cluster age. If a generic gas/dust ratio of 100 was assumed, the disk lifetime would be even shorter, only ~ 3000 yrs. The evolutionary state of this unusual protoplanetary disk is discussed.

Own contribution: I was leading this paper on one of the GASPS targets. The long author list is because (a) the GASPS data were reduced by a number of team members, (b) Riaz, Duchêne and Pascucci provided auxiliary observational data and (c) because of the GASPS consortium publication rules (PI Dent). Except for the sections detailing these observations and data reductions (sections 3.1, 3.2, 3.3, 3.5, 3.6) I wrote all the paper text and created all figures. I did most of the basic code development on ProDiMo, with some contributions from Wing-Fai Thi. The paper enabled us to successfully propose cycle 0 ALMA observational time, which confirmed that the disk of ET Chamaeleontis has indeed an outer radius of only about 5 AU (Woitke et al., 2013).

Link: <https://ui.adsabs.harvard.edu/abs/2011A%26A...534A...44W>

Publication 4:

Consistent dust and gas models for protoplanetary disks. I. Disk shape, dust settling, opacities, and PAHs

Woitke, P.; Min, M.; Pinte, C.; Thi, W.-F.; Kamp, I.; Rab, C.; Anthonioz, F.; Antonellini, S.; Baldovin-Saavedra, C.; Carmona, A.; Dominik, C.; Dionatos, O.; Greaves, J.; Güdel, M.; Ilee, J.D.; Liebhart, A.; Ménard, F.; Rigon, L.; Waters, L.B.F.M.; Aresu, G.; Meijerink, R.; Spaans, M.

Astronomy & Astrophysics, 2016, Volume 586, id. A103, pp. 1–35

Abstract: We propose a set of standard assumptions for the modelling of Class II and III protoplanetary disks, which includes detailed continuum radiative transfer, thermo-chemical modelling of gas and ice, and line radiative transfer from optical to cm wavelengths. The first paper of this series focuses on the assumptions about the shape of the disk, the dust opacities, dust settling, and polycyclic aromatic hydrocarbons (PAHs). In particular, we propose new standard dust opacities for disk models, we present a simplified treatment of PAHs in radiative equilibrium which is sufficient to reproduce the PAH emission features, and we suggest using a simple yet physically justified treatment of dust settling. We roughly adjust parameters to obtain a model that predicts continuum and line observations that resemble typical multi-wavelength continuum and line observations of Class II T Tauri stars. We systematically study the impact of each model parameter (disk mass, disk extension and shape, dust settling, dust size and opacity, gas/dust ratio, etc.) on all mainstream continuum and line observables, in particular on the SED, mm-slope, continuum visibilities, and emission lines including [OI] 63 μm , high-J CO lines, (sub-)mm CO isotopologue lines, and CO fundamental ro-vibrational lines. We find that evolved dust properties, i.e. large grains, often needed to fit the SED, have important consequences for disk chemistry and heating/cooling balance, leading to stronger near- to far-IR emission lines in general. Strong dust settling and missing disk flaring have similar effects on continuum observations, but opposite effects on far-IR gas emission lines. PAH molecules can efficiently shield the gas from stellar UV radiation because of their strong absorption and negligible scattering opacities in comparison to evolved dust. The observable millimetre-slope of the SED can become significantly more gentle in the case of cold disk midplanes, which we find regularly in our T Tauri models. We propose to use line observations of robust chemical tracers of the gas, such as O, CO, and H₂, as additional constraints to determine a number of key properties of the disks, such as disk shape and mass, opacities, and the dust/gas ratio, by simultaneously fitting continuum and line observations.

Own contribution: This paper was the first common publication that emerged from my FP7-SPACE project DIANA (PI Woitke). It has set new standards for the physical and chemical modelling of protoplanetary discs including stellar irradiation, dust opacities, PAHs and dust settling. All consortium members were involved in the definition of these standards, yet the numerical implementation of these equations was mostly done by myself concerning ProDiMo, by Christophe Pinte concerning MCFOST, and by Michiel Min concerning MCMax. I did a lot of cross-checking between the three modelling codes. The full consortium appears in the author list, yet I have written all paper text, and all figures were created by myself, with the exception of figure B.1 which was provided by Christophe Pinte, and section A.3 which was provided by Armin Liebhart and Manuel Güdel.

Link: <https://ui.adsabs.harvard.edu/abs/2016A%26A...586A.103W>

Publication 5:

Modelling mid-infrared molecular emission lines from T Tauri stars

Woitke, P.; Min, M.; Thi, W.-F.; Roberts, C.; Carmona, A.; Kamp, I.; Ménard, F.; Pinte, C.

Astronomy & Astrophysics, 2018, Volume 618, id. A57, pp. 1–18

Abstract: We introduce a new modelling framework including the Fast Line Tracer (FLiTs) to simulate infrared line emission spectra from protoplanetary discs. This paper focusses on the mid-IR spectral region between 9.7 and 40 μm for T Tauri stars. The generated spectra contain several tens of thousands of molecular emission lines of H_2O , OH, CO, CO_2 , HCN, C_2H_2 , H_2 , and a few other molecules, as well as the forbidden atomic emission lines of Si I, Si II, Si III, Si II, Fe II, Ne II, Ne III, Ar II, and Ar III. In contrast to previously published works, we do not treat the abundances of the molecules nor the temperature in the disc as free parameters, but use the complex results of detailed 2D ProDiMo disc models concerning gas and dust temperature structure, and molecular concentrations. FLiTs computes the line emission spectra by ray tracing in an efficient, fast, and reliable way. The results are broadly consistent with $R=600$ Spitzer/IRS observational data of T Tauri stars concerning line strengths, colour, and line ratios. In order to achieve that agreement, however, we need to assume either a high gas/dust mass ratio of order 1000, or the presence of illuminated disc walls at distances of a few au, for example, due to disc-planet interactions. These walls are irradiated and heated by the star which causes the molecules to emit strongly in the mid-IR. The molecules in the walls cannot be photodissociated easily by UV because of the large densities in the walls favouring their re-formation. Most observable molecular emission lines are found to be optically thick. An abundance analysis is hence not straightforward, and the results of simple slab models concerning molecular column densities can be misleading. We find that the difference between gas and dust temperatures in the disc surface is important for the line formation. The mid-IR emission features of different molecules probe the gas temperature at different depths in the disc, along the following sequence: OH (highest) – CO – H_2O – CO_2 – HCN – C_2H_2 (deepest), just where these molecules start to become abundant. We briefly discuss the effects of C/O ratio and choice of chemical rate network on these results. Our analysis offers new ways to infer the chemical and temperature structure of T Tauri discs from future James Webb Space Telescope (JWST)/MIRI observations, and to possibly detect secondary illuminated disc walls based on their specific mid-IR molecular signature.

Own contribution: The paper presents the results of a part project in the FP7-SPACE project DIANA (PI Woitke), in which Michiel Min developed the Fast Line Tracer (FLiTs). FLiTs uses the molecular abundances, dust opacity, temperatures, and non-LTE populations from ProDiMo, and I coded the interface from ProDiMo to FLiTs. I also performed all combined ProDiMo \rightarrow FLiTs runs, created all figures and tables, and wrote the main text of the paper and scientific discussions, except for sections 4.1 and 4.2, which were provided by Michiel Min. Wing-Fai Thi provided some of the atomic and molecular data used, and my former master student Clayton Roberts helped with post-processing the Spitzer spectroscopic data and identification of molecular features in figure 4. The other co-authors had advisory functions.

Link: <https://ui.adsabs.harvard.edu/abs/2018A%26A...618A..57W>

Publication 6:

Consistent dust and gas models for protoplanetary disks. III. Models for Selected Objects from the FP7 DIANA Project

Woitke, P.; Kamp, I.; Antonellini, S.; Anthonioz, F.; Baldovin-Saveedra, C.; Carmona, A.; Dionatos, O.; Dominik, C.; Greaves, J.; Güdel, M.; Ilee, J.D.; Liebhardt, A.; Menard, F.; Min, M.; Pinte, C.; Rab, C.; Rigon, L.; Thi, W.-F.; Thureau, N.; Waters, L.B.F.M.

Publications of the Astronomical Society of the Pacific, 2019, Volume 131, pp.064301, 71 pages.

Abstract: The European FP7 project DIANA has performed a coherent analysis of a large set of observational data of protoplanetary disks by means of thermo-chemical disk models. The collected data include extinction-corrected stellar UV and X-ray input spectra (as seen by the disk), photometric fluxes, low and high resolution spectra, interferometric data, emission line fluxes, line velocity profiles and line maps, which probe the dust, polycyclic aromatic hydrocarbons (PAHs) and the gas in these objects. We define and apply a standardized modeling procedure to fit these data by state-of-the-art modeling codes (ProDiMo, MCFOST, MCMax), solving continuum and line radiative transfer (RT), disk chemistry, and the heating and cooling balance for both the gas and the dust. 3D diagnostic RT tools (e.g., FLiTs) are eventually used to predict all available observations from the same disk model, the DIANA-standard model. Our aim is to determine the physical parameters of the disks, such as total gas and dust masses, the dust properties, the disk shape, and the chemical structure in these disks. We allow for up to two radial disk zones to obtain our best-fitting models that have about 20 free parameters. This approach is novel and unique in its completeness and level of consistency. It allows us to break some of the degeneracies arising from pure Spectral Energy Distribution (SED) modeling. In this paper, we present the results from pure SED fitting for 27 objects and from the all inclusive DIANA-standard models for 14 objects. Our analysis shows a number of Herbig Ae and T Tauri stars with very cold and massive outer disks which are situated at least partly in the shadow of a tall and gas-rich inner disk. The disk masses derived are often in excess to previously published values, since these disks are partially optically thick even at millimeter wavelength and so cold that they emit less than in the Rayleigh-Jeans limit. We fit most infrared to millimeter emission line fluxes within a factor better than 3, simultaneously with SED, PAH features and radial brightness profiles extracted from images at various wavelengths. However, some line fluxes may deviate by a larger factor, and sometimes we find puzzling data which the models cannot reproduce. Some of these issues are probably caused by foreground cloud absorption or object variability. Our data collection, the fitted physical disk parameters as well as the full model output are available to the community through an online database.

Own contribution: This paper summarised the modelling results of the FP7-SPACE project DIANA (PI Woitke). All authors contributed to either the multi-wavelength data collection or the various modelling efforts, but as the work package leader for the disk modelling, it was my task to bring the various modelling results from the different co-authors to common standards, re-calculating all final models to create homogeneous figures. I have written most of the paper text, and edited some text passages that were provided by my team members.

Link: <https://ui.adsabs.harvard.edu/abs/2019PASP...131f4301W>

Publication 7:

Consistent dust and gas models for protoplanetary disks. IV. A panchromatic view of protoplanetary disks

Dionatos, O.; **Woitke, P.**; Güdel, M.; Degroote, P.; Liebhart, A.; Anthonioz, F.; Antonellini, S.; Baldovin-Saavedra, C.; Carmona, A.; Dominik, C.; Greaves, J.; Ilee, J. D.; Kamp, I.; Ménard, F.; Min, M.; Pinte, C.; Rab, C.; Rigon, L.; Thi, W.-F.; Waters, L.B.F.M.

Astronomy & Astrophysics, 2019, Volume 625, id. A66, pp. 1–32

Abstract: Consistent modeling of protoplanetary disks requires the simultaneous solution of both continuum and line radiative transfer, heating and cooling balance between dust and gas and, of course, chemistry. Such models depend on panchromatic observations that can provide a complete description of the physical and chemical properties and energy balance of protoplanetary systems. Along these lines, we present a homogeneous, panchromatic collection of data on a sample of 85 T Tauri and Herbig Ae objects for which data cover a range from X-rays to centimeter wavelengths. Datasets consist of photometric measurements, spectra, along with results from the data analysis such as line fluxes from atomic and molecular transitions. Additional properties resulting from modeling of the sources such as disk mass and shape parameters, dust size, and polycyclic aromatic hydrocarbon (PAH) properties are also provided for completeness. The purpose of this data collection is to provide a solid base that can enable consistent modeling of the properties of protoplanetary disks. To this end, we performed an unbiased collection of publicly available data that were combined to homogeneous datasets adopting consistent criteria. Targets were selected based on both their properties and the availability of data. Data from more than 50 different telescopes and facilities were retrieved and combined in homogeneous datasets directly from public data archives or after being extracted from more than 100 published articles. X-ray data for a subset of 56 sources represent an exception as they were reduced from scratch and are presented here for the first time. Compiled datasets, along with a subset of continuum and emission-line models are stored in a dedicated database and distributed through a publicly accessible online system. All datasets contain metadata descriptors that allow us to track them back to their original resources. The graphical user interface of the online system allows the user to visually inspect individual objects but also compare between datasets and models. It also offers to the user the possibility to download any of the stored data and metadata for further processing.

Own contribution: This paper published the data collection done for the FP7-SPACE project DIANA (PI Woitke). Many team members were responsible for various types of observational data, and Odysseas Dionatos was leading the corresponding work package. I provided the archival Spitzer/IRS, the Herschel/SPIRE and the UV data collections, I created and hosted the computer account where team members could initially upload their data, to oversee the data collection process. I created figures 1, 2, 3, C.1, C.2, and wrote the appendix B. Some of the tables, for example tables 4 and C.1, resulted from spreadsheets I updated regularly. I would estimate my contribution to this paper to be about 35%.

Link: <https://ui.adsabs.harvard.edu/abs/2019A%26A...625A...66D>

7 International Research Activities

1. European Marie-Curie Training network H2020-MSCA-ITN-2019 project 860470 entitled “Virtual Laboratories for Exoplanets and Planet-Forming Disks” (or short CHAMELEON), funded with a total European contribution of 4.100.000 from 06/2020 to 05/2024, see <https://chameleon.iwf.oeaw.ac.at/>. CHAMELEON combines 6 European universities (Graz, Antwerp, Copenhagen, Edinburgh, Groningen, Leuven) and 5 non-university institutions, which includes the LUCA School of Arts (Antwerp), the Netherlands Institute for Space Research (SRON), MPIA Heidelberg, Copenhagen Games Lab, and the Scottish Parliament Information Centre. This MC ITN EJD network involves 15 staff members and educates 15 PhD students. I am leading the work package 1 entitled “Modelling planet-forming disks”.
2. European FP7-SPACE collaboration project 284405 “DiscAnalysis” (or short, DI-ANA), funded with a total European contribution of €2.000.000 from 01/2012 to 03/2016, see <https://diana.iwf.oeaw.ac.at/>. I was the PI and scientific coordinator. Besides my former host University of St Andrews, there were four other European institutions involved: Astronomical Institute Anton Pannekoek (Amsterdam, NL), Université Joseph Fourier (UJF Grenoble, France), Kapteyn Astronomical Institute (Groningen, NL) and Universität Wien (Vienna, Austria). Tasks included the management of the consortium, organisation of team meetings, reporting, recruitment and sub-contracting, funds for outreach and conference organisation.
3. FAPESP/BEPE: In November 2016, a joint application with my Brazilian collaborator Prof. S. Pilling to the São Paulo Research Foundation (FAPESP) for a Research Internship entitled “Formation of complex molecules on astrophysical ices in star forming regions triggered by UV and X-rays by employing the ProDiMo code and laboratory data” was successful. It had a financial volume of about £50.000. Dr. Will Rocha worked as a post-doc at St Andrews University under my supervision for 12 months in 2017, fully funded by Brazil.
4. St Andrews astronomy group-application for STFC consolidation grant 04/2012 (Co-PI), about £1.400.000 total, and in 04/2015 (Co-PI), about £1.600.000 total, 3 PDRA positions.
5. FWF National Research Program “Pathways to Habitability” (PI Manuel Güdel) for period 03/2012 to 02/2020, the largest Austrian key project in Astronomy with a total of about €7.000.000, organised in 7 sub-projects (SPs), see <http://path.univie.ac.at>. My contribution was to co-edit the application for SP 2 “Disks”.
6. Nederlandse Onderzoekschool Voor Astronomie (NOVA)-2 project *Pulsations, Winds and Dust Formation in AGB Stars*, PhD position for 2.8 years (2005 – 2008), in cooperation with A. Quirrenbach (Leiden Observatory), volume €134.400.
7. Netherlands National Computing Facilities Foundation (NCF) project June 2004 – May 2005 (renewal August 2005 – July 2006), *AstroHydro3D* group application for supercomputing time on TERAS/ASTER/LISA parallel machines, 200.000 CPU hours per year.

8 List of Teaching Courses

Selected Topics in Space Physics and Aeronomy (*Summer 2022*): I contributed two lectures to the course PHM.024UB led by Philippe-André in the Joined Physics Teaching Programme of the TU Graz and the University of Graz for advanced students. My lectures were entitled “*The chemical diversity of planetary atmospheres*” and “*Chemical Rates and Networks*”.

Physics 1A (*Autumn 2016 – 2020*) at the University of St Andrews. I have coordinated this most important physics module for first-semester students of St Andrews University since 2016, and have lectured the mechanics part (about 1/3 of all lectures). 30 credits. The module was run with an increasing number of students (from 146 students in 2016 to 181 students in 2020) including about 35–50 students from other schools and about 10–15 Gateway students. I have coordinated the work of 3 lecturers, 11–16 tutors, and 5 lab demonstrators. We have been running 4 lectures and 1 workshop each week, as well as 20 tutorial groups to keep the size of the tutorial groups at an optimum of about 6–8 students. classtest and exam correction work and set the final grades which have then been discussed with the external examiners. I have re-structured the Mechanics course, have invented a number of new procedures, and have sailed the PH1011-ship through the difficult COVID times.

Computational Astrophysics (*Spring 2012 – 2021*) at the University of St Andrews. 3rd-yr students get hands-on experience in developing their own FORTRAN-90 programs under LINUX, study and test numerical algorithms, plot their results with PYTHON, and develop skills for systematic work and scientific report writing. 15 credits. Numerical methods and astrophysical topics include numerical integration (initial mass function), solving systems of coupled ordinary differential equations (stellar orbits) and Bayesian analysis (planet transits). 15 credits, about 15–35 students, initial 6 lectures, 2x3.5 hours lab contact time during 13 weeks, weekly, full continuous assessment (4 assessed exercises). I was the module coordinator, the course was partly shared with other lecturers.

Stars and Nebulae II (*Spring 2015 – 2021*) at the University of St Andrews about stellar interiors and atmospheres, radiative transfer, interaction of radiation with matter, line formation and emergent spectrum. 15 credits, 14 lectures, about 15 4th-yr students. Computer-aided tutorial exercises, assessed homework, written exams. The course is mostly shared with Prof. Andrew Cameron, but in 2020 I taught all parts with 28 lectures.

Summer School (*June 2014*): I have co-organised a summer school entitled “*Protoplanetary discs: theory and modelling meet observations*”, Ameland, NL, where 57 participants (mostly PhD-students) learnt about the basic theories of protoplanetary discs, their formation and evolution, chemistry, radiative transfer, and the diversity of observational data such as SEDs, images, line emission and interferometry. I contributed two lectures about SED-fitting and gas heating & cooling. The summer school aimed at introducing this exciting field to the next generation of scientists. From these lectures, we compiled a book published in 2015 (<https://diana.iwf.oeaw.ac.at/summer-school>). I have co-edited this volume.

Astrophysics I (*Winter 2011/12*): compulsory lecture for 4th-yr astronomy students at Vienna university on theoretical astrophysics (hydrostatics, stars, planets, white dwarfs, Bonnor-Ebert spheres, stellar structure, fragmentation, stability, virial theorem, shock waves, radiative transfer, radiative processes, MHD, waves, dissipation), 2x2 hours weekly, about 40 students, assessed tutorials, oral examinations.

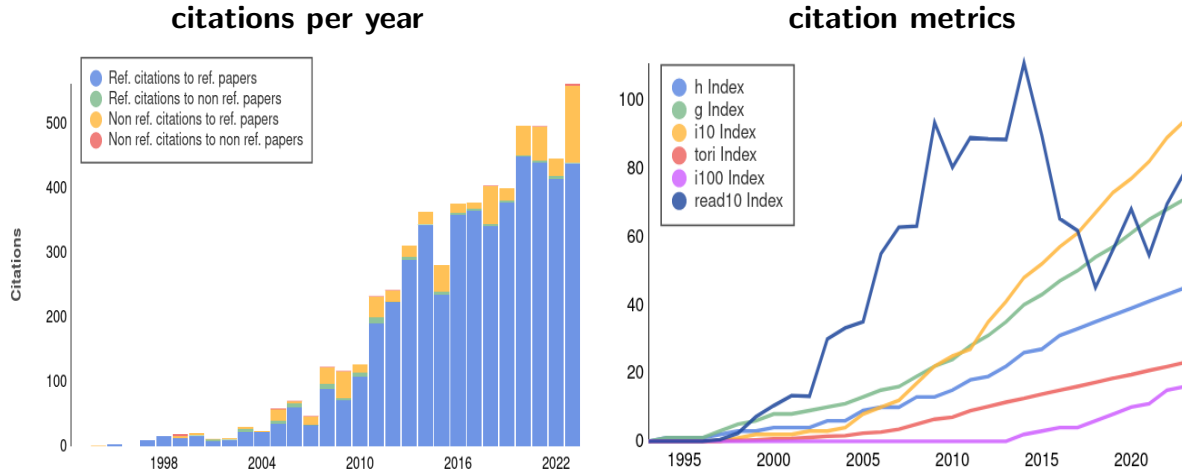
Astrophysics II (*Spring 2011*): compulsory lecture for 4th-yr astronomy students at Vienna university on theoretical astrophysics (interstellar medium, heating & cooling, shock waves, ionisation fronts, HII regions, stellar winds, supernovae, galactic astrophysics, gravitation, motion in mean gravitational potentials, spiral structure), 2x2 hours weekly, about 40 students, assessed tutorials, oral examinations.

9 List of Publications

1993 – 2023 200 (120 refereed) > 5500 citations $h = 45$

2013 – 2023 101 (68 refereed) > 2200 citations $h = 27$

citation metrics from ADS <https://ui.adsabs.harvard.edu>, October 2023:



- My refereed publications since 2013 have attracted a total of 2237 citations (about 32 times per paper) and have been read about 41000 times (about 600 times per paper).
- Five of my ten best-cited papers are first-author papers.

In the following, I have listed these publications separately in categories *Books*, *Refereed Articles*, and *Conference Proceedings* (only those listed by ADS are included).

Books

1. KAMP, I., **Woitke, P.**, ILEE, J. (2015, September). Summer School “Protoplanetary Disks: Theory and Modelling Meet Observations”, *Preface*. In European Physical Journal Web of Conferences, Band 102, pp. 1.
2. **Woitke, P.** (2015b, September). Summer School “Protoplanetary Disks: Theory and Modelling Meet Observations”, *Modelling and interpretation of SEDs*. In European Physical Journal Web of Conferences, Band 102, chapter 7.
3. **Woitke, P.** (2015a, September). Summer School “Protoplanetary Disks: Theory and Modelling Meet Observations”, *Heating and cooling processes in disks*. In European Physical Journal Web of Conferences, Band 102, chapter 11.
4. SIMIS, Y., **Woitke, P.** (2003). Dynamics and Instabilities in Dusty Winds. In H. J. Habing & H. Olofsson (eds.), *Asymptotic giant branch stars*, Astronomy and astrophysics library, New York, Berlin: Springer, 2003, pp. 291.
5. **Woitke, P.** (1997). *Heating and Cooling in Circumstellar Envelopes*. Dissertation, Thesis, Tech. Univ. Berlin, (1997).

Refereed Articles

1. MARIGO, P., **Woitke, P.**, TOGNELLI, E., GIRARDI, L., ARINGER, B., BRESSAN, A. (2023, October). AESOPUS 2.0: Low-Temperature Opacities with Solid Grains. *arXiv e-prints*, arXiv:2310.14588.
2. JANSSEN, L. J., **Woitke, P.**, HERBORT, O., MIN, M., CHUBB, K. L., HELLING, C., CARONE, L. (2023, October). The sulphur species in hot rocky exoplanet atmospheres. *arXiv e-prints*, arXiv:2310.07701.
3. KANWAR, J., KAMP, I., **Woitke, P.**, RAB, C., THI, W.-F., MIN, M. (2023, October). Hydrocarbon chemistry in inner regions of planet forming disks. *arXiv e-prints*, arXiv:2310.04505.
4. STEINMEYER, M.-L., **Woitke, P.**, JOHANSEN, A. (2023, September). Sublimation of refractory minerals in the gas envelopes of accreting rocky planets. *A&A* **677**, A181.
5. BALDUIN, T., **Woitke, P.**, THI, W.-F., GRÅE JØRGENSEN, U., NARITA, Y. (2023, August). Size-dependent charging of dust particles in protoplanetary disks Can turbulence cause charge separation and lightning? *arXiv e-prints*, arXiv:2308.04335.
6. ROCHA, W. R. M., **Woitke, P.**, PILLING, S., THI, W. F., JØRGENSEN, J. K., KRISTENSEN, L. E., PEROTTI, G., KAMP, I. (2023, May). Simulation of CH₃OH ice UV photolysis under laboratory conditions. *A&A* **673**, A70.
7. KAEUFER, T., **Woitke, P.**, MIN, M., KAMP, I., PINTE, C. (2023, April). Analysing the SEDs of protoplanetary disks with machine learning. *A&A* **672**, A30.
8. HELLING, C., SAMRA, D., LEWIS, D., CALDER, R., HIRST, G., **Woitke, P.**, BAEYENS, R., CARONE, L., HERBORT, O., CHUBB, K. L. (2023, March). Exoplanet weather and climate regimes with clouds and thermal ionospheres. A model grid study in support of large-scale observational campaigns. *A&A* **671**, A122.
9. RENSEN, F., MIGUEL, Y., ZILINSKAS, M., LOUCA, A., **Woitke, P.**, HELLING, C., HERBORT, O. (2023, February). The Deep Atmospheric Composition of Jupiter from Thermochemical Calculations Based on Galileo and Juno Data. *Remote Sensing* **15**(3), 841.
10. ERKAEV, N. V., SCHERF, M., HERBORT, O., LAMMER, H., ODERT, P., KUBYSHKINA, D., LEITZINGER, M., **Woitke, P.**, O'NEILL, C. (2023, January). Modification of the radioactive heat budget of Earth-like exoplanets by the loss of primordial atmospheres. *MNRAS* **518**(3), 3703–3721.
11. **Woitke, P.**, ARABHAVI, A. M., KAMP, I., THI, W. F. (2022, December). Mixing and diffusion in protoplanetary disc chemistry. *A&A* **668**, A164.
12. RAB, C., WEBER, M., GRASSI, T., ERCOLANO, B., PICOGNA, G., CASELLI, P., THI, W. F., KAMP, I., **Woitke, P.** (2022, December). Interpreting molecular hydrogen and atomic oxygen line emission of T Tauri disks with photoevaporative disk-wind models. *A&A* **668**, A154.

13. OBERG, N., KAMP, I., CAZAUX, S., **Woitke, P.**, THI, W. F. (2022, November). Circumplanetary disk ices. I. Ice formation vs. viscous evolution and grain drift. *A&A* **667**, A95.
14. ARABHAVI, A. M., **Woitke, P.**, CAZAUX, S. M., KAMP, I., RAB, C., THI, W.-F. (2022, October). Ices in planet-forming disks: Self-consistent ice opacities in disk models. *A&A* **666**, A139.
15. HERBORT, O., **Woitke, P.**, HELLING, C., ZERKLE, A. L. (2022, February). The atmospheres of rocky exoplanets. II. Influence of surface composition on the diversity of cloud condensates. *A&A* **658**, A180.
16. KHORSHID, N., MIN, M., DÉSSERT, J. M., **Woitke, P.**, DOMINIK, C. (2022, November). SimAb: A simple, fast, and flexible model to assess the effects of planet formation on the atmospheric composition of gas giants. *A&A* **667**, A147.
17. RIMMER, P. B., JORDAN, S., CONSTANTINOU, T., **Woitke, P.**, SHORTTLE, O., HOBBS, R., PASCHODIMAS, A. (2021, August). Hydroxide Salts in the Clouds of Venus: Their Effect on the Sulfur Cycle and Cloud Droplet pH. *The Planetary Science Journal* **2**(4), 133.
18. **Woitke, P.** AND HERBORT, O. AND HELLING, CH. AND STÜEKEN, E. AND DOMINIK, M. AND BARTH, P. AND SAMRA, D., (2021, February). Coexistence of CH₄, CO₂, and H₂O in exoplanet atmospheres, *A&A* **646**, 43.
19. RAB, CH. AND KAMP, I. AND DOMINIK, C. AND GINSKI, C. AND MURO-ARENA, G. A. AND THI, W. -F. AND WATERS, L. B. F. M. AND **Woitke, P.** (2020, October). Interpreting high spatial resolution line observations of planet-forming disks with gaps and rings: the case of HD 163296, *A&A* **642**, 165.
20. ANTONELLINI, S. AND BANZATTI, A. AND KAMP, I. AND THI, W. -F. AND **Woitke, P.** (2020, May). Model exploration of near-IR ro-vibrational CO emission as a tracer of inner cavities in protoplanetary disks, *A&A* **637**, 29.
21. HERBORT, O. AND **Woitke, P.** AND HELLING, CH. AND ZERKLE, A. (2020, April). The atmospheres of rocky exoplanets. I. Outgassing of common rock and the stability of liquid water, *A&A* **636**, 71.
22. MOLAVERDIKHANI, K. AND HELLING, CH. AND LEW, B. W. P. AND MACDONALD, R. J. AND SAMRA, D. AND IRO, N. AND **Woitke, P.** AND PARMENTIER, V. (2020, March). Understanding the atmospheric properties and chemical composition of the ultra-hot Jupiter HAT-P-7b. II. Mapping the effects of gas kinetics, *A&A* **635**, 31.
23. THI, W. F. AND HOCUK, S. AND KAMP, I. AND **Woitke, P.** AND RAB, CH. AND CAZAUX, S. AND CASELLI, P. AND D'ANGELO, M. (2020, March). Warm dust surface chemistry in protoplanetary disks. Formation of phyllosilicates. *A&A* **635**, 16.

24. THI, W. F. AND HOCUK, S. AND KAMP, I. AND **Woitke, P.** AND RAB, CH. AND CAZAUX, S. AND CASELLI, P. (2020, February). Warm dust surface chemistry. H_2 and HD formation. *A&A* **634**, 42.
25. **Woitke, Peter** AND HELLING, CHRISTIANE AND GUNN, OPHELIA (2020, February). Dust in brown dwarfs and extra-solar planets. VII. Cloud formation in diffusive atmospheres, *A&A* **634**, 23.
26. THI, W. F. AND LESUR, G. AND **Woitke, P.** AND KAMP, I. AND RAB, CH. AND CARMONA, A. (2019, December). Radiation thermo-chemical models of protoplanetary disks. Grain and polycyclic aromatic hydrocarbon charging, *A&A* **632**, 44.
27. GREENWOOD, A. J. AND KAMP, I. AND WATERS, L. B. F. M. AND **Woitke, P.** AND THI, W. -F. (2019, November). The infrared line-emitting regions of T Tauri protoplanetary disks, *A&A* **631**, 81.
28. HELLING, CH. AND IRO, N. AND CORRALES, L. AND SAMRA, D. AND OHNO, K. AND ALAM, M. K. AND STEINRUECK, M. AND LEW, B. AND MOLAVERDIKHANI, K. AND MACDONALD, R. J. AND HERBORT, O. AND **Woitke, P.** AND PARMEN-TIER, V. (2019, November). Understanding the atmospheric properties and chemical composition of the ultra-hot Jupiter HAT-P-7b. I. Cloud and chemistry mapping, *A&A* **631**, 79
29. **Woitke, P.** AND KAMP, I. AND ANTONELLINI, S. AND ANTHONIOZ, F. AND BALDOVIN-SAVEEDRA, C. AND CARMONA, A. AND DIONATOS, O. AND DOMINIK, C. AND GREAVES, J. AND GÜDEL, M. AND ILEE, J. D. AND LIEBHARDT, A. AND MENARD, F. AND MIN, M. AND PINTE, C. AND RAB, C. AND RIGON, L. AND THI, W. F. AND THUREAU, N. AND WATERS, L. B. F. M. (2019, June). Consistent Dust and Gas Models for Protoplanetary Disks. III. Models for Selected Objects from the FP7 DIANA Project, *PASP* **131**, 64301
30. HELLING, CH. AND GOURBIN, P. AND **Woitke, P.** AND PARMENTIER, V. (2019, June). Sparkling nights and very hot days on WASP-18b: the formation of clouds and the emergence of an ionosphere, *A&A* **626**, 133
31. GREENWOOD, A. J. AND KAMP, I. AND WATERS, L. B. F. M. AND **Woitke, P.** AND THI, W. -F. (2019, June). Effects of dust evolution on protoplanetary disks in the mid-infrared, *A&A* **626**, 6
32. DIONATOS, O. AND **Woitke, P.** AND GÜDEL, M. AND DEGROOTE, P. AND LIEBHART, A. AND ANTHONIOZ, F. AND ANTONELLINI, S. AND BALDOVIN-SAAVEDRA, C. AND CARMONA, A. AND DOMINIK, C. AND GREAVES, J. AND ILEE, J. D. AND KAMP, I. AND MÉNARD, F. AND MIN, M. AND PINTE, C. AND RAB, C. AND RIGON, L. AND THI, W. F. AND WATERS, L. B. F. M. (2019, May). Consistent dust and gas models for protoplanetary disks. IV. A panchromatic view of protoplanetary disks, *A&A* **625**, 66.
33. RAB, CH. AND KAMP, I. AND GINSKI, C. AND OBERG, N. AND MURO-ARENA, G. A. AND DOMINIK, C. AND WATERS, L. B. F. M. AND THI, W. -F. AND

- Woitke, P.** (2019, April). Observing the gas component of circumplanetary disks around wide-orbit planet-mass companions in the (sub)mm regime, *A&A* **624**, 16.
34. D'ANGELO, M. AND CAZAUX, S. AND KAMP, I. AND THI, W. -F. AND **Woitke, P.** (2019, February). Water delivery in the inner solar nebula. Monte Carlo simulations of forsterite hydration, *A&A* **622**, 208.
 35. **Woitke, P.** AND MIN, M. AND THI, W. -F. AND ROBERTS, C. AND CARMONA, A. AND KAMP, I. AND MÉNARD, F. AND PINTE, C. (2018, October). Modelling mid-infrared molecular emission lines from T Tauri stars, *A&A* **618**, 57.
 36. **Woitke, P.** AND HELLING, CH. AND HUNTER, G. H. AND MILLARD, J. D. AND TURNER, G. E. AND WORTERS, M. AND BLECIC, J. AND STOCK, J. W. (2018, June). Equilibrium chemistry down to 100 K. Impact of silicates and phyllosilicates on the carbon to oxygen ratio, *A&A* **614**, 1.
 37. RAB, CH. AND GÜDEL, M. AND **Woitke, P.** AND KAMP, I. AND THI, W. -F. AND MIN, M. AND ARESU, G. AND MEIJERINK, R. (2018, January). X-ray radiative transfer in protoplanetary disks. The role of dust and X-ray background fields, *A&A* **609**, 91.
 38. PINTE, C. AND MÉNARD, F. AND DUCHÊNE, G. AND HILL, T. AND DENT, W. R. F. AND **Woitke, P.** AND MARET, S. AND VAN DER PLAS, G. AND HALES, A. AND KAMP, I. AND THI, W. F. AND DE GREGORIO-MONSALVO, I. AND RAB, C. AND QUANZ, S. P. AND AVENHAUS, H. AND CARMONA, A. AND CASASSUS, S. (2018, January). Direct mapping of the temperature and velocity gradients in discs. Imaging the vertical CO snow line around IM Lupi, *A&A* **609**, 47.
 39. KAMP, I. AND THI, W. -F. AND **Woitke, P.** AND RAB, C. AND BOUMA, S. AND MÉNARD, F. (2017, November). Consistent dust and gas models for protoplanetary disks. II. Chemical networks and rates, *A&A* **607**, 41.
 40. RAB, CH. AND ELBAKYAN, V. AND VOROBYOV, E. AND GÜDEL, M. AND DIONATOS, O. AND AUDARD, M. AND KAMP, I. AND THI, W. -F. AND **Woitke, P.** AND POSTEL, A. (2017, July). The chemistry of episodic accretion in embedded objects. 2D radiation thermo-chemical models of the post-burst phase, *A&A* **604**, 15.
 41. HELLING, CH. AND TOOTILL, D. AND **Woitke, P.** AND LEE, G. (2017, July). Dust in brown dwarfs and extrasolar planets. V. Cloud formation in carbon- and oxygen-rich environments, *A&A* **603**, 123.
 42. RAB, CH. AND GÜDEL, M. AND PADOVANI, M. AND KAMP, I. AND THI, W. -F. AND **Woitke, P.** AND ARESU, G. (2017, July). Stellar energetic particle ionization in protoplanetary disks around T Tauri stars, *A&A* **603**, 96.
 43. GREENWOOD, A. J. AND KAMP, I. AND WATERS, L. B. F. M. AND **Woitke, P.** AND THI, W. -F. AND RAB, CH. AND ARESU, G. AND SPAANS, M. (2017, May). Thermochemical modelling of brown dwarf discs, *A&A* **601**, 44.

44. ANTONELLINI, S. AND BREMER, J. AND KAMP, I. AND RIVIERE-MARICHALAR, P. AND LAHUIS, F. AND THI, W. -F. AND **Woitke, P.** AND MEIJERINK, R. AND ARESU, G. AND SPAANS, M. (2017, January). Mid-IR water and silicate relation in protoplanetary disks, *A&A* **597**, 72.
45. DRABEK-MAUNDER, E. AND MOHANTY, S. AND GREAVES, J. AND KAMP, I. AND MEIJERINK, R. AND SPAANS, M. AND THI, W. -F. AND **Woitke, P.** (2016, December). HCO⁺ Detection of Dust-depleted Gas in the Inner Hole of the LkCa 15 Pre-transitional Disk, *ApJ* **833**, 260
46. HAWORTH, THOMAS J. AND ILEE, JOHN D. AND FORGAN, DUNCAN H. AND FACCHINI, STEFANO AND PRICE, DANIEL J. AND BONEBERG, DOMINIKA M. AND BOOTH, RICHARD A. AND CLARKE, CATHIE J. AND GONZALEZ, JEAN-FRANÇOIS AND HUTCHISON, MARK A. AND KAMP, INGA AND LAIBE, GUILLAUME AND LYRA, WLADIMIR AND MERU, FARZANA AND MOHANTY, SUBHANJOY AND PANIĆ, OLJA AND RICE, KEN AND SUZUKI, TAKERU AND TEAGUE, RICHARD AND WALSH, CATHERINE AND **Woitke, Peter** AND COMMUNITY AUTHORS (2016, October). Grand Challenges in Protoplanetary Disc Modelling, *PASA* **33**, e053
47. GREAVES, J. S. AND HOLLAND, W. S. AND MATTHEWS, B. C. AND MARSHALL, J. P. AND DENT, W. R. F. AND **Woitke, P.** AND WYATT, M. C. AND MATRÀ, L. AND JACKSON, A. (2016, October). Gas and dust around A-type stars at tens of Myr: signatures of cometary breakup, *MNRAS* **461**, 3910.
48. LEE, G. AND DOBBS-DIXON, I. AND HELLING, CH. AND BOGNAR, K. AND **Woitke, P.** (2016, October). Dynamic mineral clouds on HD 189733b. I. 3D RHD with kinetic, non-equilibrium cloud formation, *A&A* **594**, 48.
49. MIN, M. AND BOUWMAN, J. AND DOMINIK, C. AND WATERS, L. B. F. M. AND PONTOPPIDAN, K. M. AND HONY, S. AND MULDER, G. D. AND HENNING, TH. AND VAN DISHOCK, E. F. AND **Woitke, P.** AND EVANS, NEAL J., II AND DIGIT TEAM (2016, August). The abundance and thermal history of water ice in the disk surrounding HD 142527 from the DIGIT Herschel Key Program, *A&A* **593**, 11.
50. HEIN BERTELSEN, R. P., KAMP, I., VAN DER PLAS, G., VAN DEN ANCKER, M. E., WATERS, L. B. F. M., THI, W.-F., **Woitke, P.** (2016, May). Variability in the CO ro-vibrational lines from HD163296. *MNRAS* **458**, 1466–1477.
51. HEIN BERTELSEN, R. P., KAMP, I., VAN DER PLAS, G., VAN DEN ANCKER, M. E., WATERS, L. B. F. M., THI, W.-F., **Woitke, P.** (2016, May). A proposed new diagnostic for Herbig disc geometry. FWHM versus J of CO ro-vibrational lines. *A&A* **590**, A98.
52. **Woitke, P.**, MIN, M., PINTE, C., THI, W.-F., KAMP, I., RAB, C., ANTHONIOZ, F., ANTONELLINI, S., BALDOVIN-SAAVEDRA, C., CARMONA, A., DOMINIK, C., DIONATOS, O., GREAVES, J., GÜDEL, M., ILEE, J. D., LIEBHART, A., MÉNARD, F., RIGON, L., WATERS, L. B. F. M., ARESU, G., MEIJERINK, R., SPAANS, M. (2016, February). Consistent dust and gas models for protoplanetary disks. I. Disk shape, dust settling, opacities, and PAHs. *A&A* **586**, A103.

53. ANTONELLINI, S., KAMP, I., LAHUIS, F., **Woitke, P.**, THI, W.-F., MEIJERINK, R., ARESU, G., SPAANS, M., GÜDEL, M., LIEBHART, A. (2016, January). Mid-IR spectra of pre-main sequence Herbig stars: An explanation for the non-detections of water lines. *A&A* **585**, A61.
54. MIN, M., RAB, C., **Woitke, P.**, DOMINIK, C., MÉNARD, F. (2016, January). Multiwavelength optical properties of compact dust aggregates in protoplanetary disks. *A&A* **585**, A13.
55. ANTONELLINI, S., KAMP, I., RIVIERE-MARICHALAR, P., MEIJERINK, R., **Woitke, P.**, THI, W.-F., SPAANS, M., ARESU, G., LEE, G. (2015, October). Understanding the water emission in the mid- and far-IR from protoplanetary disks around T Tauri stars. *A&A* **582**, A105.
56. VAN DER WIEL, M. H. D., NAYLOR, D. A., KAMP, I., MÉNARD, F., THI, W.-F., **Woitke, P.**, OLOFSSON, G., PONTOPPIDAN, K. M., DI FRANCESCO, J., GLAUSER, A. M., GREAVES, J. S., IVISON, R. J. (2014, November). Signatures of warm carbon monoxide in protoplanetary discs observed with Herschel SPIRE. *MNRAS* **444**, 3911–3925.
57. GARUFI, A., PODIO, L., KAMP, I., MÉNARD, F., BRITAIN, S., EIROA, C., MONTESINOS, B., ALONSO-MARTÍNEZ, M., THI, W. F., **Woitke, P.** (2014, July). The protoplanetary disk of FT Tauri: multiwavelength data analysis and modelling. *A&A* **567**, A141.
58. CARMONA, A., PINTE, C., THI, W. F., BENISTY, M., MÉNARD, F., GRADY, C., KAMP, I., **Woitke, P.**, OLOFSSON, J., ROBERGE, A., BRITAIN, S., DUCHÊNE, G., MEEUS, G., MARTIN-ZAÏDI, C., DENT, B., LE BOUQUIN, J. B., BERGER, J. P. (2014, July). Constraining the structure of the transition disk HD 135344B (SAO 206462) by simultaneous modelling of multiwavelength gas and dust observations. *A&A* **567**, A51.
59. KEANE, J. T., PASCUCCI, I., ESPAILLAT, C., **Woitke, P.**, ANDREWS, S., KAMP, I., THI, W.-F., MEEUS, G., DENT, W. R. F. (2014, June). Herschel Evidence for Disk Flattening or Gas Depletion in Transitional Disks. *ApJ* **787**, 153.
60. ARESU, G., KAMP, I., MEIJERINK, R., SPAANS, M., VICENTE, S., PODIO, L., **Woitke, P.**, MENARD, F., THI, W.-F., GÜDEL, M., LIEBHART, A. (2014, June). [O I] disk emission in the Taurus star-forming region. *A&A* **566**, A14.
61. HELLING, C., **Woitke, P.**, RIMMER, P. B., KAMP, I., THI, W.-F., MEIJERINK, R. (2014, April). Disk Evolution, Element Abundances and Cloud Properties of Young Gas Giant Planets. *Life* **4**, 142–173.
62. PODIO, L., KAMP, I., CODELLA, C., NISINI, B., ARESU, G., BRITAIN, S., CABRIT, S., DOUGADOS, C., GRADY, C., MEIJERINK, R., SANDELL, G., SPAANS, M., THI, W.-F., WHITE, G. J., **Woitke, P.** (2014, March). Probing the Gaseous Disk of T Tau N with CN 5-4 Lines. *ApJL* **783**, L26.

63. HEIN BERTELSEN, R. P., KAMP, I., GOTO, M., VAN DER PLAS, G., THI, W.-F., WATERS, L. B. F. M., VAN DEN ANCKER, M. E., **Woitke, P.** (2014, January). CO ro-vibrational lines in HD 100546. A search for disc asymmetries and the role of fluorescence. *A&A* **561**, A102.
64. THI, W.-F., PINTE, C., PANTIN, E., AUGEREAU, J. C., MEEUS, G., MÉNARD, F., MARTIN-ZAÏDI, C., **Woitke, P.**, RIVIERE-MARICHALAR, P., KAMP, I., CARMONA, A., SANDELL, G., EIROA, C., DENT, W., MONTESINOS, B., ARESU, G., MEIJERINK, R., SPAANS, M., WHITE, G., ARDILA, D., LEBRETON, J., MENDIGUTÍA, I., BRITAIN, S. (2014, January). Gas lines from the 5-Myr old optically thin disk around HD 141569A. Herschel observations and modelling. *A&A* **561**, A50.
65. KAMP, I., THI, W.-F., MEEUS, G., **Woitke, P.**, PINTE, C., MEIJERINK, R., SPAANS, M., PASCUCI, I., ARESU, G., DENT, W. R. F. (2013, November). Uncertainties in water chemistry in disks: An application to TW Hydrae. *A&A* **559**, A24.
66. MEIJERINK, R., SPAANS, M., KAMP, I., ARESU, G., THI, W.-F., **Woitke, P.** (2013, October). Tracing the Physical Conditions in Active Galactic Nuclei with Time-Dependent Chemistry. *Journal of Physical Chemistry A* **117**, 9593–9604.
67. THI, W. F., MÉNARD, F., MEEUS, G., CARMONA, A., RIVIERE-MARICHALAR, P., AUGEREAU, J.-C., KAMP, I., **Woitke, P.**, PINTE, C., MENDIGUTÍA, I., EIROA, C., MONTESINOS, B., BRITAIN, S., DENT, W. (2013a, September). Nature of the gas and dust around 51 Ophiuchi. Modelling continuum and Herschel line observations. *A&A* **557**, A111.
68. ROBERGE, A., KAMP, I., MONTESINOS, B., DENT, W. R. F., MEEUS, G., DONALDSON, J. K., OLOFSSON, J., MOÓR, A., AUGEREAU, J.-C., HOWARD, C., EIROA, C., THI, W.-F., ARDILA, D. R., SANDELL, G., **Woitke, P.** (2013, July). Herschel Observations of Gas and Dust in the Unusual 49 Ceti Debris Disk. *ApJ* **771**, 69.
69. DENT, W. R. F., THI, W. F., KAMP, I., WILLIAMS, J. P., MENARD, F., ANDREWS, S., ARDILA, D., ARESU, G., AUGEREAU, J.-C., BARRADO Y NAVASCUES, D., BRITAIN, S., CARMONA, A., CIARDI, D., DANCHI, W., DONALDSON, J., DUCHENE, G., EIROA, C., FEDELE, D., GRADY, C., DE GREGORIO-MOLSALVO, I., HOWARD, C., HUÉLAMO, N., KRIVOV, A., LEBRETON, J., LISEAU, R., MARTIN-ZAÏDI, C., MATHEWS, G., MEEUS, G., MENDIGUTÍA, I., MONTESINOS, B., MORALES-CALDERON, M., MORA, A., NOMURA, H., PANTIN, E., PASCUCI, I., PHILLIPS, N., PINTE, C., PODIO, L., RAMSAY, S. K., RIAZ, B., RIVIERE-MARICHALAR, P., ROBERGE, A., SANDELL, G., SOLANO, E., TILLING, I., TORRELLES, J. M., VANDENBUSCHE, B., VICENTE, S., WHITE, G. J., **Woitke, P.** (2013, May). GASPS - A Herschel Survey of Gas and Dust in Protoplanetary Disks: Summary and Initial Statistics. *PASP* **125**, 477–505.
70. PODIO, L., KAMP, I., CODELLA, C., CABRIT, S., NISINI, B., DOUGADOS, C., SANDELL, G., WILLIAMS, J. P., TESTI, L., THI, W.-F., **Woitke, P.**, MEIJERINK,

- R., SPAANS, M., ARESU, G., MÉNARD, F., PINTE, C. (2013b, March). Water Vapor in the Protoplanetary Disk of DG Tau. *ApJL* **766**, L5.
71. THI, W. F., KAMP, I., **Woitke, P.**, VAN DER PLAS, G., BERTELSEN, R., WIESENFELD, L. (2013, March). Radiation thermo-chemical models of protoplanetary discs. IV. Modelling CO ro-vibrational emission from Herbig Ae discs. *A&A* **551**, A49.
 72. ARESU, G., MEIJERINK, R., KAMP, I., SPAANS, M., THI, W.-F., **Woitke, P.** (2012, November). Far-ultraviolet and X-ray irradiated protoplanetary disks: a grid of models. II. Gas diagnostic line emission. *A&A* **547**, A69.
 73. MEIJERINK, R., ARESU, G., KAMP, I., SPAANS, M., THI, W.-F., **Woitke, P.** (2012, November). Far-ultraviolet and X-ray irradiated protoplanetary disks: a grid of models. I. The disk structure. *A&A* **547**, A68.
 74. LEBRETON, J., AUGEREAU, J.-C., THI, W.-F., ROBERGE, A., DONALDSON, J., SCHNEIDER, G., MADDISON, S. T., MÉNARD, F., RIVIERE-MARICHALAR, P., MATHEWS, G. S., KAMP, I., PINTE, C., DENT, W. R. F., BARRADO, D., DUCHÊNE, G., GONZALEZ, J.-F., GRADY, C. A., MEEUS, G., PANTIN, E., WILLIAMS, J. P., **Woitke, P.** (2012, March). An icy Kuiper belt around the young solar-type star HD 181327. *A&A* **539**, A17.
 75. RIVIERE-MARICHALAR, P., MÉNARD, F., THI, W. F., KAMP, I., MONTESINOS, B., MEEUS, G., **Woitke, P.**, HOWARD, C., SANDELL, G., PODIO, L., DENT, W. R. F., MENDIGUTÍA, I., PINTE, C., WHITE, G. J., BARRADO, D. (2012, February). Detection of warm water vapour in Taurus protoplanetary discs by Herschel. *A&A* **538**, L3.
 76. TILLING, I., **Woitke, P.**, MEEUS, G., MORA, A., MONTESINOS, B., RIVIERE-MARICHALAR, P., EIROA, C., THI, W.-F., ISELLA, A., ROBERGE, A., MARTINZAIDI, C., KAMP, I., PINTE, C., SANDELL, G., VACCA, W. D., MÉNARD, F., MENDIGUTÍA, I., DUCHÊNE, G., DENT, W. R. F., ARESU, G., MEIJERINK, R., SPAANS, M. (2012, February). Gas modelling in the disc of HD 163296. *A&A* **538**, A20.
 77. **Woitke, P.**, RIAZ, B., DUCHÊNE, G., PASCUCCHI, I., LYO, A.-R., DENT, W. R. F., PHILLIPS, N., THI, W.-F., MÉNARD, F., HERCZEG, G. J., BERGIN, E., BROWN, A., MORA, A., KAMP, I., ARESU, G., BRITAIN, S., DE GREGORIO-MONSALVO, I., SANDELL, G. (2011, October). The unusual protoplanetary disk around the T Tauri star ET Chamaeleontis. *A&A* **534**, A44.
 78. KAMP, I., TILLING, I., **Woitke, P.**, THI, W.-F., HOGERHEIJDE, M. (2010, January). Radiation thermo-chemical models of protoplanetary disks. II. Line diagnostics. *A&A* **510**, A18.
 79. DE KOK, R. J., HELLING, C., STAM, D. M., **Woitke, P.**, WITTE, S. (2011, July). The influence of non-isotropic scattering of thermal radiation on spectra of brown dwarfs and hot exoplanets. *A&A* **531**, A67.

80. THI, W.-F., MÉNARD, F., MEEUS, G., MARTIN-ZAÏDI, C., **Woitke, P.**, TATULLI, E., BENISTY, M., KAMP, I., PASCUCCI, I., PINTE, C., GRADY, C. A., BRITTAİN, S., WHITE, G. J., HOWARD, C. D., SANDELL, G., EIROA, C. (2011, June). Detection of CH^+ emission from the disc around HD 100546. *A&A* **530**, L2.
81. FEDELE, D., PASCUCCI, I., BRITTAİN, S., KAMP, I., **Woitke, P.**, WILLIAMS, J. P., DENT, W. R. F., THI, W.-F. (2011, May). Water Depletion in the Disk Atmosphere of Herbig AeBe Stars. *ApJ* **732**, 106.
82. THI, W.-F., **Woitke, P.**, KAMP, I. (2011, April). Radiation thermo-chemical models of protoplanetary discs. III. Impact of inner rims on spectral energy distributions. *MNRAS* **412**, 711–726.
83. ARESU, G., KAMP, I., MEIJERINK, R., **Woitke, P.**, THI, W.-F., SPAANS, M. (2011a, February). X-ray impact on the protoplanetary disks around T Tauri stars. *A&A* **526**, A163.
84. THI, W.-F., **Woitke, P.**, KAMP, I. (2010, September). Warm non-equilibrium gas phase chemistry as a possible origin of high $\text{HDO}/\text{H}_2\text{O}$ ratios in hot and dense gases: application to inner protoplanetary discs. *MNRAS* **407**, 232–246.
85. MATHEWS, G. S., DENT, W. R. F., WILLIAMS, J. P., HOWARD, C. D., MEEUS, G., RIAZ, B., ROBERGE, A., SANDELL, G., VANDENBUSSCHE, B., DUCHÊNE, G., KAMP, I., MÉNARD, F., MONTESINOS, B., PINTE, C., THI, W. F., **Woitke, P.**, ALACID, J. M., ANDREWS, S. M., ARDILA, D. R., ARESU, G., AUGEREAU, J. C., BARRADO, D., BRITTAİN, S., CIARDI, D. R., DANCHI, W., EIROA, C., FEDELE, D., GRADY, C. A., DE GREGORIO-MONSALVO, I., HERAS, A., HUELAMO, N., KRIVOV, A., LEBRETON, J., LISEAU, R., MARTIN-ZAÏDI, C., MENDIGUTÍA, I., MORA, A., MORALES-CALDERON, M., NOMURA, H., PANTIN, E., PASCUCCI, I., PHILLIPS, N., PODIO, L., POELMAN, D. R., RAMSAY, S., RICE, K., RIVIERE-MARICHALAR, P., SOLANO, E., TILLING, I., WALKER, H., WHITE, G. J., WRIGHT, G. (2010, July). GAS in Protoplanetary Systems (GASPS). I. First results. *A&A* **518**, L127.
86. PINTE, C., **Woitke, P.**, MÉNARD, F., DUCHÊNE, G., KAMP, I., MEEUS, G., MATHEWS, G., HOWARD, C. D., GRADY, C. A., THI, W.-F., TILLING, I., AUGEREAU, J.-C., DENT, W. R. F., ALACID, J. M., ANDREWS, S., ARDILA, D. R., ARESU, G., BARRADO, D., BRITTAİN, S., CIARDI, D. R., DANCHI, W., EIROA, C., FEDELE, D., DE GREGORIO-MONSALVO, I., HERAS, A., HUELAMO, N., KRIVOV, A., LEBRETON, J., LISEAU, R., MARTIN-ZAÏDI, C., MENDIGUTÍA, I., MONTESINOS, B., MORA, A., MORALES-CALDERON, M., NOMURA, H., PANTIN, E., PASCUCCI, I., PHILLIPS, N., PODIO, L., POELMAN, D. R., RAMSAY, S., RIAZ, B., RICE, K., RIVIERE-MARICHALAR, P., ROBERGE, A., SANDELL, G., SOLANO, E., VANDENBUSSCHE, B., WALKER, H., WILLIAMS, J. P., WHITE, G. J., WRIGHT, G. (2010, July). The Herschel view of GAS in Protoplanetary Systems (GASPS). First comparisons with a large grid of models. *A&A* **518**, L126.
87. THI, W.-F., MATHEWS, G., MÉNARD, F., **Woitke, P.**, MEEUS, G., RIVIERE-MARICHALAR, P., PINTE, C., HOWARD, C. D., ROBERGE, A., SANDELL,

- G., PASCUCCI, I., RIAZ, B., GRADY, C. A., DENT, W. R. F., KAMP, I., DUCHÊNE, G., AUGEREAU, J.-C., PANTIN, E., VANDENBUSSCHE, B., TILLING, I., WILLIAMS, J. P., EIROA, C., BARRADO, D., ALACID, J. M., ANDREWS, S., ARDILA, D. R., ARESU, G., BRITTAİN, S., CIARDI, D. R., DANCHI, W., FEDELE, D., DE GREGORIO-MONSALVO, I., HERAS, A., HUELAMO, N., KRIVOV, A., LEBRETON, J., LISEAU, R., MARTIN-ZAIDI, C., MENDIGUTÍA, I., MONTESINOS, B., MORA, A., MORALES-CALDERON, M., NOMURA, H., PHILLIPS, N., PODIO, L., POELMAN, D. R., RAMSAY, S., RICE, K., SOLANO, E., WALKER, H., WHITE, G. J., WRIGHT, G. (2010, July). Herschel-PACS observation of the 10 Myr old T Tauri disk TW Hya. Constraining the disk gas mass. *A&A* **518**, L125.
88. MEEUS, G., PINTE, C., **Woitke, P.**, MONTESINOS, B., MENDIGUTÍA, I., RIVIERE-MARICHALAR, P., EIROA, C., MATHEWS, G. S., VANDENBUSSCHE, B., HOWARD, C. D., ROBERGE, A., SANDELL, G., DUCHÊNE, G., MÉNARD, F., GRADY, C. A., DENT, W. R. F., KAMP, I., AUGEREAU, J. C., THI, W. F., TILLING, I., ALACID, J. M., ANDREWS, S., ARDILA, D. R., ARESU, G., BARRADO, D., BRITTAİN, S., CIARDI, D. R., DANCHI, W., FEDELE, D., DE GREGORIO-MONSALVO, I., HERAS, A., HUELAMO, N., KRIVOV, A., LEBRETON, J., LISEAU, R., MARTIN-ZAIDI, C., MORA, A., MORALES-CALDERON, M., NOMURA, H., PANTIN, E., PASCUCCI, I., PHILLIPS, N., PODIO, L., POELMAN, D. R., RAMSAY, S., RIAZ, B., RICE, K., SOLANO, E., WALKER, H., WHITE, G. J., WILLIAMS, J. P., WRIGHT, G. (2010, July). Gas in the protoplanetary disc of HD 169142: Herschel’s view. *A&A* **518**, L124.
89. **Woitke, P.**, PINTE, C., TILLING, I., MÉNARD, F., KAMP, I., THI, W.-F., DUCHÊNE, G., AUGEREAU, J.-C. (2010, June). Continuum and line modelling of discs around young stars. I. 300000 disc models for HERSCHEL/GASPS. *MNRAS* **405**, L26–L30.
90. KAMP, I., **Woitke, P.**, PINTE, C., TILLING, I., THI, W.-F., MENARD, F., DUCHENE, G., AUGEREAU, J.-C. (2011, August). Continuum and line modelling of discs around young stars. II. Line diagnostics for GASPS from the DENT grid. *A&A* **532**, A85.
91. **Woitke, P.**, THI, W.-F., KAMP, I., HOGERHEIJDE, M. R. (2009, July). Hot and cool water in Herbig Ae protoplanetary disks. A challenge for Herschel. *A&A* **501**, L5–L8.
92. **Woitke, P.**, KAMP, I., THI, W.-F. (2009, July). Radiation thermo-chemical models of protoplanetary disks. I. Hydrostatic disk structure and inner rim. *A&A* **501**, 383–406.
93. PINTE, C., HARRIES, T. J., MIN, M., WATSON, A. M., DULLEMOND, C. P., **Woitke, P.**, MÉNARD, F., DURÁN-ROJAS, M. C. (2009, May). Benchmark problems for continuum radiative transfer. High optical depths, anisotropic scattering, and polarisation. *A&A* **498**, 967–980.
94. HELLING, C., ACKERMAN, A., ALLARD, F., DEHN, M., HAUSCHILDT, P., HOMEIER, D., LODDERS, K., MARLEY, M., RIETMEIJER, F., TSUJI, T., **Woitke, P.**

- (2008a, December). A comparison of chemistry and dust cloud formation in ultracool dwarf model atmospheres. *MNRAS* **391**, 1854–1873.
95. HELLING, C., **Woitke, P.**, THI, W.-F. (2008, July). Dust in brown dwarfs and extra-solar planets. I. Chemical composition and spectral appearance of quasi-static cloud layers. *A&A* **485**, 547–560.
 96. HELLING, C., DEHN, M., **Woitke, P.**, HAUSCHILDT, P. H. (2008b, April). Erratum: “Consistent Simulations of Substellar Atmospheres and Nonequilibrium Dust Cloud Formation”. *ApJL* **677**, L157–L157.
 97. JOHNAS, C. M. S., HELLING, C., DEHN, M., **Woitke, P.**, HAUSCHILDT, P. H. (2008, March). The influence of dust formation modelling on Na I and K I line profiles in substellar atmospheres. *MNRAS* **385**, L120–L124.
 98. HELLING, C., DEHN, M., **Woitke, P.**, HAUSCHILDT, P. H. (2008a, March). Consistent Simulations of Substellar Atmospheres and Nonequilibrium Dust Cloud Formation. *ApJL* **675**, L105–L108.
 99. HELLING, C., ACKERMAN, A. S., ALLARD, F., DEHN, M., HAUSCHILDT, P., HUBENY, I., HOMEIER, D., LODDERS, K., MARLEY, M., TSUJI, T., **Woitke, P.** (2007, September). Comparative study of dust cloud modelling for substellar atmospheres. *Astronomische Nachrichten* **328**, 655.
 100. **Woitke, P.** (2006b, December). Too little radiation pressure on dust in the winds of oxygen-rich AGB stars. *A&A* **460**, L9–L12.
 101. HELLING, C., **Woitke, P.** (2006a, August). Dust in brown dwarfs. V. Growth and evaporation of dirty dust grains. *A&A* **455**, 325–338.
 102. **Woitke, P.** (2006a, June). 2D models for dust-driven AGB star winds. *A&A* **452**, 537–549.
 103. HELLING, C., THI, W.-F., **Woitke, P.**, FRIDLUND, M. (2006, May). Detectability of dirty dust grains in brown dwarf atmospheres. *A&A* **451**, L9–L12.
 104. **Woitke, P.**, NICCOLINI, G. (2005, April). Dust cloud formation in stellar environments. II. Two-dimensional models for structure formation around AGB stars. *A&A* **433**, 1101–1115.
 105. HELLING, C., KLEIN, R., **Woitke, P.**, NOWAK, U., SEDLMAYR, E. (2004, August). Dust in brown dwarfs. IV. Dust formation and driven turbulence on mesoscopic scales. *A&A* **423**, 657–675.
 106. PASCUCCI, I., WOLF, S., STEINACKER, J., DULLEMOND, C. P., HENNING, T., NICCOLINI, G., **Woitke, P.**, LOPEZ, B. (2004, April). The 2D continuum radiative transfer problem. Benchmark results for disk configurations. *A&A* **417**, 793–805.
 107. **Woitke, P.**, HELLING, C. (2004b, January). Dust in brown dwarfs. III. Formation and structure of quasi-static cloud layers. *A&A* **414**, 335–350.

108. SCHIRRMACHER, V., **Woitke, P.**, SEDLMAYR, E. (2003, June). On the gas temperature in the shocked circumstellar envelopes of pulsating stars. III. Dynamical models for AGB star winds including time-dependent dust formation and non-LTE cooling. *A&A* **404**, 267–282.
109. RICHTER, H., WOOD, P. R., **Woitke, P.**, BOLICK, U., SEDLMAYR, E. (2003, March). On the shock-induced variability of emission lines in M-type Mira variables. II. Fe II and [Fe II] emission lines as a diagnostic tool. *A&A* **400**, 319–328.
110. NICCOLINI, G., **Woitke, P.**, LOPEZ, B. (2003b, February). High precision Monte Carlo radiative transfer in dusty media. *A&A* **399**, 703–716.
111. **Woitke, P.**, HELLING, C. (2003a, February). Dust in brown dwarfs. II. The coupled problem of dust formation and sedimentation. *A&A* **399**, 297–313.
112. **Woitke, P.** (2001a). Dust Induced Structure Formation. In R. E. Schielicke (Hrsg.), *Reviews in Modern Astronomy*, Band 14 of *Reviews in Modern Astronomy*, pp. 185.
113. **Woitke, P.**, SEDLMAYR, E., LOPEZ, B. (2000, June). Dust cloud formation in stellar environments. I. A radiative/thermal instability of dust forming gases. *A&A* **358**, 665–670.
114. **Woitke, P.**, HELLING, C., WINTERS, J. M., JEONG, K. S. (1999, August). On the formation of warm molecular layers. *A&A* **348**, L17–L20.
115. **Woitke, P.**, SEDLMAYR, E. (1999, July). Heating and cooling by iron in cool star winds. *A&A* **347**, 617–629.
116. CLAYTON, G. C., AYRES, T. R., LAWSON, W. A., DRILLING, J. S., **Woitke, P.**, ASPLUND, M. (1999, April). First Observations of an R Coronae Borealis Star with the Space Telescope Imaging Spectrograph: RY Sagittarii near Maximum Light. *ApJ* **515**, 351–355.
117. **Woitke, P.**, GOERES, A., SEDLMAYR, E. (1996a, September). On the gas temperature in the shocked circumstellar envelopes of pulsating stars. II. Shock induced condensation around R Coronae Borealis stars. *A&A* **313**, 217–228.
118. **Woitke, P.**, KRUEGER, D., SEDLMAYR, E. (1996, July). On the gas temperature in the shocked circumstellar envelopes of pulsating stars. I. Radiative heating and cooling rates. *A&A* **311**, 927–944.
119. KRUEGER, D., **Woitke, P.**, SEDLMAYR, E. (1995, November). A general multi-component method for the description of dust grain processing. *A&AS* **113**, 593.
120. **Woitke, P.**, DOMINIK, C., SEDLMAYR, E. (1993, July). Dust destruction in the transition region between stellar wind and interstellar medium. *A&A* **274**, 451.
121. **Woitke, P.**, DOMINIK, C., WINTERS, J. M., SEDLMAYR, E. (1993). Dust formation in the Ejecta of SN 1987A. In B. Baschek, G. Klare, & J. Lequeux (Hrsg.), *New Aspects of Magellanic Cloud Research*, Band 416 of *Lecture Notes in Physics*, Berlin Springer Verlag, pp. 224–225.

Conference Proceedings

1. SCHERF, M., BENEDIKT, M., ERKAEV, N., LAMMER, H., HERBORT, O., MARCQ, E., **Woitke, P.**, ODERT, P., O'NEILL, C., KUBYSHKINA, D., LEITZINGER, M. (2022, September). Escape of moderately volatile elements from protoplanets and its potential effect on habitability. In *European Planetary Science Congress*, pp. EPSC2022–999.
2. JORGE, D., KAMP, I., WATERS, R., **Woitke, P.**, SPAARGAREN, R. (2021, September). Forming planets around stars with non-solar composition. In *European Planetary Science Congress*, pp. EPSC2021–853.
3. KHORSHID, N., MIN, M., DESERT, J. M., DOMINIK, C., **Woitke, P.** (2021, September). Planet formation and its effect on planet atmosphere composition. In *European Planetary Science Congress*, pp. EPSC2021–660.
4. **Woitke, P.**, HELLING, C. (2021, April). GGchem: Fast thermo-chemical equilibrium code. *Bibcode: 2021ascl.soft04018W*.
5. HERBORT, O., **Woitke, P.**, HELLING, C., ZERKLE, A. (2021, March). From clouds to crust — Cloud diversity and surface conditions in atmospheres of rocky exoplanets. In *Bulletin of the American Astronomical Society*, Band 53, pp. 1134.
6. WATERS, L. B. F. M., VAN HOOLST, T., **Woitke, P.**, HELLING, C., KAMP, I., VAZAN, A., VAN DER VLEUT, B., SPAARGAREN, R., NOACK, L., LOES TEN KATE, I., MIN, M., ORMEL, C. (2021, January). The impact of planet formation scenarios on the composition of rocky exoplanets. In *43rd COSPAR Scientific Assembly. Held 28 January - 4 February*, Band 43, pp. 520.
7. NIKOLAOU, ATHANASIA AND MUGNAI, LORENZO AND HERBORT, OLIVER AND PASCALE, ENZO AND **Woitke, Peter**, (2020, September). Characteristics of an hybrid atmosphere with disk-captured and degassing contributions over a rocky planet's magma ocean. A modeling approach, in European Planetary Science Congress, EPSC2020-937.
8. RAB, C. AND ELBAKYAN, V. AND VOROBYOV, E. AND POSTEL, A. AND GÜDEL, M. AND DIONATOS, O. AND AUDARD, M. AND KAMP, I. AND THI, W. -F. AND **Woitke, P.** (2020, January). The chemistry of episodic accretion, in *Laboratory Astrophysics: From Observations to Interpretation*, p.440-442,
9. RAB, C. AND MURO-ARENA, G. A. AND KAMP, I. AND DOMINIK, C. AND WATERS, L. B. F. M. AND THI, W. -F. AND **Woitke, P.** (2020, January). The gas structure of the HD 163296 planet-forming disk - gas gaps or not?, in *Laboratory Astrophysics: From Observations to Interpretation*, p.445-447
10. RAB, CH. AND MURO-ARENA, G. A. AND KAMP, I. AND DOMINIK, C. AND WATERS, L. B. F. M. AND THI, W. -F. AND **Woitke, P.** (2020, January). Searching for chemical signatures of planet formation, in *Origins: From the Protosun to the First Steps of Life*, p. 362-364.

11. RAB, CH. AND PADOVANI, M. AND GÜDEL, M. AND KAMP, I. AND THI, W. -F. AND **Woitke, P.** (2020, January). Constraining the stellar energetic particle flux in young solar-like stars, in *Origins: From the Protosun to the First Steps of Life*, p. 310-311.
12. **Woitke, P.**, DENT, W. R. F., THI, W.-F., MENARD, F., PINTE, C., DUCHENE, G., SANDELL, G., LAWSON, W., KAMP, I. (2013, July). ET Cha - a single T Tauri star with a disk of radius ~ 5 AU ? In *Protostars and Planets VI Posters*, pp. 13.
13. THI, W.-F., PINTE, C., PANTIN, E., AUGEREAU, J.-C., MEEUS, G., MÉNARD, F., MARTIN-ZAIDI, C., **Woitke, P.**, RIVIERE-MARICHALAR, P., KAMP, I., CARMONA, A., SANDELL, G., EIROA, C., DENT, W., MONTESINOS, B., ARESU, G., MEIJERINK, R., SPAANS, M., WHITE, G., ARDILA, D., LEBRETON, J., MENDIGUTIA, I., BRITAIN, S. (2013, July). Herschel-PACS observation of gas lines from the disc around HD141569A. In *Protostars and Planets VI Posters*, pp. 21.
14. RAB, C., **Woitke, P.**, GÜDEL, M., MIN, M., DIANA TEAM (2013, July). X-ray Radiative Transfer in Protoplanetary Disks with ProDiMo. In *Protostars and Planets VI Posters*, pp. 38.
15. MIN, M., RAB, C., DOMINIK, C., **Woitke, P.** (2013, July). The appearance of large aggregates in protoplanetary disks. In *Protostars and Planets VI Posters*, pp. 44.
16. ANTONELLINI, S., KAMP, I., **Woitke, P.**, THI, W.-F. (2013, July). H₂O in Protoplanetary Disks: the Snow Line and the Planets' Nest. In *Protostars and Planets VI Posters*, pp. 35.
17. HEIN BERTELSEN, R., KAMP, I., GOTO, M., VAN DER PLAS, G., THI, W.-F., WATERS, R., **Woitke, P.**, VAN DEN ANCKER, M. (2013, July). Co Ro-Vib Observations of HD100546: a Symmetric Disk or Not? In *Protostars and Planets VI Posters*, pp. 11.
18. LAHUIS, F., KAMP, I., THI, W.-F., VAN DISHOCK, E., HARSONO, D., **Woitke, P.** (2013, July). Time variation in the molecular infrared spectrum of IRS 46. In *Protostars and Planets VI Posters*, pp. 25.
19. PODIO, L., KAMP, I., CODELLA, C., CABRIT, S., NISINI, B., DOUGADOS, C., SANDELL, G., WILLIAMS, J. P., TESTI, L., THI, W.-F., **Woitke, P.**, MEIJERINK, R., SPAANS, M., ARESU, G., MÉNARD, F., PINTE, C. (2013a, July). Water Vapor in the Protoplanetary Disk of DG Tau. In *Protostars and Planets VI Posters*, pp. 28.
20. DENT, W. R. F., THI, W. F., KAMP, I., WILLIAMS, J. P., MENARD, F., ANDREWS, S., ARDILA, D., ARESU, G., AUGEREAU, J.-C., BARRADO Y NAVASCUES, D., BRITAIN, S., CARMONA, A., CIARDI, D., DANCHI, W., DONALDSON, J., DUCHENE, G., EIROA, C., FEDELE, D., GRADY, C., DE GREGORIO-MONSALVO, I., HOWARD, C., HUELAMO, N., KRIVOV, A., LEBRETON, J., LISEAU, R., MARTIN-ZAIDI, C., MATHEWS, G., MEEUS, G., MENDIGUTIA, I.,

- MONTESINOS, B., MORALES-CALDERON, M., MORA, A., NOMURA, H., PANTIN, E., PASCUCCHI, I., PHILLIPS, N., PINTE, C., PODIO, L., RAMSAY, M. K., RIAZ, B., RIVIERE-MARICHALAR, P., ROBERGE, A., SANDELL, G., SOLANO, E., TILLING, I., TORRELLES, J. M., VANDENBUSSCHE, B., VICENTE, S., WHITE, G. J., **Woitke, P.** (2013, August). VizieR Online Data Catalog: Gas Survey of Protoplanetary Systems. I. (Dent+, 2013). *VizieR Online Data Catalog* **612**, 50477.
21. ARESU, G., KAMP, I., MEIJERINK, R., **Woitke, P.**, THI, W. F., SPAANS, M. (2011b, May). X-rays in protoplanetary disks: their impact on the thermal and chemical structure, a grid of models. In J. Cernicharo & R. Bachiller (Hrsg.), *IAU Symposium*, Band 280 of *IAU Symposium*, pp. 87P.
 22. HELLING, C., ACKERMAN, A., ALLARD, F., DEHN, M., HAUSCHILDT, P., HOMER, D., LODDERS, K., MARLEY, M., RIETMEIJER, F., TSUJI, T., **Woitke, P.** (2008b, May). Comparison of cloud models for Brown Dwarfs. In Y.-S. Sun, S. Ferraz-Mello, & J.-L. Zhou (Hrsg.), *IAU Symposium*, Band 249 of *IAU Symposium*, pp. 173–177.
 23. DEHN, M., HELLING, C., **Woitke, P.**, HAUSCHILDT, P. (2007, May). The influence of convective energy transport on dust formation in brown dwarf atmospheres. In F. Kupka, I. Roxburgh, & K. L. Chan (Hrsg.), *IAU Symposium*, Band 239 of *IAU Symposium*, pp. 227–229.
 24. HELLING, C., **Woitke, P.** (2005, March). Rain and clouds in brown dwarf atmospheres: a coupled problem from small to large. In F. Favata, G. A. J. Hussain, & B. Battrock (Hrsg.), *13th Cambridge Workshop on Cool Stars, Stellar Systems and the Sun*, Band 560 of *ESA Special Publication*, pp. 249.
 25. DEHN, M., HELLING, C., **Woitke, P.**, HAUSCHILDT, P. (2005). First Steps Towards Modelling a Brown Dwarf Atmosphere Including the Formation of Dust. In *Protostars and Planets V Posters*, pp. 8158.
 26. HELLING, C., **Woitke, P.** (2004, December). Theory of Precipitating Dust Formation in Substellar Atmospheres. In J. Beaulieu, A. Lecavelier Des Etangs, & C. Terquem (Hrsg.), *Extrasolar Planets: Today and Tomorrow*, Band 321 of *Astronomical Society of the Pacific Conference Series*, pp. 199.
 27. HELLING, C., KLEIN, R., **Woitke, P.**, NOWAK, U., SELDMAYR, E. (2003, July). On the Sub-grid Modelling of Turbulent Dust Formation in Substellar Atmospheres. *Astronomische Nachrichten Supplement* **324**, 2.
 28. HELLING, C., KLEIN, R., **Woitke, P.**, SELDMAYR, E. (2003). Dust Formation in Brown Dwarf Atmospheres Under Conditions of Driven Turbulence. In N. Piskunov, W. W. Weiss, & D. F. Gray (Hrsg.), *Modelling of Stellar Atmospheres*, Band 210 of *IAU Symposium*, pp. 12P.
 29. HELLING, C., **Woitke, P.** (2006b, August). Time-dependent modelling of oxygen-rich dust formation. In *IAU Joint Discussion*, Band 11 of *IAU Joint Discussion*, pp. 13.

30. HELLING, C., **Woitke, P.**, KLEIN, R., SEDLMAYR, E. (2005). Dust Formation in Substellar Atmospheres: A Multi-Scale Problem. In H. U. Käufl, R. Siebenmorgen, & A. Moorwood (Hrsg.), *High Resolution Infrared Spectroscopy in Astronomy*, pp. 503–509.
31. HELLING, C., **Woitke, P.**, WINTERS, J. M., SEDLMAYR, E. (1998). Influence of molecular opacities on the generation of cool star winds. In *IAU Symposium*, Band 191 of *IAU Symposium*, pp. 209P.
32. JOHNAS, C. M. S., HELLING, C., WITTE, S., DEHN, M., **Woitke, P.**, HAUSCHILDT, P. H. (2008). The Consistent Modelling of Alkali Lines and Dust Formation in Extreme Exo-Planets. In D. Fischer, F. A. Rasio, S. E. Thorsett, & A. Wolszczan (Hrsg.), *Extreme Solar Systems*, Band 398 of *Astronomical Society of the Pacific Conference Series*, pp. 393.
33. KAMP, I., ARESU, G., CHAPARRO, G., **Woitke, P.**, THI, W. F. (2011, May). The structure and appearance of irradiated protoplanetary disks: the role of chemistry. In J. Cernicharo & R. Bachiller (Hrsg.), *IAU Symposium*, Band 280 of *IAU Symposium*, pp. 213P.
34. KEANE, J. T., PASCUCCI, I., ANDREWS, S. M., DENT, B., ESPAILLAT, C., MEEUS, G., THI, W., **Woitke, P.** (2013, January). From Classical Disks to Transition Disks: An Increasing Dust-to-Gas Ratio? In *American Astronomical Society Meeting Abstracts #221*, Band 221 of *American Astronomical Society Meeting Abstracts*, pp. #220.02.
35. LAHUIS, F., KAMP, I., THI, W. F., VAN DISHOECK, E. F., **Woitke, P.** (2011, May). Epic changes in the IRS46 mid-infrared spectrum; an inner disk chemistry study. In J. Cernicharo & R. Bachiller (Hrsg.), *IAU Symposium*, Band 280 of *IAU Symposium*, pp. 223P.
36. LÜTTKE, M., HELLING, C., JOHN, M., JEONG, K. S., **Woitke, P.**, SEDLMAYR, E. (2000). Dust Formation in Brown Dwarfs. In R. E. Schielicke (Hrsg.), *Astronomische Gesellschaft Meeting Abstracts*, Band 17 of *Astronomische Gesellschaft Meeting Abstracts*, pp. 7.
37. MEIER, S., PATZER, A. B. C., LÜTTKE, M., **Woitke, P.**, SEDLMAYR, E. (2000). Circumstellar Dust Shells of Pulsating Red Giants as Dynamical Systems. In R. E. Schielicke (Hrsg.), *Astronomische Gesellschaft Meeting Abstracts*, Band 17 of *Astronomische Gesellschaft Meeting Abstracts*, pp. 14.
38. NICCOLINI, G., LOPEZ, B., **Woitke, P.** (2003). Radiative Transfer and Dust formation in the Envelopes of Evolved Stars. In F. Combes, D. Barret, T. Contini, & L. Pagani (Hrsg.), *SF2A-2003: Semaine de l'Astrophysique Francaise*, pp. 555.
39. PERVAN, Š., HELLING, C., **Woitke, P.**, SEDLMAYR, E. (2003, July). Study on Synthetic Spectra of Substellar Objects. *Astronomische Nachrichten Supplement* **324**, 127.

40. RICHTER, H., **Woitke, P.**, BOLICK, U., SEDLMAYR, E., WOOD, P. R. (2003, July). Fe II and [Fe II] Emission Lines as a Diagnostic Tool to Probe the Shocked Atmospheres of M-type Miras. *Astronomische Nachrichten Supplement* **324**, 17.
41. RICHTER, H., **Woitke, P.**, SEDLMAYR, E., WOOD, P. R. (2000). The Variability of Emission Lines in Shocked M Mira Atmospheres. In R. E. Schielicke (Hrsg.), *Astronomische Gesellschaft Meeting Abstracts*, Band 17 of *Astronomische Gesellschaft Meeting Abstracts*, pp. 24.
42. RICHTER, H., WOOD, P. R., BOLICK, U., **Woitke, P.**, SEDLMAYR, E. (2003, January). NLTE Modelling of FeII and [FeII] Lines in the Shocked Atmospheres of M-type Miras. In I. Hubeny, D. Mihalas, & K. Werner (Hrsg.), *Stellar Atmosphere Modelling*, Band 288 of *Astronomical Society of the Pacific Conference Series*, pp. 344.
43. SCHIRRMACHER, V., **Woitke, P.**, SEDLMAYR, E. (2000). Dynamical Model Calculations of AGB Star Winds Including Time Dependent Dust Formation and Non-LTE Radiative Cooling. In R. E. Schielicke (Hrsg.), *Astronomische Gesellschaft Meeting Abstracts*, Band 17 of *Astronomische Gesellschaft Meeting Abstracts*, pp. 31.
44. SCHIRRMACHER, V., **Woitke, P.**, SEDLMAYR, E. (2001). A Radiative Instability in Post-shock-cooling Circumstellar Gas. In E. R. Schielicke (Hrsg.), *Astronomische Gesellschaft Meeting Abstracts*, Band 18 of *Astronomische Gesellschaft Meeting Abstracts*, pp. 65.
45. SCHNABEL, K., HELLING, C., **Woitke, P.**, SEDLMAYR, E. (2001). Radiation Transfer Through an Extended Planetary Atmosphere. In E. R. Schielicke (Hrsg.), *Astronomische Gesellschaft Meeting Abstracts*, Band 18 of *Astronomische Gesellschaft Meeting Abstracts*, pp. 44.
46. THI, W. F., MENARD, F., MEEUS, G., MARTIN-ZAIDI, C., **Woitke, P.**, TATULLI, E., BENISTY, M., KAMP, I., PASCUCCI, I., PINTE, C., GRADY, C. A., BRITTAIN, S., WHITE, G. J., HOWARD, C. D., SANDELL, G., EIROA, C. (2011, May). Modelling CH⁺ in the protoplanetary disk HD100546. In J. Cernicharo & R. Bachiller (Hrsg.), *IAU Symposium*, Band 280 of *IAU Symposium*, pp. 355P.
47. **Woitke, P.** (1998). Time-Dependent Behavior of Cool-Star Winds. In L. Kaper & A. W. Fullerton (Hrsg.), *Cyclical Variability in Stellar Winds*, pp. 278.
48. **Woitke, P.** (1999). Dust formation in Radioactive Environments. In R. Diehl & D. Hartmann (Hrsg.), *Astronomy with Radioactivities*, pp. 163.
49. **Woitke, P.** (2001b). Self-organization of Dust Forming Media. In E. R. Schielicke (Hrsg.), *Astronomische Gesellschaft Meeting Abstracts*, Band 18 of *Astronomische Gesellschaft Meeting Abstracts*, pp. 809.
50. **Woitke, P.** (2003). Modelling the Mass Loss of Cool AGB Stars. In N. Piskunov, W. W. Weiss, & D. F. Gray (Hrsg.), *Modelling of Stellar Atmospheres*, Band 210 of *IAU Symposium*, pp. 387.

51. **Woitke, P.** (2005, January). 2D models for the winds of AGB stars. In A. Wilson (Hrsg.), *ESA Special Publication*, Band 577 of *ESA Special Publication*, pp. 461–462.
52. **Woitke, P.** (2007, November). What Drives the Mass Loss of Oxygen-Rich AGB Stars? In F. Kerschbaum, C. Charbonnel, & R. F. Wing (Hrsg.), *Why Galaxies Care About AGB Stars: Their Importance as Actors and Probes*, Band 378 of *Astronomical Society of the Pacific Conference Series*, pp. 156.
53. **Woitke, P.** (2008a, October). Dust-driven Winds Beyond Spherical Symmetry. In L. Deng & K. L. Chan (Hrsg.), *IAU Symposium*, Band 252 of *IAU Symposium*, pp. 229–234.
54. **Woitke, P.** (2008b). Monte Carlo Radiative Transfer in Multi-D Dynamical Models of Dust-Driven Winds. In S. Wolf, F. Allard, & P. Stee (Hrsg.), *EAS Publications Series*, Band 28 of *EAS Publications Series*, pp. 75–83.
55. **Woitke, P.** (2012, March). Modelling planet-forming circumstellar discs. In *From Atoms to Pebbles: Herschel’s view of Star and Planet Formation*, pp. 39.
56. **Woitke, P., DENT, B., THI, W.-F., SIBTHORPE, B., RICE, K., WILLIAMS, J., SICILIA-AGUILAR, A., BROWN, J., KAMP, I., PASCUCCI, I., ALEXANDER, R., ROBERGE, A.** (2009, February). Gas Evolution in Protoplanetary Disks. In E. Stempels (Hrsg.), *15th Cambridge Workshop on Cool Stars, Stellar Systems, and the Sun*, Band 1094 of *American Institute of Physics Conference Series*, pp. 225–233.
57. **Woitke, P., GASPS CONSORTIUM** (2010). Gas in Protoplanetary Systems. In *38th COSPAR Scientific Assembly*, Band 38 of *COSPAR Meeting*, pp. 2474.
58. **Woitke, P., GOERES, A., SEDLMAYR, E.** (1996b). Shock-induced condensation in R CrB stars. In C. S. Jeffery & U. Heber (Hrsg.), *Hydrogen Deficient Stars*, Band 96 of *Astronomical Society of the Pacific Conference Series*, pp. 83.
59. **Woitke, P., HELLING, C.** (2003b, July). The Structure of Quasi-static Cloud Layers in Brown Dwarf Atmospheres. *Astronomische Nachrichten Supplement* **324**, 126.
60. **Woitke, P., HELLING, C.** (2004a, August). 2D Models for the Winds of AGB Stars. *Astronomische Nachrichten Supplement* **325**, 95.
61. **Woitke, P., HELLING, C.** (2005, March). 2D dynamical models for dust-driven winds of AGB stars. In F. Favata, G. A. J. Hussain, & B. Battrick (Hrsg.), *13th Cambridge Workshop on Cool Stars, Stellar Systems and the Sun*, Band 560 of *ESA Special Publication*, pp. 1039.
62. **Woitke, P., KRÜGER, D., GOERES, A., SEDLMAYR, E.** (1994). On the temperature in the shocked envelopes of R CrB stars. In G. Klare (Hrsg.), *Astronomische Gesellschaft Abstract Series*, Band 10 of *Astronomische Gesellschaft Abstract Series*, pp. 160.
63. **Woitke, P., QUIRRENBACH, A.** (2008). The Chaotic Winds of AGB Stars: Observation Meets Theory. In A. Richichi, F. Delplancke, F. Paresce, & A. Chelli (Hrsg.), *The Power of Optical/IR Interferometry: Recent Scientific Results and 2nd Generation*, pp. 181.

64. **Woitke, P.**, SEDLMAYR, E. (1998). Thermal Bifurcations in the Circumstellar Envelopes of C-Stars. In *IAU Symposium*, Band 191 of *IAU Symposium*, pp. 317P.
65. NICCOLINI, G., **Woitke, P.**, LOPEZ, B. (2003a, April). Formation and evolution of dust clumps around cool stars. In Y. Nakada, M. Honma, & M. Seki (Hrsg.), *Mass-Losing Pulsating Stars and their Circumstellar Matter*, Band 283 of *Astrophysics and Space Science Library*, pp. 245–246.